

Electronic Thesis and Dissertation Repository

---

5-2-2016 12:00 AM

## Bed Agglomeration Behavior in a Bubbling Fluidized-Bed Combustor

Ehsan Ghiasi, *The University of Western Ontario*

Supervisor: Prof. Charles Xu, *The University of Western Ontario*

Joint Supervisor: Prof Honghi Tran, *The University of Western Ontario*

A thesis submitted in partial fulfillment of the requirements for the Master of Science degree in Chemical and Biochemical Engineering

© Ehsan Ghiasi 2016

Follow this and additional works at: <https://ir.lib.uwo.ca/etd>

 Part of the [Other Chemical Engineering Commons](#)

---

### Recommended Citation

Ghiasi, Ehsan, "Bed Agglomeration Behavior in a Bubbling Fluidized-Bed Combustor" (2016). *Electronic Thesis and Dissertation Repository*. 3758.

<https://ir.lib.uwo.ca/etd/3758>

This Dissertation/Thesis is brought to you for free and open access by Scholarship@Western. It has been accepted for inclusion in Electronic Thesis and Dissertation Repository by an authorized administrator of Scholarship@Western. For more information, please contact [wlsadmin@uwo.ca](mailto:wlsadmin@uwo.ca).

## Abstract

Agglomeration is a major operational problem during the combustion of biomass containing a high amount of alkali compounds. The agglomerate formation is mainly due to the presence of alkali elements in biomass ashes that form low-melting compounds during the combustion.

In the first part of this project, the critical amount of liquid that would lead to a severe agglomeration/de-fluidization was studied and determined in a lab scale bubbling fluidized bed (BFB) heated at elevated temperatures. To simulate the biomass ashes, various percentages of KCl and KCl-K<sub>2</sub>SO<sub>4</sub> compounds at eutectic composition were mixed with silica sand as the bed material. The results indicated that the formation of channeling/bed-material agglomeration was severe in the presence of KCl or mixture of KCl-K<sub>2</sub>SO<sub>4</sub> with an amount of 0.4-0.6 wt.% with respect to the weight of bed material, being in a good agreement with that was reported by the author's group in a previous study carried out in a cold BFB test rig using glycerol-water mixture to simulate melted biomass ash. Kaolin and aluminum sulfates were investigated as additives in the BFB and proved to be effective for preventing the bed material agglomeration.

In the second part of this research, we examined the de-fluidization time for BFB combustion of corn stalk (with a high K, Mg, Ca-containing ash) with different bed materials operating at different superficial air velocities. Corn stalk has a high tendency for the unwanted bed agglomeration problems during combustion due to its high contents of K, Ca and Mg in the ash. In combustion of corn stalk, there was a lower deposition tendency of K compounds onto the olivine bed material than that onto the silica sand material, which might account for the longer time to onset of de-fluidization (>12h) for the olivine bed material than that for the silica bed material (8h) during corn stalk combustion. With increasing the superficial gas velocity, the deposited amount of the alkali/alkaline earth elements (K, Ca, Mg) on the bed material (either silica or olivine sand) reduced substantially, which would contribute to reduced tendency of bed agglomeration and de-fluidization.

**Keywords:** Agglomeration, bubbling fluidized bed, biomass, additives, bed material

## Co-Authorship Statement

**Study of Bed Material Agglomeration in a Bubbling Fluidized Bed (BFB) using KCl and K<sub>2</sub>SO<sub>4</sub> at High Temperatures to Simulate Molten Ash** (based on Chapter 3)

**Authors:** Ghiasi, E., Montes, A., Nanda, M., Tran, H. and Xu, C.

The experiment work was conducted by Ehsan Ghiasi under the supervision of Prof. Charles (Chunbao) Xu and Prof. Honghi Tran, and the guidance of Dr. Malaya Nanda and Alejandro Montes. Writing and data analysis of this publication was conducted by Ehsan Ghiasi. It was reviewed and revised by Prof. Charles (Chunbao) Xu and Prof. Honghi Tran. The manuscript will be submitted to “*Powder Technology*” for consideration of publication.

**Behavior and Mechanism of Bed Material Agglomeration in Fluidized-bed Combustion of Corn Stalk Using Silica or Olivine as Bed Material** (based on Chapter 4)

**Authors:** Ghiasi, E., Tran, H. and Xu, C.

The experiment work and data analysis were conducted by Ehsan Ghiasi. Prof. Charles (Chunbao) Xu, and Prof. Honghi Tran provided general guidance, consultation regarding experimental work and interpretation of results. The manuscript draft was written and revised by Ehsan Ghiasi, and reviewed by Prof. Charles (Chunbao) Xu and Prof. Honghi Tran. The manuscript will be submitted to “*Energy & Fuels*” for consideration of publication.

## **Dedication**

*To*

*My beloved wife, Fatemeh,*

*&*

*My wonderful parents, Mohammadreza & Khadijeh,*

*For their endless love, encouragement, and support.*

## **Acknowledgments**

I would like to express my sincere gratitude to my supervisors Professor Charles (Chunbao) Xu at Western University and Professor Honghi Tran at University of Toronto for their valuable guidance, continuous support, encouragement, advice and help throughout my MSc project.

I would like to acknowledge the industrial support from various pulp and paper companies and the Natural Sciences and Engineering Research Council of Canada (NSERC) via the CRD Grant, for their financial support for this project and my master studies.

I would like to thank the faculty and staff of Institute for Chemical and Fuels from Alternative Resources (ICFAR) and Chemical and Biochemical Engineering Department at Western University for providing support and education during my studies.

My gratitude is also extended to all the people I had the pleasure of working with at ICFAR and Western Research Park in Sarnia in the past two years, especially Malaya Nanda, Fang (Flora) Cao, Hojat Seyedy for their contributions and assistance in my research.

My deepest appreciation and sincere gratitude goes to my family; without whom I would have never been able to reach this point. Words cannot express how grateful I am to my parents for their love and support. At last, I would like to gratefully thank my beloved wife, Fatemeh Ferdosian, for her patience, care, unconditional love, encouragement and great support during all these years.

*Ehsan Ghiasi*  
*Western University*  
*May 2016*

# Table of Contents

Abstract.....	i
Co-Authorship Statement.....	ii
Dedication.....	iii
Acknowledgments.....	iv
Table of Contents.....	v
List of Tables.....	ix
List of Figures.....	x
List of Appendices.....	xiii
List of Abbreviations and Symbols.....	xiv
1. Chapter 1.....	1
General Introduction.....	1
1.1 Introduction.....	2
1.2 Fluidized Bed Combustion.....	3
1.3 Bed Agglomeration.....	4
1.4 Knowledge Gaps and Needs of Research.....	5
1.5 Thesis Objective.....	6
1.6 Thesis Structure.....	6
1.7 References.....	8
2. Chapter 2.....	10
Literature Review.....	10
2.1 Biomass.....	11
2.2 Conversion of Biomass to Energy.....	13
2.2.1 Gasification.....	14

2.2.2	Pyrolysis.....	15
2.2.3	Combustion.....	15
2.3	Fluidization and Fluidized Bed .....	16
2.3.1	Minimum Fluidization Velocity .....	17
2.3.2	Experimental approach .....	19
2.3.3	Fluidized Bed Combustor .....	20
2.3.4	Scope of Fluidized Bed Combustor .....	20
2.4	Bed Material Agglomeration and De-fluidization .....	21
2.4.1	Effects of Type of Biomass.....	23
2.4.2	Effects of Bed Materials .....	26
2.4.3	Effects of Air Velocity.....	29
2.4.4	Effects of Operation Temperature .....	30
2.4.5	Effects of Additives .....	31
2.5	Summary .....	33
2.6	References .....	35
3.	Chapter 3.....	41
	Study of Bed Material Agglomeration in a Bubbling Fluidized Bed (BFB) using KCl and K <sub>2</sub> SO <sub>4</sub> at High Temperatures to Simulate Molten Ash .....	41
	Abstract.....	42
3.1	Introduction .....	43
3.2	Experimental .....	45
3.2.1	Experimental Set-up.....	45
3.2.2	Materials .....	47
3.2.3	Procedure .....	47
3.3	Results & Discussion .....	48

3.3.1	Effects of KCl on formation of agglomerates .....	49
3.3.2	Effects of eutectic mixture of KCl-K <sub>2</sub> SO <sub>4</sub> on formation of agglomerates .....	54
3.3.3	Effects of Additives .....	57
3.4	Conclusions .....	59
3.5	References .....	60
4.	Chapter 4.....	62
	Behavior and Mechanism of Bed Material Agglomeration in Fluidized-bed Combustion of Corn Stalk Using Silica or Olivine as Bed Material .....	62
	Abstract .....	63
4.1	Introduction .....	64
4.2	Experimental .....	66
4.2.1	Fluidized Bed Combustor (FBC) .....	66
4.2.2	Fuel Preparation .....	68
4.2.3	Methods.....	68
4.3	Results & Discussions.....	69
4.3.1	Temperature Profiles.....	69
4.3.2	Composition of Coated Ash-layer on Bed Material .....	72
4.3.3	De-Fluidization Time and Surface Composition of Agglomerates .....	75
4.3.4	Composition of Bottom and Fly Ash.....	79
4.4	Conclusions .....	82
4.5	References .....	84
5.	Chapter 5.....	90
	Conclusions and Recommendations .....	90
5.1	Conclusions .....	91
5.2	Recommendations .....	92



Appendix.....	94
Curriculum Vitae .....	102

## List of Tables

Table 2-1 Major advantages and disadvantages of biomass energy. ....	12
Table 2-2 Different modes of pyrolysis of wood [18,19]. ....	15
Table 2-3 Different values for $C_1$ and $C_2$ . ....	19
Table 2-4 Ash analysis (wt%) of three biomass fuels [46]. ....	25
Table 2-5 Physical properties of alumina and silica sands [25]. ....	26
Table 2-6 Initial de-fluidization temperature of various biomass fuels [30]. ....	27
Table 3-1 SEM-EDX and XPS analytical results for the agglomerates collected after the tests with various amounts of KCl addition. ....	52
Table 3-2 ICP results of washing liquids from pure silica sand and from agglomerates of silica sand with 0.6wt% KCl. ....	53
Table 3-3 SEM-EDX and XPS analysis results for the agglomerates collected after the tests with various amounts of KCl- $K_2SO_4$ addition. ....	56
Table 3-4 AAS, IC analysis results of the eutectic mixture of KCl- $K_2SO_4$ after heating at 800°C for various lengths of time. ....	57
Table 3-5 SEM-EDX analysis results for the bed materials collected after the experiments with co-presence of alkali compounds and an additive (Kaolin or $Al_2(SO_4)_3$ ). ....	59
Table 4-1 Chemical composition and properties of bed materials. ....	67
Table 4-2 Mineral composition of corn stalk. ....	68
Table 4-3 Operation conditions and de-fluidization time for the combustion of corn stalk in a BFB combustor using silica sand and olivine sand as bed material at $2.5U_{mf}$ . ....	76

## List of Figures

Figure 1-1 Biomass resource conversion processes [5].....	2
Figure 1-2 Circulating fluidized bed (a) and Bubbling fluidized bed (b) [9,10]. .....	3
Figure 1-3 Chain stoker grate [12].....	4
Figure 1-4 schematic of two possible mechanisms of agglomerate formation.....	5
Figure 2-1 Consumption of energy in the United States in 2008 [1].....	11
Figure 2-2 Main conversion options for biomass to secondary energy carriers, reprinted with permission from ref. [11]. Copyright (2006) Springer. ....	14
Figure 2-3 Fluidization regimes [27]. .....	17
Figure 2-4 variation in bed pressure drop ( $\Delta P$ ) with superficial velocity ( $V_g$ ) [29]. .....	20
Figure 2-5 Schematic mechanism of formation of agglomerates (1) Coating-induced mechanism and (2) melt induced mechanism [34]. .....	21
Figure 2-6 SEM micrographs at different magnifications of a typical agglomerate sample (A), details of the external surface (B), cross-section of an agglomerate (C), and details of the agglomerates cross-section (D). Pine seed shells $T= 850^\circ\text{C}$ , $d_p=212\text{-}400 \mu\text{m}$ , reprinted with permission from ref. [36]. Copyright (2008) Elsevier. ....	22
Figure 2-7 Degree of ash sintering for different biomass fuels at various temperatures [47]. .....	25
Figure 2-8 Effects of bed material size on the de-fluidization time at various temperatures, reprinted with permission from ref. [2]. Copyright (2003) Elsevier.....	28
Figure 2-9 Influence of bed material size on de-fluidization time, reprinted with permission from ref. [48]. Copyright (2011) Elsevier. ....	28
Figure 2-10 De-fluidization time as a function of gas velocity [53].....	29

Figure 2-11 Influence of temperature on time of agglomeration, reprinted with permission from ref. [48]. Copyright (2011) Elsevier. ....	30
Figure 2-12 Retention of KCl within zeolite 24A and kaolin at various temperatures [61].....	32
Figure 3-1 Schematic diagram (A) and photo of lab scale (B) BFB combustor.....	46
Figure 3-2 Variation of differential pressure ( $\Delta P$ ) and temperature signals with experimental time in BFB of silica sand particles with 0.0wt% KCl (a); 0.2wt% KCl (b); 0.4wt% KCl (c); 0.6wt% KCl (d). ....	50
Figure 3-3 Formed agglomerates and the bottom view of the BFB reactor. ....	51
Figure 3-4 SEM mapping images of the agglomerates from the test with 0.6% KCl. ....	52
Figure 3-5 Photos of the bed material after the experiment with (A) and without (B) 0.6wt% KCl .....	54
Figure 3-6 Variation of differential pressure ( $\Delta P$ ) and temperature signals with experimental time in BFB of silica sand particles with 0.0wt% KCl-K <sub>2</sub> SO <sub>4</sub> (a); 0.2wt% KCl-K <sub>2</sub> SO <sub>4</sub> (b); 0.4wt% KCl-K <sub>2</sub> SO <sub>4</sub> (c); 0.6wt% KCl-K <sub>2</sub> SO <sub>4</sub> (d). ....	55
Figure 3-7 SEM image (a) and EDX spectra (b) of the formed agglomerates after the BFB test with 0.6wt% KCl-K <sub>2</sub> SO <sub>4</sub> .....	55
Figure 3-8 SEM mapping images of agglomerates from the test with 0.6% KCl-K <sub>2</sub> SO <sub>4</sub> . ....	56
Figure 3-9 Variation of $\Delta P$ and temperature signals with experimental time in in BFB of silica sand particles with 0.6wt% KCl and 0.6wt% kaolin (a); 0.6wt% KCl and 0.6wt% aluminum sulfate (b); 0.6wt% KCl-K <sub>2</sub> SO <sub>4</sub> and 0.6wt% kaolin(c); 0.6wt% KCl-K <sub>2</sub> SO <sub>4</sub> and 0.6wt% aluminum sulfate (d). .....	58
Figure 4-1 Temperature profiles along the height of the reactor in combustion of corn stalk in the presence of silica and olivine sand (at $U_g = 2.5 U_{mf}$ ).....	70

Figure 4-2 Effects of superficial air velocity on the temperature profiles along the reactor height in combustion of corn stalk with silica sand (a) or olivine sand (b) bed material. ....	72
Figure 4-3 EDX results of the surface composition of bed material (silica or olivine sand) after 2, 4, and 6 hours combustion of corn stalk at two air velocities $U_g = 2.5U_{mf}$ (a) and $4U_{mf}$ (b). ....	74
Figure 4-4 T- $\Delta$ P signals at the dense phase bed during combustion of corn stalk in BFB of silica (2 <sup>nd</sup> day) (a) and olivine sand (3 <sup>rd</sup> day) (b) at $U_g = 2.5U_{mf}$ . ....	75
Figure 4-5 EDX elemental analysis of the agglomerated silica in two points (A and B as shown in Figure 4-7 (I)) and non-agglomerated olivine particles after 12h combustion tests. ....	77
Figure 4-6 Ternary phase diagram of CaO-K <sub>2</sub> O-SiO <sub>2</sub> [5]. ....	78
Figure 4-7 SEM micrograph of typical silica agglomerates (I), optical photograph of a small silica sand agglomerate (II). ....	79
Figure 4-8 Bottom ash particles collected from the olivine bed (a) and silica bed (b) after 8h BFB combustion of corn stalk. ....	80
Figure 4-9 Results of ICP analysis of bottom ash particles collected from the silica or olivine bed after 8h BFB combustion of corn stalk. ....	81
Figure 4-10 Results of ICP analysis of fly ashes collected after 8h BFB combustion of corn stalk in silica sand or olivine sand in comparison with composition of the original corn stalk ash. ....	82

## **List of Appendices**

Appendix 1: Permission to Reuse Copyrighted Materials

## List of Abbreviations and Symbols

<b>Abbreviation</b>	<b>Meaning</b>
BFB	Bubbling Fluidized Bed
CFBC	Circulating Fluidized Bed Combustor
BFBC	Bubbling Fluidized Bed Combustor
FCC	Fluid Catalytic Cracking
HHV	Higher Heating Value
LHV	Lower Heating Value
MSW	Municipal Solid Waste
FBC	Fluidized Bed Combustion
DDGS	Distiller's Dried Grain with Solubles
IDT	Initial De-fluidization Temperature
SEM	Scanning Electron Microscopy
EDX	Energy Dispersive X-ray
ICP	Inductively Coupled Plasma
AAS	Atomic Absorption Spectroscopy
IC	Ion Chromatography
XPS	X-ray Photoelectron Spectroscopy

<b>Symbol</b>	<b>Meaning</b>
$\rho_g$	Gas density (kg/m <sup>3</sup> )
$\mu_g$	Gas viscosity (Pa.s)
$\rho_p$	Particle density (Kg/m <sup>3</sup> )
$d_p$	Particle diameter ( $\mu\text{m}$ )
$G$	Gravity (m/s <sup>2</sup> )
$U_{mf}$	Minimum fluidization velocity (m/s)
$\varepsilon$	Bed voidage
$\varepsilon_{mf}$	Bed voidage at minimum fluidization condition
$\Phi_s$	Sphericity of solid particles
$V_g$	Superficial gas velocity (m/s)
$W_{\text{bed particles}}$	Net bed weight of the particles (kg)
$A$	Bed cross sectional area (m <sup>2</sup> )
$L_{\text{bed}}$	Bed height (m)
$\Delta P_{\text{bed}}$	Bed pressure drop (psi)
$A_r$	Archimides number
$Re_{mf}$	Reynold number at minimum fluidization number
$\rho_b$	Bulk density of the bed (kg/m <sup>3</sup> )



# **Chapter 1**

## **General Introduction**

## 1.1 Introduction

Currently, fossil fuels provide almost 80% of the total energy [1]. Relying on single source, depleting the fossil fuel sources, increasing the global energy demand and environmental damages such as global warming and acid rain have forced modern society to seek for reliable and renewable alternative energy sources [2]. There are several types of renewable energy sources such as solar, wind, hydroelectric and biomass. Of these, biomass has received a great attention as it is the only renewable source that can convert into solid, liquid and gaseous fuels, and more importantly chemicals [3]. Biomass has ranked the fourth largest source of energy, providing around 14% of world primary energy [4]. The energy in biomass from plant matter originally comes from solar energy through the process known as photosynthesis [3]. Biomass can be converted into energy or chemicals through various pathways, e.g., physico-chemical, bio-chemical and thermo-chemical (Figure 1-1).

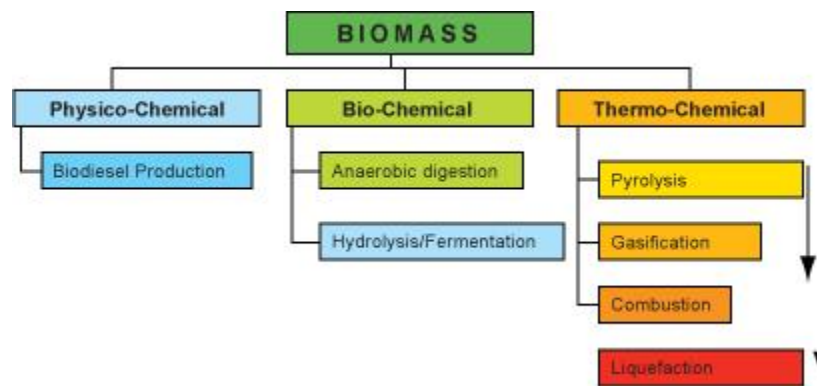


Figure 1-1 Biomass resource conversion processes [5].

Among all these three processes, thermochemical conversion is the fastest and most efficient one. Typical thermochemical conversion processes include combustion, gasification, pyrolysis and liquefaction, etc. [6].

Direct combustion of biomass is the most common method to generate heat and energy from biomass, for cooking, industries, homes or generation of electricity [7]. Among different biomass combustion technologies, fluidized bed combustion is one the most promising techniques as it can provide three T's rule for complete combustion: sufficiently high Temperature, strong Turbulence of the air-gas mixture and a long residence Time.

## 1.2 Fluidized Bed Combustion

Fluidized beds are widely used in various industrial processes, including fluid catalytic cracking (FCC), drying, coating on solid item, and solid fuel (such as biomass) conversion for generation of steam, electricity and hydrogen.

Many fluidized bed combustors have been constructed in US, Europe, and southeast of Asia using a wide range of biomass as fuel. Fluidized bed combustion has some advantages such as fuel flexibility (different shapes, sizes, and moisture contents), high efficiency, and low emission level. Fluidized bed boilers are used in pulp and paper mills and sawmills to produce high pressure steam and electric power, particularly in Europe and North America. Fluidized bed combustors can be classified into two main types, circulating fluidized bed combustor (CFBC) and bubbling fluidized bed combustor (BFBC) (Figure1-2). CFBC is preferred in large units especially for sulfur capturing in coal firing while BFBC uses simpler technologies in smaller units to burn biomass [8].

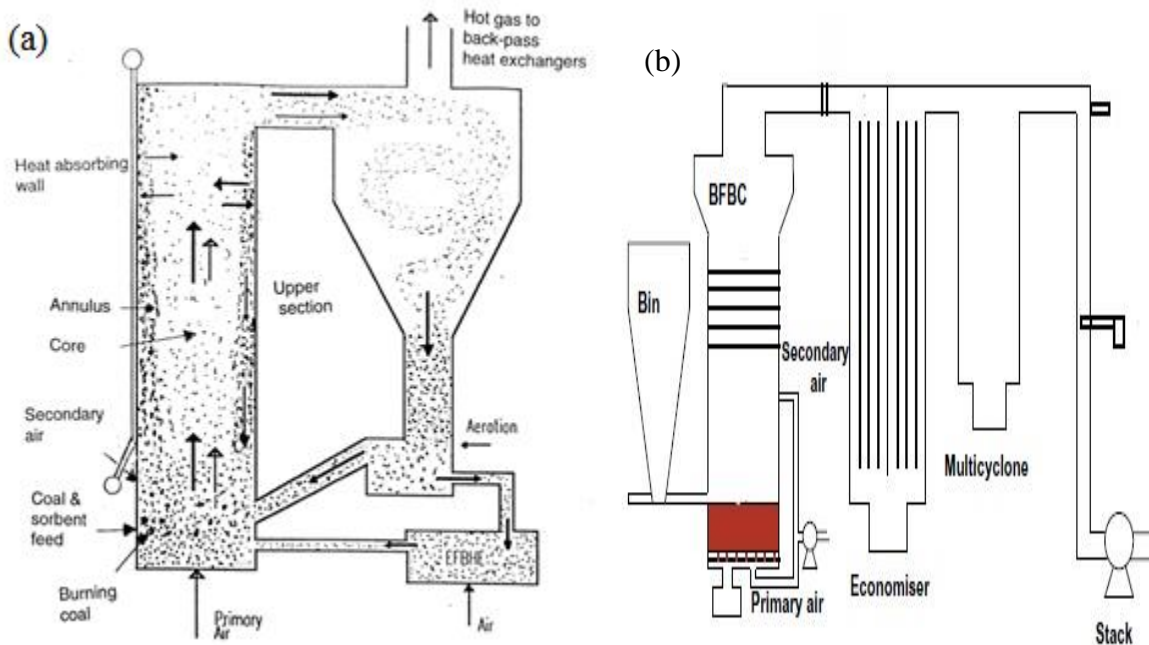


Figure 1-2 Circulating fluidized bed (a) and Bubbling fluidized bed (b) [9,10].

Bubbling fluidized bed (BFB) and chain stoker grate (Figure 1-3) are two main types of biomass boilers that are currently used in pulp and paper mills. Older industries mostly use stoker grate boilers while newer mills use bubbling fluidized boilers as they are larger and most efficient [11].

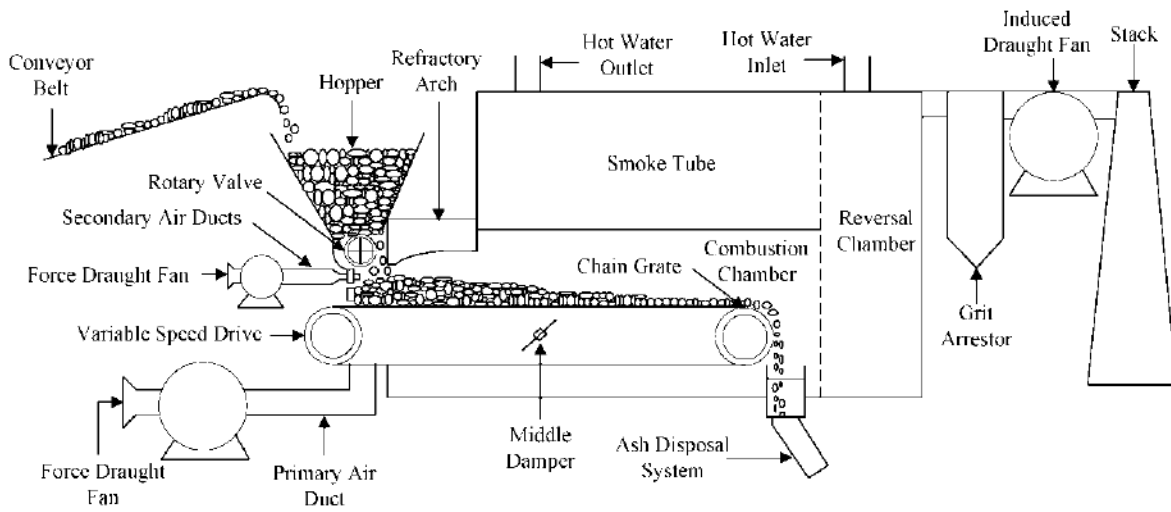


Figure 1-3 Chain stoker grate [12].

Despite all the advantages of fluidized bed combustion, there are some shortcomings such as sintering, deposition of ash particles and bed material agglomeration [13]. Bed material agglomeration is a major operational problem, as discussed in details in the following section.

### 1.3 Bed Agglomeration

Bed agglomeration is one of the major problems during the combustion of biomass which could cause partial or complete bed de-fluidization and as a result unscheduled plant shut down. Figure 1-2 shows the schematic mechanism of bed material agglomeration. When two or more particles stick together, they will lose their original weight and cannot be fluidized by the initial gas velocity that was chosen based on the original particle size.

Many researchers investigated the causes and mechanism of the bed material agglomeration [14–17]. Most of these researchers reached a common agreement that the main cause of the bed material agglomeration is the presence of low melting alkali compounds acting as a binder to form agglomerates. Biomass ash contains inorganic alkali compounds which can react with bed material, commonly silica sand, to form a low melting alkali silicate that would contribute to the formation of bed material agglomeration. Bed materials will be covered by low melting alkali silicate, during the fluidization coated bed materials collide with each other and stick together to form agglomerates. The formation of agglomerates can lead to either partial or complete de-fluidization.

Figure 1-4 shows the schematic of two possible mechanisms of agglomerate formation. The mechanism of agglomeration and factors affecting it will be discussed with more details in chapter 2 “literature review”.

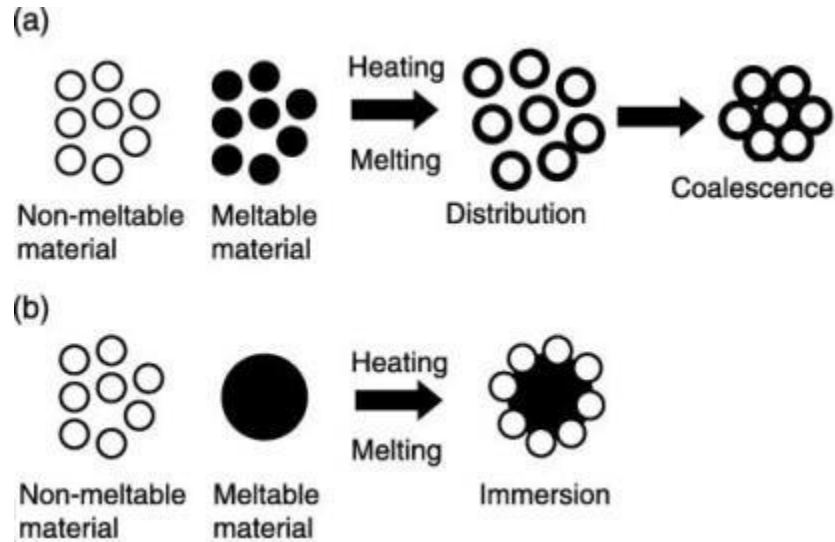


Figure 1-4 schematic of two possible mechanisms of agglomerate formation.

#### 1.4 Knowledge Gaps and Needs of Research

It is not known what is the minimum or critical amount of liquid (molten alkali compounds) required to agglomerate the bed material and cause de-fluidization of the bed, except for some research results obtained by our group based on cold/mild-temperature tests using model compounds. Therefore, the main objective of the present thesis work is to determine experimentally the critical amount of liquid required to agglomerate silica sand particles in a bubbling fluidized bed (BFB) leading to de-fluidization at higher temperatures. To simulate the real biomass combustion in BFB, various model systems have been employed, including hot BFB with KCl, and KCl-K<sub>2</sub>SO<sub>4</sub> eutectic compounds to simulate molten biomass ash in real biomass combustion. The results on bed material agglomeration behavior in fluidization of silica sand particles with KCl or KCl-K<sub>2</sub>SO<sub>4</sub> at elevated temperatures and effects of kaolin or aluminum sulfate additive are presented and discussed in this thesis. The second objective of this project is to examine the de-fluidization time for BFB combustion of corn stalk (with a high K, Mg, Ca-containing ash) with different bed materials operating at different superficial air velocities.

## 1.5 Thesis Objective

This research project is a part of a large NSERC CRD project titled “FUNDAMENTAL STUDIES OF DRYING, COMBUSTION AND ASH PROPERTIES OF BIOMASS, AND IMPACTS ON BOILER AND PULP AND PAPER MILL OPERATIONS”, led by The University of Toronto.

The main objective of this CRD project is to obtain fundamental data on drying, combustion and ash properties of biomass mixtures and to use this information to develop viable control strategies and new technologies to improve biomass boiler and mill operations.

This research project carried out by Western University includes 2 parts of studies. Part 1 includes Stage I and Stage II, Part 2 Stage III and Stage IV, as defined below:

- Stage I involving experiments in a cold BFB test rig using glycerol-water as the model system to simulate molten ash (the results were reported previously in a published paper by Monte, et al. [18]);
- Stage II using a hot BFB (heated to  $\sim 400^{\circ}\text{C}$ ) and a low melting point salt (KOH) to simulate molten ash (the results are reported in another recent publication by Montes et al. [19]);
- Stage III involving a hot BFB (heated up to  $800^{\circ}\text{C}$  electrically) with addition of different amounts of KCl,  $\text{K}_2\text{SO}_4$  and their eutectic mixture to simulate molten ash, and
- Stages IV involving a hot BFB (heated to  $\sim 800^{\circ}\text{C}$ ) with addition of different amount of agricultural residues (corn stalk) with high K contents.

Part 1 of this project (Stage 1 and Stage 2) has been already completed, and drawn the following key conclusions: in the fluidization systems studied the critical liquid amount is 0.2-0.5 wt% (in relation to the weight of bed material loaded) to cause bed material agglomeration and approx. 1wt% to cause severe channeling and very poor fluidization [18,19].

The research results for stages III and IV are presented in Chapters 3 and 4, respectively in this thesis.

## 1.6 Thesis Structure

This thesis consists of five chapters organized in the following manner:

Chapter 1 briefly describes the importance of renewable energies especially biomass, and introduces the available technologies for conversion of biomass to energy, in particular combustion of biomass and their problems. Finally, the research objectives and thesis structure are outlined.

Chapter 2 presents a summary of available literature studies on biomass energy conversion, with main focus on fluidized bed combustion. Agglomeration as the main operating problem in fluidized bed combustion, and factors affecting the formation of agglomerates and measures to prevent agglomeration are described.

Chapter 3 provides results and discussion from an investigation on critical amount of liquid for bed material agglomeration at high temperature (800°C) in a bubbling fluidized bed using KCl and K<sub>2</sub>SO<sub>4</sub> to simulate the molten ash. The effect of two additives, i.e., kaolin and aluminum sulfate on prevention of agglomeration were investigated.

Chapter 4 aims to examine the de-fluidization time for BFB combustion of corn stalk (with a high K, Mg, Ca-containing ash) with different bed materials operating at different superficial air velocities.

Chapter 5 presents the main conclusions drawn from the present research and suggests directions of future studies.

## 1.7 References

- [1] Saidur R, Abdelaziz E a., Demirbas a., Hossain MS, Mekhilef S. A review on biomass as a fuel for boilers. *Renew Sustain Energy Rev* 2011;15:2262–89. doi:10.1016/j.rser.2011.02.015.
- [2] Boström D, Grimm A, Boman C, Björnbom E, Öhman M. Influence of kaolin and calcite additives on ash transformations in small-scale combustion of oat. *Energy and Fuels* 2009;23:5184–90. doi:10.1021/ef900429f.
- [3] Demirbaş A. Biomass resource facilities and biomass conversion processing for fuels and chemicals. *Energy Convers Manag* 2001;42:1357–78. doi:10.1016/S0196-8904(00)00137-0.
- [4] Demirbas A. Potential applications of renewable energy sources, biomass combustion problems in boiler power systems and combustion related environmental issues. *Prog Energy Combust Sci* 2005;31:171–92. doi:10.1016/j.pecs.2005.02.002.
- [5] Frontier Associates. *Texas Renewable Energy Resource Assessment* 2008:1–196.
- [6] Zhang L, Xu C (Charles), Champagne P. Overview of recent advances in thermo-chemical conversion of biomass. *Energy Convers Manag* 2010;51:969–82. doi:10.1016/j.enconman.2009.11.038.
- [7] Nussbaumer T. *Combustion and Co-combustion of Biomass: Fundamentals, Technologies, and Primary Measures for Emission Reduction*. *Energy and Fuels* 2003;17:1510–21. doi:10.1021/ef030031q.
- [8] Hupa M. Ash-related issues in fluidized-bed combustion of biomasses: Recent research highlights. *Energy and Fuels* 2012;26:4–14. doi:10.1021/ef201169k.
- [9] Basu P. Combustion of coal in circulating fluidized-bed boilers: a review. *Chem Eng Sci* 1999;54:5547–57. doi:10.1016/S0009-2509(99)00285-7.
- [10] Fernández Llorente MJ, Escalada Cuadrado R, Murillo Laplaza JM, Carrasco García JE. Combustion in bubbling fluidised bed with bed material of limestone to reduce the biomass ash agglomeration and sintering. *Fuel* 2006;85:2081–92. doi:10.1016/j.fuel.2006.03.018.



- [11] Montes A. Factors Affecting Bed Agglomeration in Bubbling Fluidized Bed Biomass Boilers. Western University, 2014.
- [12] Thai SM, Wilcox SJ, Chong AZS, Ward J, Proctor A. Development of fuzzy based methodology to commission co-combustion of unprepared biomass on chain grate stoker fired boilers. *J Energy Inst* 2011;84:123–31. doi:10.1179/014426011X12968328625630.
- [13] Shimizu T, Han J, Choi S, Kim L, Kim H. Fluidized-Bed Combustion Characteristics of Cedar Pellets by Using an Alternative Bed Material. *Energy & Fuels* 2006;20:2737–42. doi:10.1021/ef0601723.
- [14] Brus E, Marcus O, Nordin A. Mechanisms of Bed Agglomeration during Fluidized-Bed Combustion of Biomass Fuels. *Energy & Fuels* 2005;1:825–32.
- [15] Chirone R, Miccio F, Scala F. Mechanism and prediction of bed agglomeration during fluidized bed combustion of a biomass fuel: Effect of the reactor scale. *Chem Eng J* 2006;123:71–80. doi:10.1016/j.cej.2006.07.004.
- [16] Bartels M, Lin W, Nijenhuis J, Kapteijn F, van Ommen JR. Agglomeration in fluidized beds at high temperatures: Mechanisms, detection and prevention. *Prog Energy Combust Sci* 2008;34:633–66. doi:10.1016/j.pecs.2008.04.002.
- [17] Skrifvars B, Ohman M, Nordin A, Hupa M. Predicting Bed Agglomeration Tendencies for Biomass Fuels Fired in FBC Boilers : A Comparison of Three Different Prediction Methods. *Energy & Fuels* 1999;13:359–63.
- [18] Montes A, Hamidi M, Briens C, Berruti F, Tran H, Xu C (Charles). Study on the critical amount of liquid for bed material agglomeration in a bubbling fluidized bed. *Powder Technol* 2015;284:437–42. doi:10.1016/j.powtec.2015.07.017.
- [19] Montes A, Ghiasi E, Tran H, Xu C (Charles). Study of bed materials agglomeration in a heated bubbling fluidized bed (BFB) using silica sand as the bed material and KOH to simulate molten ash. *Powder Technol* 2016;291:178–85. doi:10.1016/j.powtec.2015.12.030.

## **Chapter 2**

### **Literature Review**

This chapter introduces some general aspects of biomass, biomass conversion to energy and fluidization technology. Following a brief overview of mechanism of agglomeration, key factors that are believed to play a role in the formation of agglomerates are discussed.

## 2.1 Biomass

Biomass is an ancient source of energy that was utilized by mankind because of its availability and accessibility [1]. It is a renewable, carbon-neutral, and abundant source of energy, and is being considered as an alternative to fossil fuels for energy and chemical production [2]. The current production of biomass in the world is estimated to be around 146 billion metric tons a year [3], approx. 8 times the total energy consumption. Biomass is currently the fourth source of energy in the world, after petroleum, coal and natural gas. According to Oregon Department of Energy, biomass accounts for approximately 3% of the total primary energy in the United States (in 2008) (Figure 2-1). The annual biomass energy use reaches ~69 MTOE (million tons of oil equivalent) of energy in Europe in 2003 [4] .

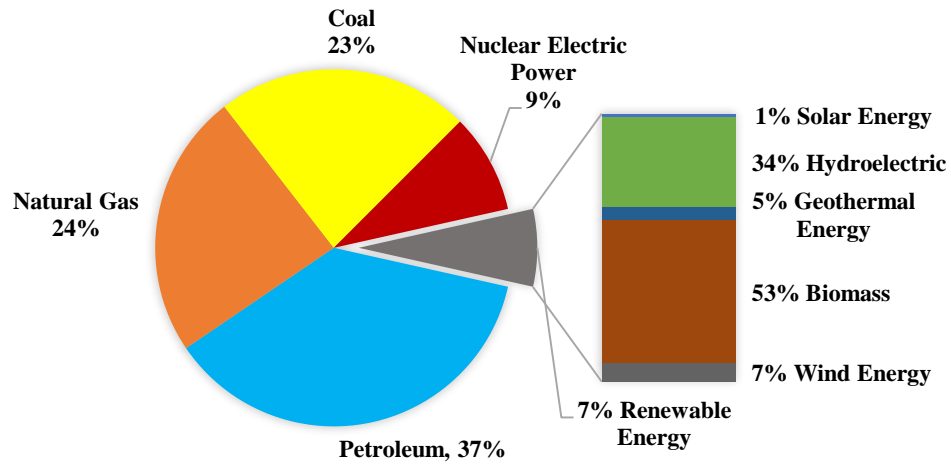


Figure 2-1 Consumption of energy in the United States in 2008 [1].

Usage of biomass as a source of energy has several advantages and disadvantages. The major advantages and disadvantages are summarized in Table 2-1.

Table 2-1 Major advantages and disadvantages of biomass energy.

<b>Advantages</b>	<b>Disadvantages</b>
<ul style="list-style-type: none"> <li>• Renewable and inexhaustible fuel source</li> <li>• Commonly low content of ash, C, S, N</li> <li>• It reduces environmental hazards</li> <li>• Capturing of some hazardous components by ash during combustion</li> <li>• Relatively cheap resource</li> <li>• It may generate additional coproducts that are valuable</li> </ul>	<ul style="list-style-type: none"> <li>• Commonly high contents of moisture, Cl, K, Na, Mn,</li> <li>• Low energy density</li> <li>• Odor, potential emission and leaching of hazardous components during disposal and heat treatment</li> <li>• Potential competition with food and feed production</li> <li>• Great harvesting, collection, transportation and storage cost</li> <li>• Many forms of biomass are available only seasonally</li> <li>• Perishable</li> </ul>

The most important sources of biomass are wood, wood wastes, agricultural crops and residues, municipal solid waste (MSW) and food processing wastes, etc. [5]. Biomasses are characterized based on the following parameters:

1. Structural analysis
2. Proximate analysis
3. Ultimate analysis
4. Ash analysis
5. Heating value

Structural analysis is to determine the constituents of biomass such as cellulose, hemicellulose and lignin. Structural analysis is particularly important in the development of methods for production of bio-fuels as well as for combustion [6,7]. Proximate analysis gives the percentages of volatile matter, moisture content, fixed carbon and ash contents. This analysis is essential in study of biomass combustion [8]. While ultimate analysis gives the major composition of biomass in weight percentage of carbon, hydrogen, oxygen, nitrogen and sulfur. Ash analysis provides the amount of inorganic material in biomass, either structural or extractable. Structural ash is inorganic material that is bound in the physical structure of the biomass, while extractable ash is inorganic material that can be removed/extracted physically such as by washing [9]. Biomass ash contents play an important role in the process of combustion due to some serious problems including fouling and slagging that are associated with the interaction of the molten ash and bed materials. Ash content and composition of biomass varies and depends on several factors such as weather conditions, soil quality, fertilizer, nutrients and varies depending on the time of harvesting. Heating value of

biomass is the amount of heat produced from the combustion of the fuel and it is measured as a unit of energy per unit mass or volume of fuel. Heating value divided in two types, lower heating value (LHV) and higher heating value (HHV), where LHV is determined by combustion of the fuel completely to form CO<sub>2</sub> and H<sub>2</sub>O vapor, and HHV is determined by combustion of the fuel completely to form CO<sub>2</sub> and condensed H<sub>2</sub>O liquid.

## **2.2 Conversion of Biomass to Energy**

The stored energy in biomass can be released and converted to useful energy via several processes. The moisture content and ash content of the biomass are among the most important parameters that shall be considered in the selection of an appropriate conversion process [1,10]. Usually, thermochemical conversion, biochemical conversion and mechanical extraction are the three major methods used for the conversion of biomass to useful energy, and chemicals in different forms (solid, liquid and gas) (Figure 2-2). Biomass with high water content is preferred for biochemical conversion through fermentation and digestion to gaseous and liquid fuels. Mechanical extraction is defined as mechanical pressing to remove the majority of oil from seeds and plants parts. As the mechanical extraction does not remove all the oil, so chemical extraction is also applied to remove the remaining oil. Thermochemical conversion processes include torrefaction, combustion, gasification, pyrolysis (and liquefaction) of biomass to generate fuels and chemicals. Biomass with low moisture content and high energy density is normally preferable for the thermochemical conversion processes.

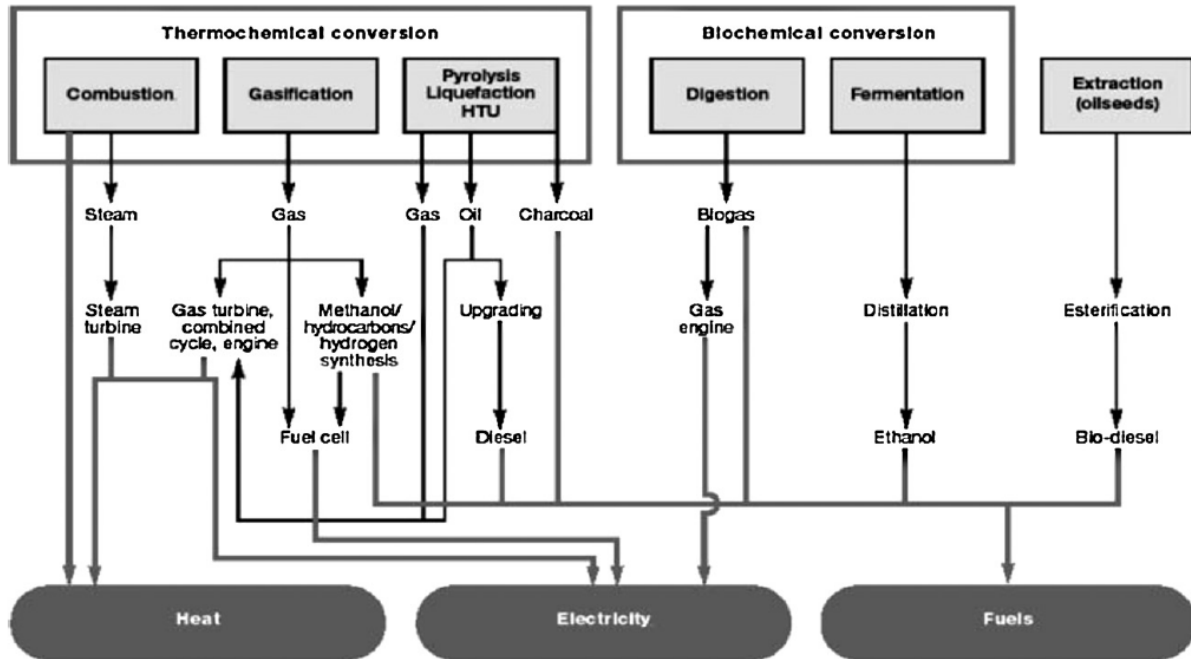


Figure 2-2 Main conversion options for biomass to secondary energy carriers, reprinted with permission from ref. [11]. Copyright (2006) Springer.

### 2.2.1 Gasification

Gasification was used for the first time in the early 1800s to convert coal to gas and attracted major attention during the energy crisis of the 1970s to produce syngas as a source of clean energy for small industries [12]. There are two types of gasification depending on the types of gasifying agents, i.e., air-blown gasification and steam-gasification. Air-blown gasification is an energy self-sufficient partial oxidation process which converts biomass to gaseous fuel rich in CO and CO<sub>2</sub>, while the steam-gasification is an endothermic process to produce H<sub>2</sub> and CO rich gaseous products. In gasification, biomass converts to carbon monoxide, hydrogen, methane, carbon dioxide and water at high temperature (>700 °C) in presence of oxygen or/and steam [13,14]. The formed gases known as syngas and can be used as fuel for internal combustion engines, as a substitute of furnace oil, or can be a feedstock for the production of liquid transportation fuel and chemicals through F-T synthesis. Gasification technologies can be further classified based on type of reactor and pressure, in addition to the gasifying agents as discussed above [12,15].

### 2.2.2 Pyrolysis

Pyrolysis is a thermal decomposition of organic matter at elevated temperatures in the absence of oxygen [16]. In practice, it is not possible to achieve a completely oxygen-free atmosphere as oxygen is present in any biomass, so some oxidation reactions may also occur during the process. Organic materials are transformed in pyrolysis into different products, i.e., gases, liquid, and a solid residue (char) containing mainly carbon and ash. Different proportion of pyrolytic products can be produced by controlling and adjusting the operating conditions, e.g., temperature, pressure, residence time, pyrolysis method and type of biomass. Pyrolysis of biomass could be divided into four stages including removal of moisture (dehydration), decomposition of hemicellulose, cellulose and lignin. Each of these steps proceeds over different temperature ranges [17]. Pyrolysis can be divided into three categories according to the process conditions; i.e. slow pyrolysis, intermediate pyrolysis and fast pyrolysis [18,19]. The conditions of each process are shown in Table 2-2. Slow pyrolysis is carried out at a low temperature for a long vapor residence time which leads to produce more charcoal. The intermediate pyrolysis is carried out at a moderate temperature and residence time. In contrast, fast pyrolysis is conducted at a high temperature, a short residence time, and in the absence of oxygen to produce more liquid fuels [20]. Increasing attention is now being paid on fast pyrolysis process, as the obtained liquid product, fast pyrolysis oil, could be used as fuels and chemicals [18]. Fast pyrolysis process is significantly influenced by factors such as mass and heat transfer, as well as chemical reaction kinetics [16,20].

Table 2-2 Different modes of pyrolysis of wood [18,19].

Types of pyrolysis	Residence Time	Temperature (°C)	Yield (%)		
			Liquid	Char	Gas
Slow	Hours/Days	400	30	35	35
Intermediate	10-30s	500	50	25	25
Fast	~1s	500	75	12	13

### 2.2.3 Combustion

Combustion is simple process in which a flammable material burns directly in the presence of air or oxygen to produce heat. Direct burning of biomass is an ancient process used for millennia for production of heat and energy from biomass. The generated heat has been used for cooking, industrial processes, heating homes or converting to the other kinds of energy like electricity. The

basic reactions of combustion are oxidation of C and H to form carbon dioxide and water. Combustion of biomass, although being ancient, still requires improvement in combustion efficiency, emissions and cost reduction to be a reliable substitute for fossil fuels. Besides C, H and O, there are some undesired elements such as N, K and Cl in biomass that are sources of NO<sub>x</sub> emission and KCl – causing operating problems (agglomeration and fouling) [23].

When compared to fossil fuel-fired boilers, biomass boilers emit a larger amount of NO<sub>x</sub>. Several options have been proposed to reduce the emission of NO<sub>x</sub> during biomass combustion, such as (1) the usage of native wood owing to its low contents of nitrogen and ash, and (2) co-firing of biomass and another fuel (such as coal) to reduce the NO<sub>x</sub> emission by providing lower combustion temperature [24]. For large-scale industrial applications, biomass combustion technologies include pulverized bed combustion, fixed bed combustion and fluidized bed combustion. Among these technologies, fluidized bed combustion is widely adopted for burning biomass even for the low quality of biomass with high ash content and low heating value [25].

### **2.3 Fluidization and Fluidized Bed**

Fluidization is a process in which the solid bed materials can behave as a fluid by passing the gas or liquid upward through the bed. Usually, fluidization is applied in industries for two types of processes that require rapid heat and mass transfer in the process [26]:

- 1) Physical processes, such as drying, mixing of particles.
- 2) Chemical processes, such as fluid catalytic cracking (FCC), solid fuel conversion and gas-solid reactions.

Typically, a fluidized bed reactor involves a cylindrical column, filled with solid particles as heat-transfer carriers or catalysts, and equipped with an air distributor at the bottom and a cyclone at the top to remove/recycle the solid fines from the vented fluidizing gas. The velocity of fluid must be sufficient to fluidize the particles in the column. With increasing the velocity of the fluid, different fluidization regimes can be obtained, as illustrated in Figure 2-3.



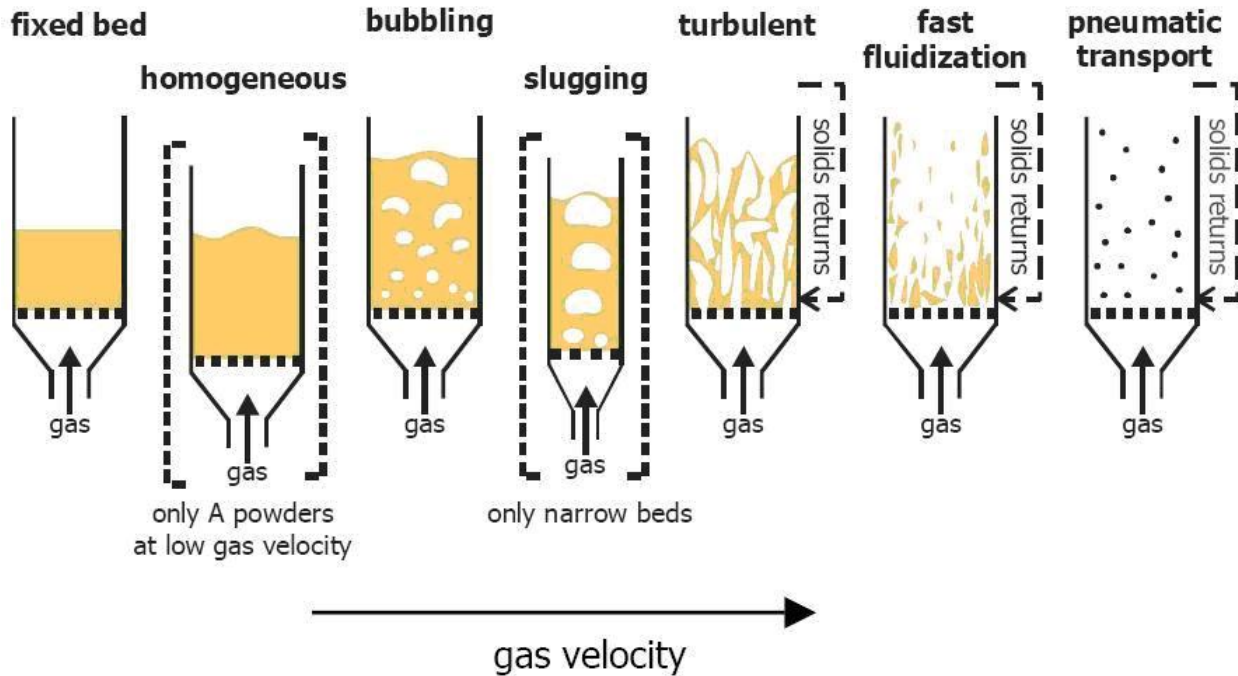


Figure 2-3 Fluidization regimes [27].

### 2.3.1 Minimum Fluidization Velocity

The minimum fluidization velocity ( $U_{mf}$ ) (“incipient fluidization velocity”) is the superficial gas velocity ( $V_g$ ) that can suspend/fluidize the solid particles in the bed. At this point the bed material behaves as a liquid. The minimum fluidization velocity depends upon a number of factors, such as, particle density, particles size, particles shape, viscosity and density of fluid, temperature and pressure.  $U_{mf}$  can be determined by using some empirical correlations based on the famous Ergun’s equation and more accurately by experiments.

#### 2.3.1.1 Empirical Calculation of $U_{mf}$

Leva [28] proposed a correlation in 1959 which is most commonly used in industries. It works well when  $Re_{mf} < 30$  ( $Re_{mf}$  is the Reynold number at minimum fluidization condition) for relatively small particles:

$$U_{mf} = \frac{7.169 \times 10^{-4} g d_p^{1.82} (\rho_p - \rho_g)^{0.94}}{\rho_g^{0.06} \mu_g^{0.88}} \quad (2-1)$$

where  $\rho_g$  is the gas density,  $\mu_g$  is the gas viscosity,  $\rho_p$  is the particle density,  $d_p$  is the mean diameter and  $g$  is gravity.

### 2.3.1.2 Theoretical Calculation of $U_{mf}$

At minimum fluidization, the bed is at boundary between fixed and fluidized condition. The frictional bed pressure drop ( $\Delta P_{fbed}$ ) can be predicted by Ergun's equation for a fixed bed with height  $H$ :

$$-\frac{\Delta P_{fbed}}{H_{bed}} = 150\mu_g V_g \frac{(1-\varepsilon)^2}{\varepsilon^3(\Phi d_p)^2} + 1.75\rho_g V_g^2 \frac{(1-\varepsilon)}{\varepsilon^3(\Phi d_p)} \quad (2-2)$$

where  $V_g$  is the superficial gas velocity,  $\mu_g$  is the viscosity of the gas,  $\varepsilon$  is the voidage,  $\Phi$  is the sphericity of the particles,  $d_p$  is the mean diameter and  $\rho_g$  is the gas density.

On the other hand, the fluidization occurs when the frictional bed pressure drop becomes equal to the weight of the bed particles per unit area

$$\Delta P_{fbed} = \frac{W_{bedparticles}}{A} = gH_{bed}(1-\varepsilon_{mf})(\rho_p - \rho_g) \quad (2-3)$$

where  $W_{bedparticles}$  is the net weight of particles,  $A$  is the bed cross sectional area and  $\varepsilon_{mf}$  is the bed voidage at the minimum fluidization condition.

$U_{mf}$  can then be calculated by combining Equations (2-2) and (2-3) for  $\Delta P_{bed}$ :

$$\frac{d_p^3 \rho_g (\rho_s - \rho_g) g}{\mu_g^2} = \frac{1.75}{\varepsilon_{mf}^3 \phi_s} \left( \frac{d_p U_{mf} \rho_g}{\mu_g} \right)^2 + \frac{150(1-\varepsilon_{mf})}{\varepsilon_{mf}^3 \phi_s^2} \left( \frac{d_p U_{mf} \rho_g}{\mu_g} \right) \quad (2-4)$$

Equation (2-4) can be simplified to:

$$A_r = \frac{150(1-\varepsilon_{mf})}{\varepsilon_{mf}^3 \phi_s^2} Re_{mf} + \frac{1.75}{\varepsilon_{mf}^3 \phi_s} Re_{mf}^2 \quad (2-5)$$

where Archimides number ( $A_r$ ) and Reynolds number ( $Re_{mf}$ ) are:

$$Re_{mf} = \left( \frac{d_p U_{mf} \rho_g}{\mu_g} \right) \quad (2-6)$$

$$A_r = \frac{d_p \rho_g (\rho_s - \rho_g) g}{\mu_g^2} \quad (2-7)$$

The solution of Equation (2-5) is

$$\text{Re}_{mf} = (C_1 + C_2 A_r)^{0.5} - C_1 \quad (2-8)$$

with

$$C_1 = 42.86 \frac{(1 - \varepsilon_{mf})}{\phi_s} \quad (2-9)$$

$$C_2 = 0.5714 \phi_s \varepsilon_{mf}^3 \quad (2-10)$$

Table 2-3 Different values for  $C_1$  and  $C_2$ .

Reference	$C_1$	$C_2$
Wen and Yu (1966)	33.7	0.0408
Richardson & St Jeronimo (1971)	25.7	0.0365
Thonglimp et al. (1894)	31.6	0.0425

Thus, the minimum fluidization velocity can be found:

- 1) If  $\phi_s$  and  $\varepsilon_{mf}$  are known,  $\text{Re}_{mf}$  and  $U_{mf}$  can be calculated directly.
- 2) If  $\phi_s$  and  $\varepsilon_{mf}$  are not known (unfortunately the usual case), correlated values for  $C_1$  and  $C_2$  must be used.

### 2.3.2 Experimental approach

The pressure drop method can be used to determine the  $U_{mf}$  by plotting  $\Delta P$  vs  $V_g$  curve. This method involves the use of data on variation in bed pressure drop across a bed of particulate solids (particle size not too small) with fluid velocity [26].

In a well-settled bed, the bed voidage ( $\varepsilon$ ) is relatively low so, the pressure drop obtained by passing the gas through the bed is shown by line A-B in Figure 2-4. The pressure drop usually reaches a maximum  $\Delta P_{\max}$  (point B), which is higher than the static pressure drop of the bed, as the fluid velocity is further increased from this point (B) the bed expands and the porosity increases from

$\epsilon_0$  to  $\epsilon_{mf}$ , resulting in a decrease in pressure drop to a value which is independent of fluid velocity (static pressure drop of the bed). At point B, the fixed bed starts to change to the fluidized bed until point C. The bed pressure drop beyond the point C remains unchanged even by increasing the superficial gas velocity ( $V_g$ ). By decreasing the upward flow of gas and retracing the path, as it shown in Figure 2-4 by line DCG. It shows that the pressure drop was less when the gas flow decreased in compare with when the upward flow gas increased. Point C is the transition point between a fixed bed and fluidized bed. The velocity corresponding to this transition point, determined graphically, is the minimum fluidization velocity ( $U_{mf}$ ) [29].

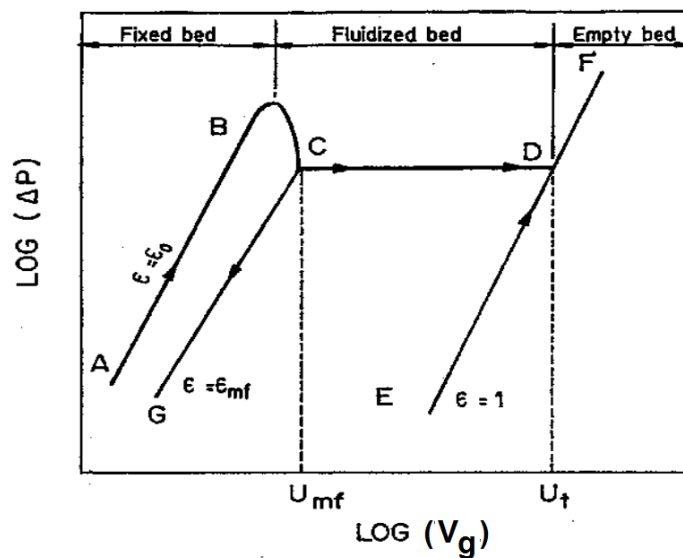


Figure 2-4 variation in bed pressure drop ( $\Delta P$ ) with superficial velocity ( $V_g$ ) [29].

### 2.3.3 Fluidized Bed Combustor

Fluidized-bed combustion (FBC) is considered as the most suitable technology for burning different types of biomass. Two most popular modes of fluidized bed combustion installations are circulating fluidized-bed combustion (CFBC) and bubbling fluidized-bed combustion (BFBC). CFBC is mainly used in large scale burning of coal and BFBC has a simpler reactor configuration so is commonly used for biomass combustion [30].

### 2.3.4 Scope of Fluidized Bed Combustor

Due to the many advantages, fluidized beds are used for a variety of applications. Some important advantages of fluidized bed biomass boilers include high combustion efficiency, fuel flexibility,

lower pollutant (particularly  $\text{NO}_x$ ) emission, and homogenous temperature distribution. In spite of the advantages of fluidized bed combustion of biomass, there are some issues in the process such as corrosion, fouling, and agglomeration. Sulfur and chlorine in the biomass that release during the combustion are the main routes of corrosion. The corrosion mechanism in a biomass combustor or boiler can be divided into three types: (1) gas species corrosion (2) solid phase corrosion (3) molten phase corrosion. Fouling or the formation of ash deposits on the surface of heat transfer equipment leads to falling of the thermal efficiency of biomass boilers.

#### 2.4 Bed Material Agglomeration and De-fluidization

Agglomeration is the most important operating problem encountered in fluidized bed biomass combustors. It causes partial or complete de-fluidization, leading to unscheduled plant shut downs [31]. Figure 2-5 shows a schematic mechanism of the formation of agglomerates. When two or more small particles stick together, they form bigger particles, which will no longer be able to fluidize with the same gas velocity [32]. The formation of a sticky molten ash layer around the bed material is the main cause of agglomerate formation. In addition, the reactions of alkali compounds that are present in the ash and bed material at high temperature may lead to formation of low melting-point compounds that might contribute to the bed material agglomeration [32,33].

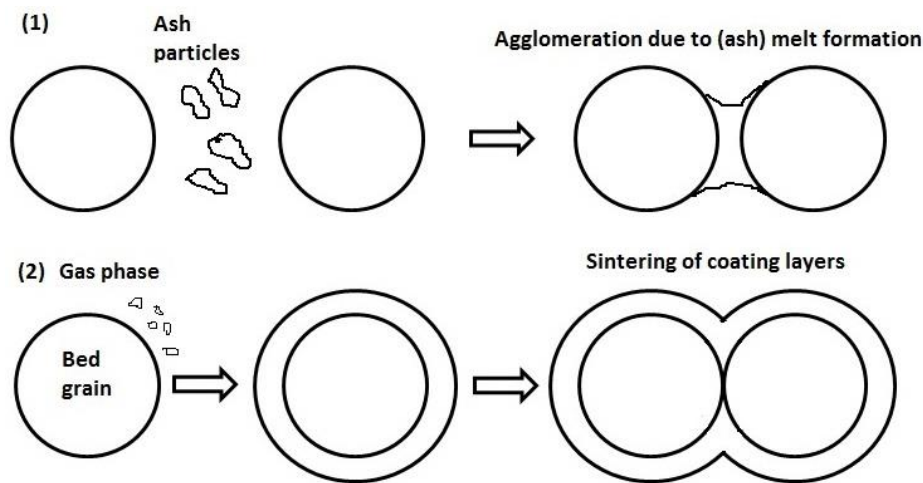


Figure 2-5 Schematic mechanism of formation of agglomerates (1) Coating-induced mechanism and (2) melt induced mechanism [34].

The presence of inorganic alkali elements such as K, Na and Ca in the biomass is mainly responsible for the formation of agglomeration of the bed particles [35]. Figure 2-6 shows the

effects of alkali melt compounds (potassium) in the agglomeration process with silica sand particles in a fluidized bed.

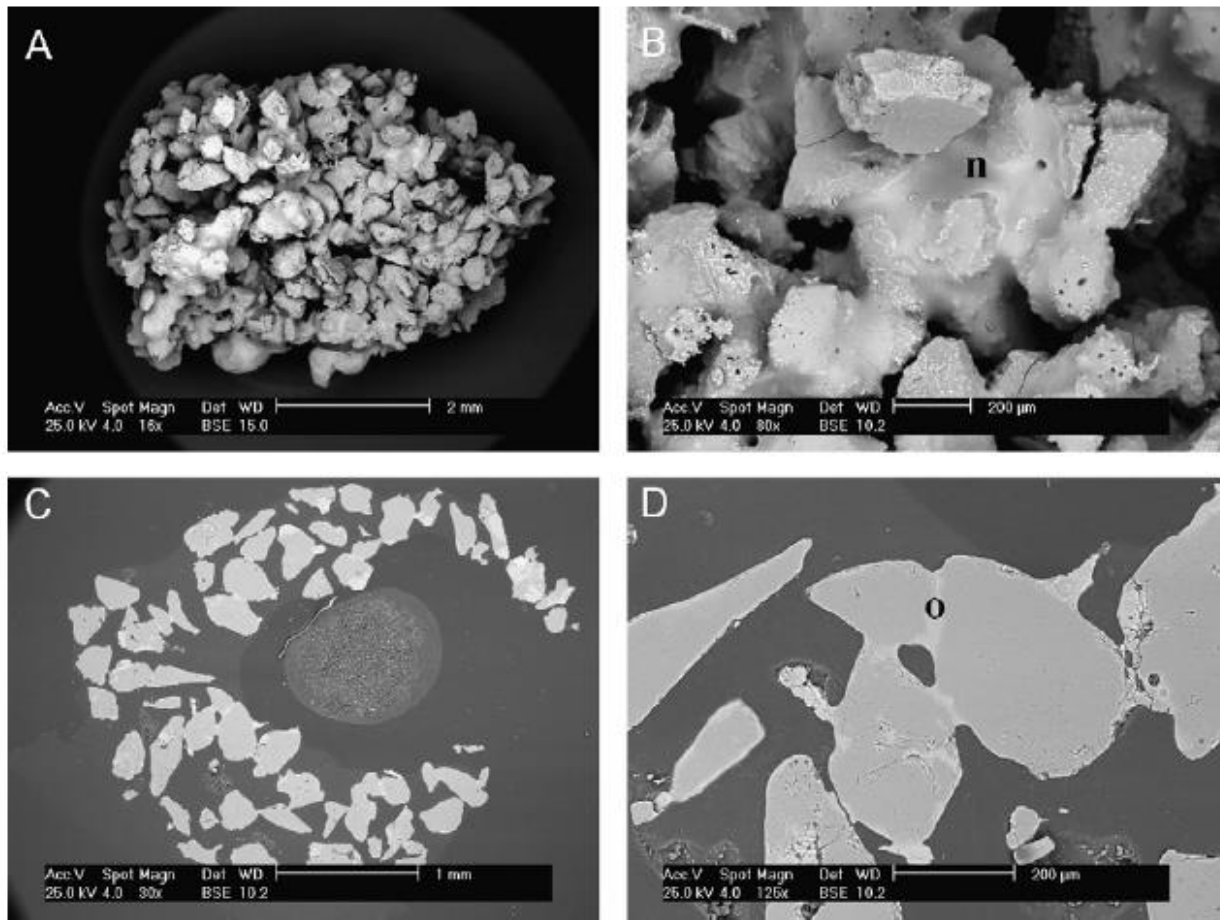


Figure 2-6 SEM micrographs at different magnifications of a typical agglomerate sample (A), details of the external surface (B), cross-section of an agglomerate (C), and details of the agglomerates cross-section (D). Pine seed shells  $T= 850^{\circ}\text{C}$ ,  $d_p=212\text{-}400\ \mu\text{m}$ , reprinted with permission from ref. [36].

Copyright (2008) Elsevier.

A comprehensive study was conducted by Montes et al. [37,38] to determine the critical amount of liquid which would cause severe bed agglomeration and de-fluidization in a lab scale cold and high temperature bubbling fluidized bed (BFB). In a cold BFB test, various amount of glycerol-water (30%v/v) solutions were injected to the bed to simulate molten ash in real biomass boiler. It was found the critical liquid amount resulting in bed agglomeration and sever channeling/de-fluidization were 0.2wt% and 0.7wt%, respectively. Furthermore, at elevated temperature ( $400^{\circ}\text{C}$ ),

KOH was used to simulate the molten ash. The results revealed that 0.5wt% and 0.8wt% were the critical amount of liquid that initiate the de-fluidization in BFB at  $3.9 U_{mf}$  and  $5.9 U_{mf}$ , respectively.

Many factors including type of biomass, nature of bed material, air velocity, operating conditions and additives can affect the formation of agglomerates in the bed.

#### **2.4.1 Effects of Type of Biomass**

Characteristics of biomass depend on the type of plant and the growth conditions. Biomasses with a larger amount of K are most problematic during the combustion due to the higher potential of bed material agglomeration. Several studies have been reported on the effect of different fuel types on the formation of agglomerates [39–42]. For example, Grimm et al. [31] conducted a study on the influence of four different biomass fuels on bed agglomeration in a bench scale bubbling fluidized-bed reactor. The used biomass fuels in this study included willow, logging residues, wheat straw, and wheat distiller's dried grain with solubles (wheat DDGS). It was found that the content of potassium had a pronounced effect on the de-fluidization temperature. Among these fuels, wheat straw consists of the higher amount of K with the lowest initial de-fluidization temperature at 750°C, and in contrast, logging residues exhibited the highest initial de-fluidization temperature approximately at 1060°C for both bed materials (olivine and silica sand). Both DDGS (rich in K and Mg) and wheat straw (rich in Si and K) demonstrated similar bed agglomeration tendency regardless of the type of bed materials.

Chaivatamaset et al. [32] studied the effects of biomass ash compositions and the operating temperature on the de-fluidization time. Two different types of biomass, i.e. palm shell and corncob were examined in a laboratory scale fluidized bed combustor using silica sand as the bed material. The de-fluidization time reduced for both biomass fuels when the operating temperature increased from 800°C to 900°C. Under constant operating conditions, corncob showed a higher bed agglomeration tendency compared to palm shell, which was attributed to the higher content of K in corncob ash. Fernandez Llorente et al. [43] studied the effect of various biomass fuels such as brassica, thistle and almond shell on initial de-fluidization temperature (IDT) in oxidising atmosphere using limestone as the bed material. The IDT could be used as a factor to predict the temperature of agglomeration and sintering in a fluidized bed combustor. The results indicated that the lowest value of IDT at 740°C was observed in the combustion of almond shell containing the highest potassium content (31wt%), whereas thistle showed the highest IDT at above 1400°C. Brus

et al. [44] investigated the mechanism of bed agglomeration during the fluidized bed combustion of five different biomass fuels including bark, reed canary grass, peat, olive residues, and straw in a bench-scale system. The fuel characteristics showed that bark, olive residues and peat contain high percentages of Ca in ash (39, 18 and 24wt%, respectively) while the percentage of K is much dominant in olive residue-ash (18wt%) and straw-ash (25wt%). It was observed that an ash-layer formed around the bed material during the combustion of all fuels except straw. In the case of olive residues and bark, the main compound of the formed layer was potassium calcium silicates. The layer formed with olive residues contains mainly potassium and silicon with small amount of calcium and magnesium. However, the ash layer from bark mainly consists of potassium, calcium and silicon. In another study, the initial agglomeration temperatures of four different agricultural residues, i.e., rice husk, bagasse, cane trash and olive flesh, were examined in a fluidized bed for combustion or gasification of these feedstocks [45]. The initial de-fluidization temperatures of all biomass fuels were lower than the predicted values from the ASTM standard ash fusion test. The initial agglomeration temperature of rice husk and bagasse were reported to be more than 1000°C, but cane trash and olive flesh have higher agglomeration tendency leading to a lower de-fluidization temperature. In addition, when lime was used as a bed material instead of silica sand, the de-fluidization happened at a higher temperature. Accordingly, rice husk and bagasse with a higher agglomeration temperature are more suitable biomass feedstocks for fluidized-bed biomass combustors.

Fryda et al. [46] characterized the agglomeration tendency of three biomass fuels in an atmospheric lab-scale fluidized bed using silica sand bed material. Table 2-4 shows the ash composition of giant reed, sweet sorghum and olive bagasse. The potassium content of giant reed (30wt%) and sweet sorghum bagasse (31.6wt%) are relatively higher than that of olive bagasse (25.8wt%), which accounts for their lower agglomeration temperatures. The de-fluidization occurred at approximately 785°C for giant reed and 810°C for sweet sorghum bagasse, while combustion of olive bagasse caused agglomeration at a higher temperature of 830°C. The XRD-EDS results reported by this literature study confirmed the presence of potassium compounds like  $K_2O \cdot SiO_2$  on the surface of bed materials after agglomerate formation.



Table 2-4 Ash analysis (wt%) of three biomass fuels [46].

Compound	Giant Reed	Sweet Soghum Bagasse	Olive Bagasse
SiO <sub>2</sub>	44.2	31.6	26.4
Al <sub>2</sub> O <sub>3</sub>	1.8	1.9	4.8
Fe <sub>2</sub> O <sub>3</sub>	0.9	0.4	7.3
CaO	1.8	10.9	27.1
MgO	2.8	6.3	4.7
TiO <sub>2</sub>	0.1	-	0.3
Na <sub>2</sub> O	0.5	0.2	-
K <sub>2</sub> O	30	31.6	25.8
P <sub>2</sub> O <sub>5</sub>	3.2	3.8	2.6
Cl	-	5.1	-
Others	14.7	8.2	1

A comprehensive study [43] has been reported on the ash sintering of nine different agricultural residues. Figure 2-7 presents the ash sintering and melting behaviours of these fuels. As shown in the Figure, wheat waste has the lowest sintering temperature at 700°C which could be due to its high contents of K, Cl, P and S in the ash, along with low contents of Ca and Si. In contrast, the highest ash sintering temperature was observed with bluegrass seed likely owing to the low concentration of K, P, Cl, S and Ca in the ash, and its large Si content (42g/kg dry fuel).

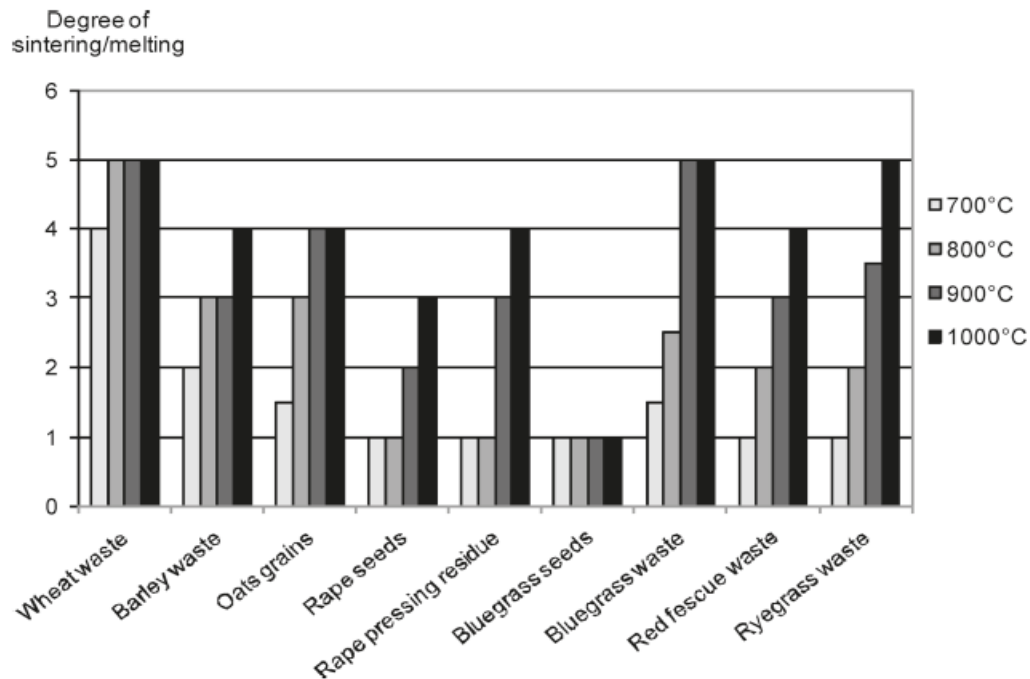


Figure 2-7 Degree of ash sintering for different biomass fuels at various temperatures [47].

### 2.4.2 Effects of Bed Materials

It is well known that silica sand is the most common bed material for biomass combustion in fluidized bed combustors due to its low price among other bed materials. However, silica sand is the most problematic type of bed material for the combustion of biomass fuels. Silica sand can react with alkali compounds from the biomass ashes, and form a low melting-point alkali silicate, which would accelerate the bed material agglomeration [48]. Many studies have been reported on the effects of types and particle size of bed materials on the bed material agglomeration [45,48,49].

Shimizu et al. [25] investigated effects of bed materials on the de-fluidization time and temperature during combustion of cedar pellet. In this study, silica sand and porous alumina were employed as bed materials (Table 2-5). The maximum operating temperature for the system with silica sand was 800°C and the system had to be stopped after 1hour operation due to the occurrence of severe agglomeration and de-fluidization of bed materials. Whereas, when alumina was used a bed material, the bed could be operated up to 950°C without apparent formation of agglomerates. The porous structure of alumina captured the volatile compounds released from the combustion of fuel pellets and most of the combustion took place in the reactor bed (dense phase). Therefore, the temperature of alumina bed was higher than that of the silica sand bed, with a higher temperature gradient between the bed material and the freeboard zone.

Table 2-5 Physical properties of alumina and silica sands [25].

Bed material	Specific surface area (m <sup>2</sup> /g)	Average diameter (µm)	Bulk density (kg/m <sup>3</sup> )	True density (kg/m <sup>3</sup> )
Alumina sand	214	500	780	3200
Silica sand	9.2	150	1223	2600

Grimm et al. [31] studied effects of two types of bed materials, i.e. olivine and quartz silica sand. The de-fluidization time for various biomass fuels including willow, logging residues, DDGS and wheat straw was reported. The initial de-fluidization temperatures of these systems are presented in Table 2-6. The results of this work demonstrated that the initial de-fluidization temperatures in silica sand bed were lower than those in the olivine bed. The elemental analysis of agglomerates showed that the composition of the inner layers is very similar to the bed material composition, while the outer layers of the agglomerates are strongly dependent on the fuel ash characteristics. For example, the agglomerates' inner layers formed in the silica sand bed contained mainly Si, K,

and Ca, and the inner layers of the agglomerates formed in the olivine bed made of primarily Mg, Si, and Ca.

Table 2-6 Initial de-fluidization temperature of various biomass fuels [30].

Fuel	Olivine bed (°C)	Silica bed (°C)
Willow	> 1060	900
Logging residues	> 1060	1030
DDGS	Total def. during comb. at ~ 800	Total def. during comb. at ~ 800
Wheat straw	740	750

The particle size of bed material is another important factor affecting bed agglomeration during the combustion of biomass fuels. Lin et al. [2] investigated the formation of agglomerates from two different sizes of silica sand particles, i.e. 0.275 and 0.328 mm. The influence of particle size on the agglomeration time at different operation temperatures is displayed in Figure 2-8. The results show that the de-fluidization time is shorter with the larger bed material size at similar operating conditions. This behaviour could be due to the lower specific outer surface area of the larger particles, making a thicker ash coating layer around them. Another reason could be that the relatively smaller value of  $V_g/U_{mf}$  for bigger particles compared with that of the finer particles leads to a poor mixing of the bed material, which consequently facilitate the formation of agglomerates. Chaivatamaset et al. also reported that the de-fluidization time is shorter with larger bed particles during the combustion of palm shell and corncob fuels in fluidized bed with silica sand bed materials [32].

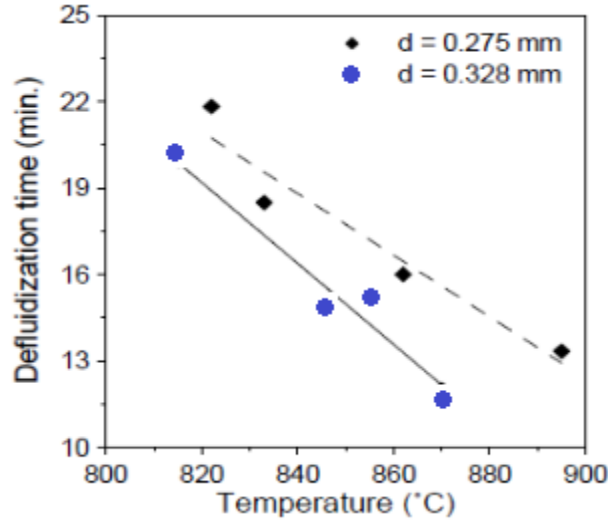


Figure 2-8 Effects of bed material size on the de-fluidization time at various temperatures, reprinted with permission from ref. [2]. Copyright (2003) Elsevier.

The influence of bed material size on agglomeration was also studied by Chunjiang et al. [48] for combustion of high-alkali straw. They adjusted the minimum fluidization velocity in accordance to the variation of the bed material particle size in order to evaluate the effects of bed particle size on bed de-fluidization. Figure 2-9 shows the de-fluidization time versus the bed material size. Again, the smaller particles demonstrated low tendency towards agglomeration due to better heat and mass transfer throughout the bed, reducing the extent of hot spot in the bed and hence the extent of ash melting, and eventually the tendency of agglomeration and de-fluidization.

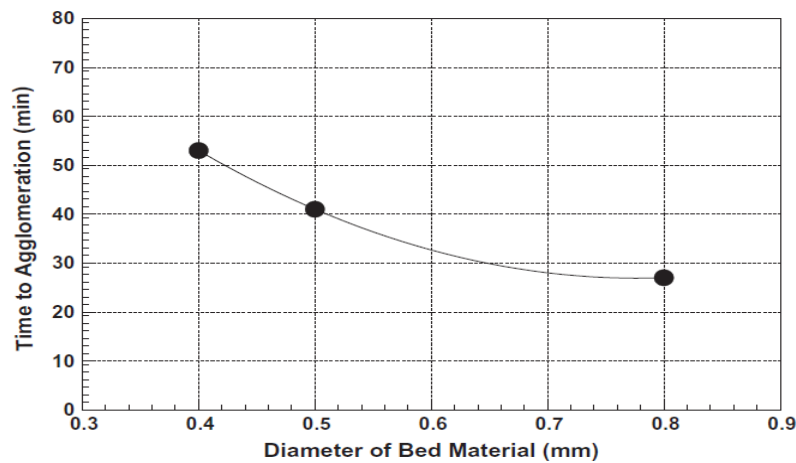


Figure 2-9 Influence of bed material size on de-fluidization time, reprinted with permission from ref. [48]. Copyright (2011) Elsevier.

### 2.4.3 Effects of Air Velocity

The ratio of superficial gas velocity to the minimum fluidization velocity,  $V_g/U_{mf}$ , is called the fluidization number. When the minimum fluidization velocity remains constant, the fluidization number increases with increasing the gas velocity. The effects of air velocity (or fluidization number) on the de-fluidization time for fluidized-bed combustion of biomass have been studied [50–52]. Rozainee et al. [51] reported that the optimum fluidization number for combustion of rice husk in a fluidized bed reactor was about 3.3. Further increasing the fluidization number would prevent the rice husk (with a light density) from being well mixed with the bed material. This results in pyrolysis of the biomass mainly in the freeboard. However, if the fluidization number is below the optimum value, the de-fluidization time becomes shorter due presumably to the poor mixing of the feedstock in the bed. Lin et al. [2] showed that increasing the fluidizing gas velocity extended the de-fluidization time due to better mixing of bed materials and forming bigger bubbles in the bed, which could break the formed agglomerates. In a study by Shiyuan et al. [53], the effects of gas velocity on de-fluidization time were investigated at 900°C. The obtained results are presented in Figure 2-10. The de-fluidization occurred at a longer time when the gas velocity increased. At a higher gas velocity, the forces of attrition and breaking acting on agglomerates increased, resulting in more fly ash particles entrained in the flue gas. Both would lead to retarding the de-fluidization time. Similar results were reported in other studies on fluidized bed combustion of biomass [32,48,54,55].

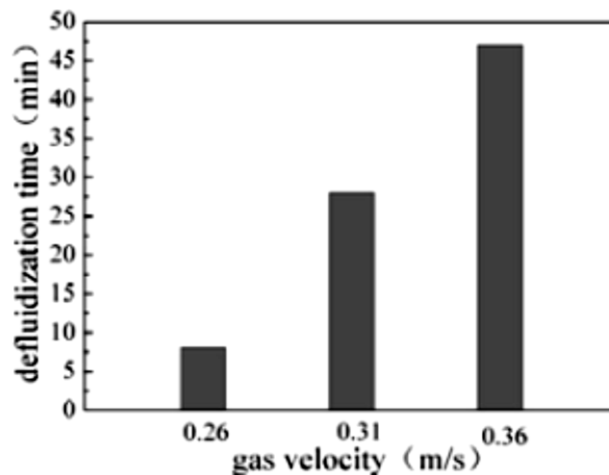


Figure 2-10 De-fluidization time as a function of gas velocity [53].

#### 2.4.4 Effects of Operating Temperature

Temperature is another pronounced factor which could be adjusted to control the formation of agglomerates in fluidized bed biomass boilers. As per Lin et al. [52], de-fluidization process was very sensitive to temperature. Their results showed that the formation of agglomerates was enhanced with increasing the operating temperature. At low temperatures, the agglomeration process was retarded with a longer de-fluidization time. In contrast, at high temperatures, alkali compounds in the ash of biomass could react with silica sand bed material and form low melting point eutectics quickly, which would cover the surface of bed particles and accelerate the agglomeration and de-fluidization. Chunjiang et al. [48] investigated the effects of operating temperature on agglomeration time for combustion of rice straw at temperatures ranging from 650°C to 900°C. Figure 2-11 displays the effects of temperature on agglomeration. As expected, the fastest de-fluidization happened at 900°C due to enhanced reactions between the alkali ash with bed material forming low melting point eutectics, which promotes the formation of agglomerates.

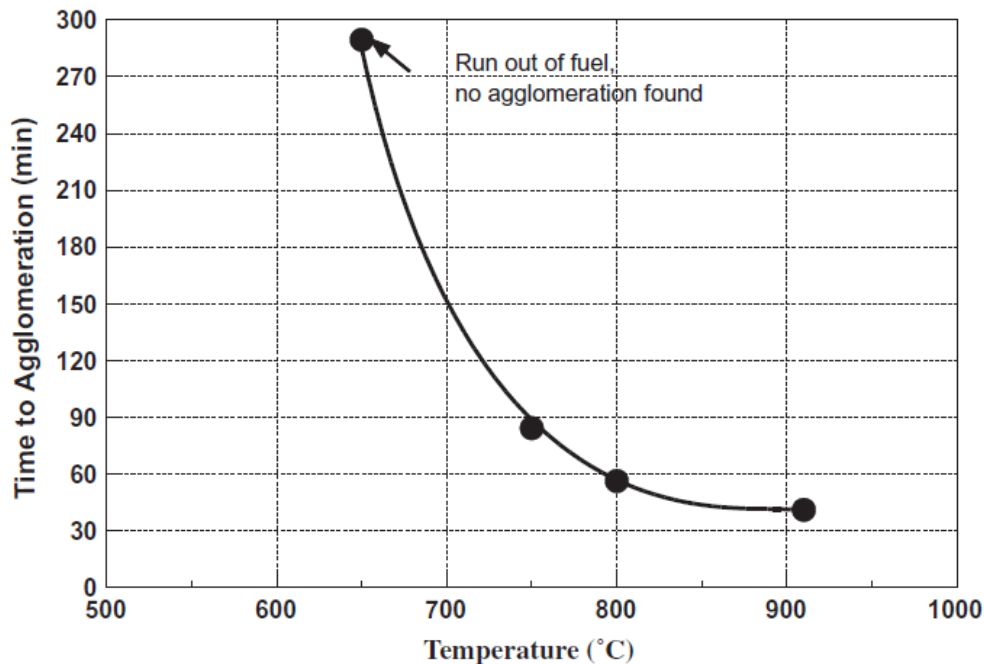


Figure 2-11 Influence of temperature on time of agglomeration, reprinted with permission from ref. [48]. Copyright (2011) Elsevier.

Similarly, Li et al. [53] reported the influence of the bed temperature on the de-fluidization time in fluidized bed combustion of wheat straw. The de-fluidization was achieved after around 14h and 0.2h at two different temperatures of 750°C and 950°C, respectively. The above results demonstrated negative effects of temperature on bed material agglomeration in fluidized bed combustors.

#### **2.4.5 Effects of Additives**

Additives refer to a group of minerals or chemicals that can retard formation of bed material agglomeration by increasing the melting temperature of ashes and capturing the problematic components. Use of additives is one of the most practical options to mitigate the ash related problems during biomass combustion. The commonly used additives can be categorized in four groups of materials based on their reactive components, including Al-silicate, sulphur, calcium and phosphorous based materials. Additives can mitigate the ash related problems through the following mechanisms:

- 1) Increasing the biomass ash melting temperature by introducing inert elements in ash residues,
- 2) Physical adsorption and elutriating troublesome ash species from combustion facilities,
- 3) Capturing problematic ash species via chemical adsorption and reactions,
- 4) Restraining biomass ash sintering via the diluting effects of the additives [56].

Potential additives for reducing biomass ash related problems have been investigated in many studies in the last decades [47,57,58].

Ohman et al. [59] investigated the role of kaolin in prevention of bed agglomeration during the fluidized bed combustion of wheat straw and bark with silica sand as the bed material. The used biomass fuels consisted of high content of potassium which could facilitate de-fluidization of the bed material. The addition of 10% w/w of kaolin to the bed material for two troublesome biomass fuels helped prevent bed agglomeration. The critical temperature for agglomeration increased from 740°C to 990°C for wheat straw and from 990°C to 1000°C for bark mixed with kaolin. It could be attributed to the capturing of potassium and formation the high melting point compounds with kaolin. The prevention effect of kaolin was much higher in wheat straw compared to that in bark

due to the higher content of potassium in wheat straw. In another investigation by Ohman et al. [60], effects of addition of kaolin and limestone were studied on the slagging of problematic and problem-free wood fuels. The authors demonstrated that, the addition of 5wt% of limestone (with respect to the bed material) to fluidized bed of silica sand with the problematic stemwood raw material resulted in complete prevention of slagging tendency probably due to the formation of high melting-point calcium-silicates and oxides. On the other hand, it was found that the addition of kaolin had a minor effect on reduction of agglomeration tendency of the problematic raw material, but surprisingly increased the slagging tendency of the problem-free stem wood. The possible reason is that with the problem-free biomass, kaolin reacted with the high melting-point Ca-Mg oxides to form low melting-point Ca-Al-K compounds, which hence accelerated the formation of agglomerates. As well known, the presence of KCl plays a major role in ash sintering and bed material agglomeration during combustion of biomass fuels. The addition of additives can also be effective for capturing the KCl and preventing the formation of agglomerates. The influence of two mineral additives, kaolin and zeolite 24A, on the capturing of KCl was investigated [61]. The results indicated that both zeolite and kaolin had high capacity for retention of KCl (Figure 2-12). As shown in the Figure, almost 50% and 40% of KCl can be captured by zeolite 24A and kaolin, respectively, at 1000°C. The KCl-capturing capacity of both additives is higher at 900°C than that at 1000°C.

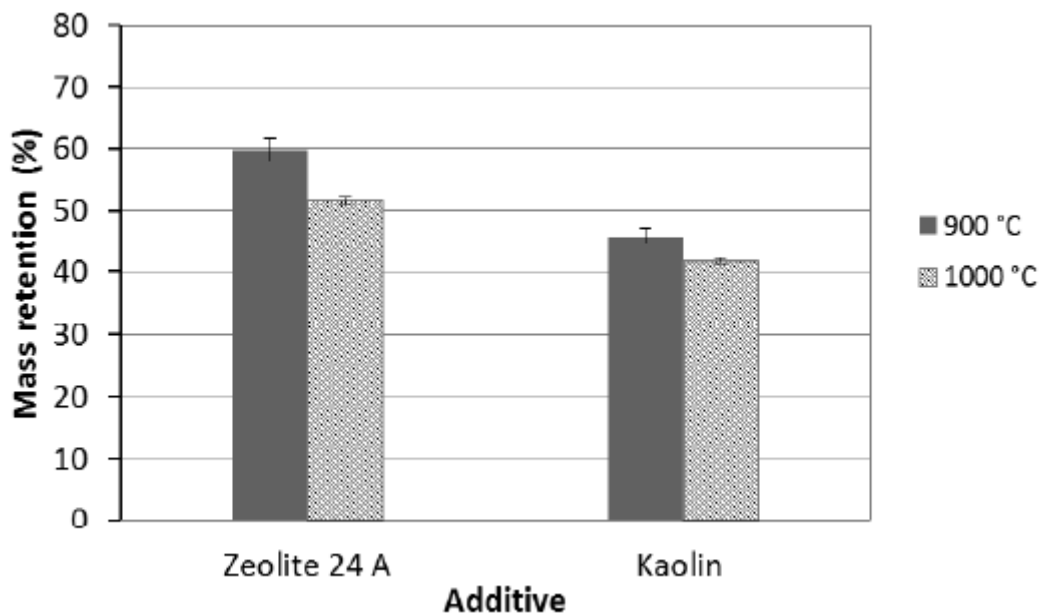
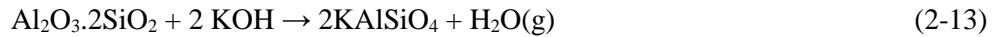
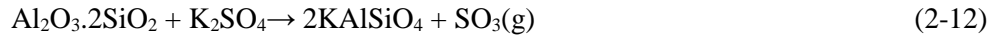


Figure 2-12 Retention of KCl within zeolite 24A and kaolin at various temperatures [61].



The mechanism of the interaction between vapor phase potassium species and kaolin was studied at temperatures ranging from 600°C to 1000°C by a surface ionization detector [21]. The possible mechanism proposed in the formation of the high melting compounds involves the following reactions:



These reactions show that different potassium species (KCl, K<sub>2</sub>SO<sub>4</sub> and KOH) can be captured by meta-kaolinite to form a Kalsilite which has high melting temperature at around 1500°C.

Peat was suggested as an innovative additive for reduction or prevention of the formation of agglomerates for fluidized bed combustion of forest biomass fuels [62]. For instance, the addition of 5wt% of the Rojnoret peat as a co-combustion biomass into the spruce bark prevented the agglomeration of the bed materials, and blending <30wt% of the peat fuels with bark could eliminate bed material agglomeration completely.

## 2.5 Summary

Fluidization has found wide applications in various industries such as petro-refinery, drying and combustion. Bubbling fluidized bed combustors are the most efficient technique for biomass combustion. Agglomeration is however the main concern in biomass combustion in fluidized bed combustors. During the combustion of biomass, alkali species (such as KCl, K<sub>2</sub>SO<sub>4</sub> and KOH, etc.) from biomass ash will react with bed material and form low melting-point alkali compounds, leading to forming a coated layer around bed materials. The melted coating layer on bed material may enhance the stickiness of particles leading to the formation of large agglomerates. Severe agglomeration of bed materials would cause de-fluidization and unscheduled shut-down of the combustor. The agglomeration formation can be affected by various parameters including operation temperature, type of bed material, particle size of bed materials and fluidizing gas velocity. With increasing the size of bed materials at a constant air velocity, the fluidized bed will face some severe issues such as agglomeration or complete de-fluidization.

However, the mechanism of agglomeration and in particular the roles of the liquid phase of molten alkali compound in the bed material agglomeration and de-fluidization are not well understood. Although there were some studies reported by the author's group [37,38] on the critical amount (about 1 wt%) of liquid phase in the bed material that would cause severe agglomeration and de-fluidization of the bed, these conclusions were based on the cold mode or mild-temperature (<400°C) BFB tests using liquid or solid model compounds to simulate molten alkali compounds in BFB combustion of biomass. More research is needed to elucidate the critical amount of liquid phase in BFB combustion of biomass, normally operating at temperatures 600-900°C. Thus, this thesis work focused on the behavior and mechanism of bed material agglomeration. Moreover, bed material agglomeration behavior and mechanism in BFB combustion of agricultural residues (corn stalk) in different bed materials were also investigated.

## 2.6 References

- [1] Saidur R, Abdelaziz E a., Demirbas a., Hossain MS, Mekhilef S. A review on biomass as a fuel for boilers. *Renew Sustain Energy Rev* 2011;15:2262–89. doi:10.1016/j.rser.2011.02.015.
- [2] Lin W, Dam-Johansen K, Frandsen F. Agglomeration in bio-fuel fired fluidized bed combustors. *Chem Eng J* 2003;96:171–85. doi:10.1016/j.cej.2003.08.008.
- [3] Demirbaş A. Biomass resource facilities and biomass conversion processing for fuels and chemicals. *Energy Convers Manag* 2001;42:1357–78. doi:10.1016/S0196-8904(00)00137-0.
- [4] Kopetz H. Biomass- a burning issue: Policies needed to spark the biomass heating market. *Refocus* 2007;8:52–4,56–8.
- [5] Demirbas MF, Balat M, Balat H. Potential contribution of biomass to the sustainable energy development. *Energy Convers Manag* 2009;50:1746–60. doi:10.1016/j.enconman.2009.03.013.
- [6] Zhang L, Xu C (Charles), Champagne P. Overview of recent advances in thermo-chemical conversion of biomass. *Energy Convers Manag* 2010;51:969–82. doi:10.1016/j.enconman.2009.11.038.
- [7] Abbasi T, Abbasi SA. Biomass energy and the environmental impacts associated with its production and utilization. *Renew Sustain Energy Rev* 2010;14:919–37. doi:10.1016/j.rser.2009.11.006.
- [8] García R, Pizarro C, Lavín AG, Bueno JL. Biomass proximate analysis using thermogravimetry. *Bioresour Technol* 2013;139:1–4. doi:10.1016/j.biortech.2013.03.197.
- [9] Sluiter JB, Ruiz RO, Scarlata CJ, Sluiter AD, Templeton DW. Compositional analysis of lignocellulosic feedstocks. 1. Review and description of methods. *J Agric Food Chem* 2010;58:9043–53. doi:10.1021/jf1008023.
- [10] Cpareda SC. *Introduction to Biomass Energy Conversions*. CRC Press, Taylor & Francis Group; 2013.
- [11] Faaij A. *Modern Biomass Conversion Technologies*. *Mitig Adapt Strateg Glob Chang*

2006;11:335–67.

- [12] Cheng J. Biomass to Renewable Energy Process. CRC Press; 2009.
- [13] McKendry P. Energy production from biomass (part 3): Gasification technologies. *Bioresour Technol* 2002;83:55–63. doi:10.1016/S0960-8524(01)00120-1.
- [14] Rajvanshi AK. Biomass Gasification. *Altern. Energy Agric. Second*, CRC Press; 1986, p. 83–102.
- [15] Ori A, Aznar MP. Biomass Gasification with Air in an Atmospheric Bubbling Fluidized Bed . Effect of Six Operational Variables on the Quality of 1996;5885:2110–20.
- [16] Balat M, Balat M, Kırtay E, Balat H. Main routes for the thermo-conversion of biomass into fuels and chemicals. Part 1: Pyrolysis systems. *Energy Convers Manag* 2009;50:3147–57. doi:10.1016/j.enconman.2009.08.014.
- [17] Mazlan MAF, Uemura Y, Osman NB, Yusup S. Fast pyrolysis of hardwood residues using a fixed bed drop-type pyrolyzer. *Energy Convers Manag* 2015;98:208–14. doi:10.1016/j.enconman.2015.03.102.
- [18] Bridgwater a. V. Review of fast pyrolysis of biomass and product upgrading. *Biomass and Bioenergy* 2012;38:68–94. doi:10.1016/j.biombioe.2011.01.048.
- [19] Bridgwater T. Biomass for energy. *J Sci Food Agric* 2006;86:1755–68. doi:10.1002/jsfa.2605.
- [20] Bridgwater a. V., Peacocke GVC. Fast pyrolysis processes for biomass. *Renew Sustain Energy Rev* 2000;4:1–73. doi:10.1016/S1364-0321(99)00007-6.
- [21] Tran KQ, Iisa K, Steenari BM, Lindqvist O. A kinetic study of gaseous alkali capture by kaolin in the fixed bed reactor equipped with an alkali detector. *Fuel* 2005;84:169–75. doi:10.1016/j.fuel.2004.08.019.
- [22] Shafizadeh F. Introduction to pyrolysis of biomass. *J Anal Appl Pyrolysis* 1982;3:283–305. doi:10.1016/0165-2370(82)80017-X.
- [23] Nussbaumer T. Combustion and Co-combustion of Biomass: Fundamentals, Technologies, and Primary Measures for Emission Reduction. *Energy and Fuels* 2003;17:1510–21. doi:10.1021/ef030031q.

- [24] Sami M, Annamalai K, Wooldridge M. Co-firing of coal and biomass fuel blends. *Prog Energy Combust Sci* 2001;27:171–214. doi:10.1016/S0360-1285(00)00020-4.
- [25] Shimizu T, Han J, Choi S, Kim L, Kim H. Fluidized-Bed Combustion Characteristics of Cedar Pellets by Using an Alternative Bed Material. *Energy & Fuels* 2006;20:2737–42. doi:10.1021/ef0601723.
- [26] Kunii D, Levenspiel O. *Fluidization engineering*. Wiley; 1969.
- [27] Ruud Van Ommen J., Ellis N. *JMBC/OSPT Course Particle Technology*. 2010.
- [28] Leva M. *Fluidization*. Mc. Graw Hill; 1959.
- [29] Gupta C., Sathiyamoorthy D. *Fluid Bed Technology in Materials Processing*. CRC Press; 1999.
- [30] Hupa M. Ash-related issues in fluidized-bed combustion of biomasses: Recent research highlights. *Energy and Fuels* 2012;26:4–14. doi:10.1021/ef201169k.
- [31] Grimm A, Marcus O, Fredriksson A, Bostro D. Bed Agglomeration Characteristics in Fluidized-Bed Combustion of Biomass Fuels Using Olivine as Bed Material. *Energy & Fuels* 2012;26:4550–9.
- [32] Chaivatamaset P, Sricharoon P, Tia S. Bed agglomeration characteristics of palm shell and corncob combustion in fluidized bed. *Appl Therm Eng* 2011;31:2916–27. doi:10.1016/j.applthermaleng.2011.05.021.
- [33] Chirone R, Miccio F, Scala F. Mechanism and prediction of bed agglomeration during fluidized bed combustion of a biomass fuel: Effect of the reactor scale. *Chem Eng J* 2006;123:71–80. doi:10.1016/j.cej.2006.07.004.
- [34] Montes A. *Factors Affecting Bed Agglomeration in Bubbling Fluidized Bed Biomass Boilers*. Western University, 2014.
- [35] Bartels M, Lin W, Nijenhuis J, Kapteijn F, van Ommen JR. Agglomeration in fluidized beds at high temperatures: Mechanisms, detection and prevention. *Prog Energy Combust Sci* 2008;34:633–66. doi:10.1016/j.pecs.2008.04.002.
- [36] Scala F, Chirone R. An SEM/EDX study of bed agglomerates formed during fluidized bed combustion of three biomass fuels. *Biomass and Bioenergy* 2008;32:252–66.

doi:10.1016/j.biombioe.2007.09.009.

- [37] Montes A, Hamidi M, Briens C, Berruti F, Tran H, Xu C (Charles). Study on the critical amount of liquid for bed material agglomeration in a bubbling fluidized bed. *Powder Technol* 2015;284:437–42. doi:10.1016/j.powtec.2015.07.017.
- [38] Montes A, Ghiasi E, Tran H, Xu C (Charles). Study of bed materials agglomeration in a heated bubbling fluidized bed (BFB) using silica sand as the bed material and KOH to simulate molten ash. *Powder Technol* 2016;291:178–85. doi:10.1016/j.powtec.2015.12.030.
- [39] Bizon KD, Jong W De, Siedlecki M, Chirone R. Investigation of Agglomeration Phenomena During Fluidized Bed Combustion of Biomass in a 1 MW Shallow Bed Boiler. 32nd Meet. Combust., 2009, p. 1–6.
- [40] Skrifvars B, Ohman M, Nordin A, Hupa M. Predicting Bed Agglomeration Tendencies for Biomass Fuels Fired in FBC Boilers : A Comparison of Three Different Prediction Methods. *Energy & Fuels* 1999;13:359–63.
- [41] Bartels M, Nijenhuis J, Lensselink J, Siedlecki M, De Jong W, Kapteijn F, et al. Detecting and counteracting agglomeration in fluidized bed biomass combustion. *Energy and Fuels* 2009;23:157–69. doi:10.1021/ef8005788.
- [42] Anthony E. Fluidized bed combustion of alternative solid fuels; status, successes and problems of the technology. *Prog Energy Combust Sci* 1995;21:239–68. doi:10.1016/0360-1285(95)00005-3.
- [43] Fernández Llorente MJ, Escalada Cuadrado R, Murillo Laplaza JM, Carrasco García JE. Combustion in bubbling fluidised bed with bed material of limestone to reduce the biomass ash agglomeration and sintering. *Fuel* 2006;85:2081–92. doi:10.1016/j.fuel.2006.03.018.
- [44] Brus E, Marcus O, Nordin A. Mechanisms of Bed Agglomeration during Fluidized-Bed Combustion of Biomass Fuels. *Energy & Fuels* 2005;1:825–32.
- [45] Natarajan E, Ohman M, Gabbra M, Nordin A, Liliedahl T. Experimental Determination of Bed Agglomeration Tendencies of Some Common Agricultural Residues in Fluidized Bed Combustion and Gasification. *Biomass and Bioenergy* 1998;15:163–9.

- [46] Fryda LE, Panopoulos KD, Kakaras E. Agglomeration in fluidised bed gasification of biomass. *Powder Technol* 2008;181:307–20. doi:10.1016/j.powtec.2007.05.022.
- [47] Steenari BM, Lundberg A, Pettersson H, Wilewska-Bien M, Andersson D. Investigation of ash sintering during combustion of agricultural residues and the effect of additives. *Energy and Fuels* 2009;23:5655–62. doi:10.1021/ef900471u.
- [48] Yu C, Qin J, Nie H, Fang M, Luo Z. Experimental research on agglomeration in straw-fired fluidized beds. *Appl Energy* 2011;88:4534–43. doi:10.1016/j.apenergy.2011.05.046.
- [49] Arromdee P, Kuprianov VI. Combustion of peanut shells in a cone-shaped bubbling fluidized-bed combustor using alumina as the bed material. *Appl Energy* 2012;97:470–82. doi:10.1016/j.apenergy.2012.03.048.
- [50] Gatternig B, Karl J. The influence of particle size, fluidization velocity and fuel type on ash-induced agglomeration in biomass combustion. *Front Energy Res* 2014;2:1–12. doi:10.3389/fenrg.2014.00051.
- [51] Rozainee M, Ngo SP, Salema a. a., Tan KG, Ariffin M, Zainura ZN. Effect of fluidising velocity on the combustion of rice husk in a bench-scale fluidised bed combustor for the production of amorphous rice husk ash. *Bioresour Technol* 2008;99:703–13. doi:10.1016/j.biortech.2007.01.049.
- [52] Lin C-L, Peng T-H, Wang W-J. Effect of particle size distribution on agglomeration/defluidization during fluidized bed combustion. *Powder Technol* 2011;207:290–5. doi:10.1016/j.powtec.2010.11.010.
- [53] Shiyuan L, Qinggang L, Haipeng T. Agglomeration During Fluidized -Bed Combustion of Biomass. 13th Int. Conf. Fluid. - New Paradig. Fluid. Eng., 2010.
- [54] Chaivatamaset P, Sricharoon P, Tia S, Bilitewski B. The characteristics of bed agglomeration/defluidization in fluidized bed firing palm fruit bunch and rice straw. *Appl Therm Eng* 2014;70:737–47. doi:10.1016/j.applthermaleng.2014.05.061.
- [55] Liu H, Feng Y, Wu S, Liu D. The role of ash particles in the bed agglomeration during the fluidized bed combustion of rice straw. *Bioresour Technol* 2009;100:6505–13. doi:10.1016/j.biortech.2009.06.098.

- [56] Wang L, Hustad JE, Skreiberg Ø, Skjevraak G, Grønli M. A critical review on additives to reduce ash related operation problems in biomass combustion applications. *Energy Procedia* 2012;20:20–9. doi:10.1016/j.egypro.2012.03.004.
- [57] Steenari BM, Lindqvist O. High-temperature reactions of straw ash and the anti-sintering additives kaolin and dolomite. *Biomass and Bioenergy* 1998;14:67–76. doi:10.1016/S0961-9534(97)00035-4.
- [58] Boström D, Grimm A, Boman C, Björnbom E, Öhman M. Influence of kaolin and calcite additives on ash transformations in small-scale combustion of oat. *Energy and Fuels* 2009;23:5184–90. doi:10.1021/ef900429f.
- [59] Öhman M, Nordin A. The Role of Kaolin in Prevention of Bed Agglomeration during Fluidized Bed Combustion of Biomass Fuels 2000, Volume 14. *Energy & Fuels* 2000;14:737–737. doi:10.1021/ef000065n.
- [60] Öhman M, Boström D, Nordin A, Hedman H. Effect of kaolin and limestone addition on slag formation during combustion of wood fuels. *Energy and Fuels* 2004;18:1370–6. doi:10.1021/ef040025+.
- [61] Wang L, Becidan M, Skreiberg Ø. Testing of Zeolite and Kaolin for Preventing Ash Sintering and Fouling during Biomass Combustion. *Chem Eng Trans* 2013;35:1159–64. doi:10.3303/CET1335193.
- [62] Lundholm K, Nordin A, Marcus O, Bostro D. Reduced Bed Agglomeration by Co-combustion Biomass with Peat Fuels in a Fluidized Bed. *Energy & Fuels* 2005;19:2273–8.



## **Chapter 3**

### **Study of Bed Material Agglomeration in a Bubbling Fluidized Bed (BFB) using KCl and K<sub>2</sub>SO<sub>4</sub> at High Temperatures to Simulate Molten Ash**

## Abstract

The agglomeration of bed material is one of the most serious problems in combustion of biomass in fluidized-bed boilers, due to the presence of some inorganic alkali elements such as K and Na in the biomass ash, which form low-melting alkali compounds during the process. In this study, the agglomeration behaviors of bed materials (silica sand particles) were investigated in a bench-scale bubbling fluidized-bed reactor operating at 800°C using simulated biomass ash components: KCl, K<sub>2</sub>SO<sub>4</sub>, and a mixture of KCl and K<sub>2</sub>SO<sub>4</sub> at eutectic composition (molar ratio K<sub>2</sub>SO<sub>4</sub>/(KCl+ K<sub>2</sub>SO<sub>4</sub>) = 0.26). The signals of temperature and differential pressure across the bed were monitored while heating up the fluidized bed of silica sand particles premixed with various amounts of KCl, K<sub>2</sub>SO<sub>4</sub> and the KCl-K<sub>2</sub>SO<sub>4</sub> mixture in bubbling bed regime. A sharp decrease in temperature and differential pressure was observed around 750°C and 690°C for 0.4-0.6wt% loading of the low melting-point KCl and KCl-K<sub>2</sub>SO<sub>4</sub> mixture, respectively, suggesting the formation of bed material agglomeration and even de-fluidization of the bed, caused by the molten KCl and KCl-K<sub>2</sub>SO<sub>4</sub> mixture forming liquid bridges between silica particles and/or by possible chemical reactions between the silica and the KCl at a high temperature, forming low melting alkali silicate compounds (e.g., K<sub>2</sub>OSiO<sub>2</sub>, with melting points of <1000°C). No agglomeration was observed when adding K<sub>2</sub>SO<sub>4</sub> to the bed materials heated up to 800°C, which could be attributed to the higher melting point of K<sub>2</sub>SO<sub>4</sub> (>1024°C). SEM-EDX analysis of the agglomerates sampled from the experiments demonstrated a substantial decrease in the amount of Cl content in relation to K, implying the loss of Cl in the form of HCl or Cl<sub>2</sub> gas during the fluidization process at a high temperature. Also, the use of kaolin and aluminum sulfate to minimize agglomeration were also investigated. The results indicated that these additives could successfully prevent the formation of agglomerates by forming compounds with high melting points.

### 3.1 Introduction

Biomass has great potential to be used as a substitute for fossil fuels for the production of energy and chemicals, as it is renewable, carbon-neutral and abundant. Therefore, the use of biomass on a large scale can contribute to reduction of greenhouse gases emission. In fact, biomass, being the fourth largest source of energy in the world, provides about 14% of the world's total energy consumption [1].

Combustion is the most common technology for conversion of biomass to energy for production of heat, electricity and steam [2]. There are various technologies for biomass combustion in different types of reactors such as fixed beds, moving beds and fluidized beds [3]. Fluidized bed combustion (FBC) technology has many advantages, such as high fuel flexibility, high combustion efficiency, lower process temperature (contributing to less NO<sub>x</sub> formation, hence lower environmental impact) over other technologies. [4,5]. Therefore, FBC has been considered as the most efficient technology for combustion among others [1]. In spite of all these advantages, combustion of biomass in fluidized bed reactors still has some areas to improve. Currently, the bed material agglomeration seems to be a major operational issue in the fluid bed reactors.

Bed material agglomeration in fluidized bed reactors occurs during the combustion of biomass via different mechanisms such as melt-induced agglomeration, direct reaction of alkali compounds with bed material and coating-induced agglomeration [6,7]. Thus, the presence of alkali elements in biomass ash was commonly believed to be one of the main reasons for agglomeration. At high temperatures (>700°C), alkali compounds in biomass ash such as potassium chloride (KCl) would melt or react with silica bed material forming silicate compounds of a low melting point, which could result in bed material agglomeration [8]. The bed material agglomeration could eventually cause bed de-fluidization and unwanted expensive shutdown [4].

Several studies have been conducted on the mechanisms of agglomeration by using various types of biomass. In addition, the effects of operation conditions including type of bed materials, bed particle size, air velocity, temperature and the presence of additives have been investigated on the formation of agglomerates [1,4,5,8,9]. For instance, Llorente et al. [10] examined the effects of fuel characterization on the initial de-fluidization temperature for different types of biomass by using limestone as a bed material. The results indicated that the initial de-fluidization temperature for

almond shell was the lowest one, while the highest value was observed with thistle attributed to its ash composition containing the lowest amount of potassium. Shimizu et al. [1] investigated the de-fluidization behaviors of two bed materials, i.e. silica sand and porous alumina during the combustion of cedar pellet. It was revealed that the operating temperature of the system containing silica sand was 800°C, while alumina bed could operate up to 950°C without any agglomerates. It was proposed that the porous structure of alumina in the bed could capture the volatile compounds released from the combustion of fuel pellets, and most of the combustion took place inside the dense phase of the alumina bed. The increase in particle size of bed materials has detrimental effects on agglomerate formation. It was found that the bigger particles have reduced de-fluidization time compared to the smaller particles. This phenomena was attributed to the fact that larger particles have lower specific outer surface area in comparison with the smaller particles, resulting in formation a thicker coating layer around particles at a given amount of molten ash [11].

The effects of gas velocity on the de-fluidization time was reported in a study [12] at a constant combustion temperature of 900°C. It was observed that the de-fluidization occurred at a longer time when the gas velocity increased. At a higher gas velocity, the attrition forces acting on agglomerates and the increased amount of fuel ash entrained in the gas would contribute to delaying de-fluidization. Yu et al. [13] investigated the effects of operating temperature on agglomeration time during the combustion of rice straw at temperatures from 650°C to 900°C. It was observed that increasing operational temperature had a detrimental effect on de-fluidization time as expected. Faster de-fluidization happened at 900°C, and a longer operation was achieved at 650°C. The shorter de-fluidization time at a higher temperature could be attributed to the formation of a larger amount of melting ash, covering the sand particles, leading to severe bed material agglomeration.

To the best of the author's knowledge, there is no answer yet for what is the minimum/critical amount of liquid phase (molten alkali compounds) required in the bubbling bed fluidization to agglomerate the bed material. In a previous work conducted in our group by Montes et al. [14,15], we have determined the critical amount of liquid (~ 1wt% with respect to the silica bed material) which would cause severe bed agglomeration and de-fluidization in a bubbling fluidized bed (BFB) under cold or low-temperature operational conditions using model compounds to simulated molten ash in real biomass boilers. For example, in the cold BFB tests, various amount of glycerol-water (30%v/v) solutions were injected to the bed to simulate molten ash in real biomass boilers. It was

found the critical liquid amount resulting in bed agglomeration and severe channeling/de-fluidization were 0.2wt% and 0.7wt% with respect to the mass of bed material, respectively [14]. Furthermore, at the elevated temperature (400°C) tests, KOH was used to simulate the molten ash. The results revealed that 0.5wt% and 0.8wt% were the critical amount of liquid that could result in de-fluidization in the BFB of silica sand at a superficial gas velocity of  $3.9 U_{mf}$  and  $5.9 U_{mf}$ , respectively [15]. In following to our previous studies, the present study aimed to investigate bed material agglomeration behavior in fluidization of silica sand particles at higher temperatures (800°C) using KCl, K<sub>2</sub>SO<sub>4</sub> or KCl-K<sub>2</sub>SO<sub>4</sub> alkali compounds to simulate the molten ash and effects of kaolin or aluminum sulfate additives on the bed material agglomeration.

## **3.2 Experimental**

### **3.2.1 Experimental Set-up**

All the experiments were carried out in a laboratory scale bubble fluidized bed (BFB) combustor. The schematic diagram of the experimental set-up along with a real photo is illustrated in Figure 3-1. The reactor and freeboard were made of stainless steel with diameter of 3' and 4", respectively. The total height of the reactor was 2m. Air distributor was located at the bottom of the reactor and pre-heated air was used for the reactor. The reactor was equipped with an electrical furnace for heating of the bed material to the desired operating temperatures for the model compound studies, or for pre-heating the reactor in real biomass combustion tests. The reactor was equipped with a screw feeder coupled with a rotary valve to achieve adjustable feeding rates, assisted with a vibrator in the feeding line along with a compressed air purging system. An external cyclone at the exit of the combustor was used to capture the particulate matter entrained by the effluent gas. Two water cooled condensers for tar removal are located after the cyclone. The reactor is also equipped with measuring instrument including pressure transducers (PT), K-type thermocouples (T), flow-meter. A pressure transducer was located at the bottom of the bed just 5 cm above the air distributor and the other at the top of the reactor to measure the differential pressure across the dense phase of the BFB reactor. Five K-type thermocouples were mounted on the air line, the bottom of the reactor, the top and middle of the reactor and on the gas outlet line. The signals from the thermocouples and the pressure transducers are collected using an Omega data acquisition system and a personal computer equipped with a custom-designed data logging software.

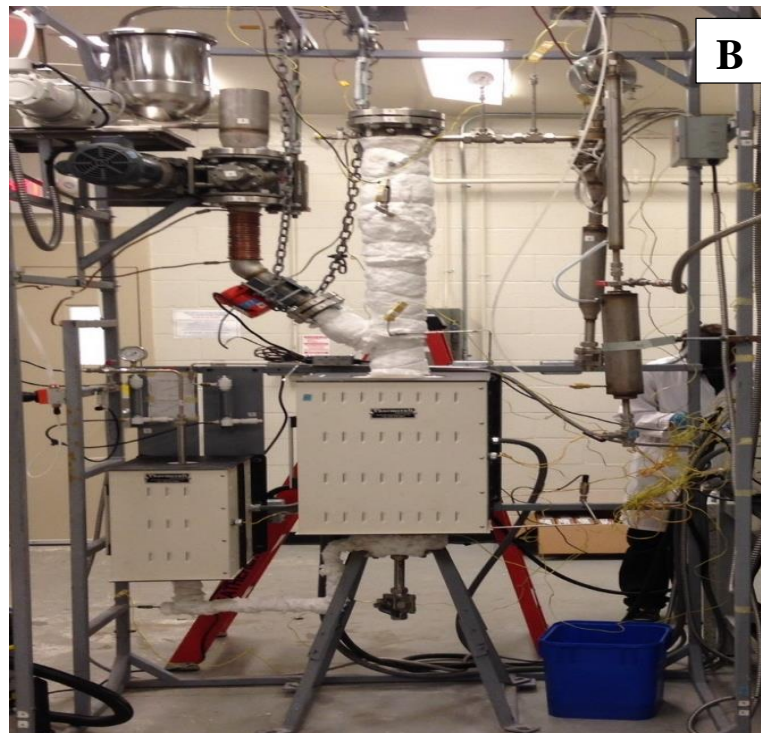
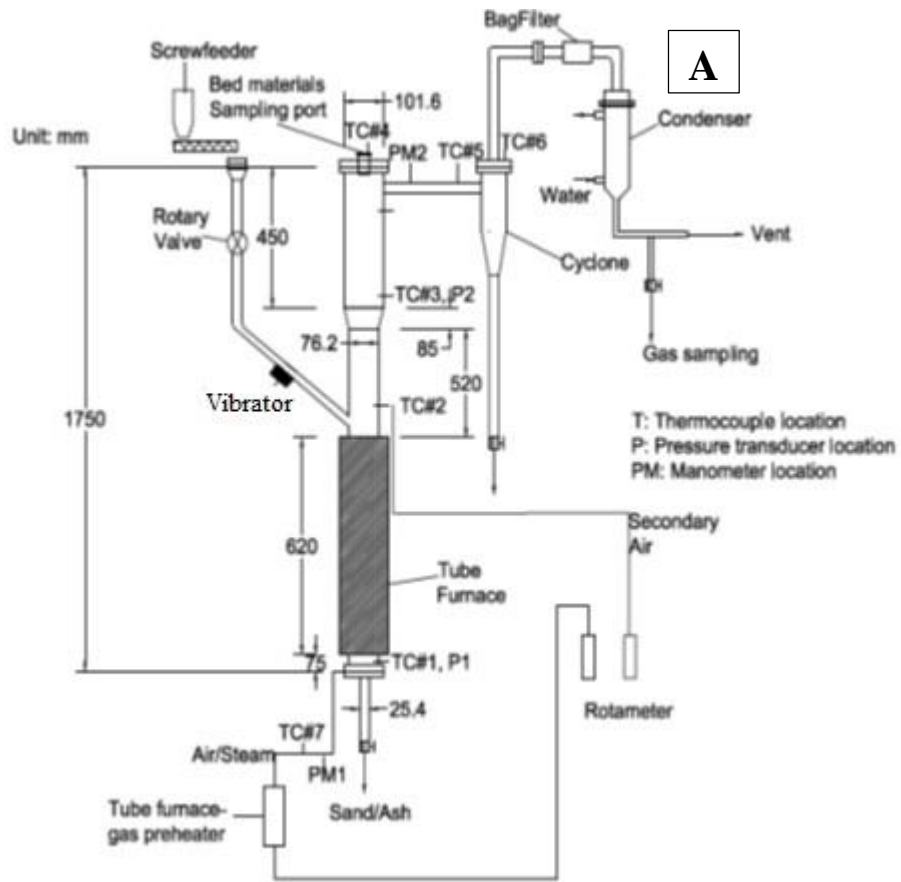


Figure 3-1 Schematic diagram (A) and photo of lab scale (B) BFB combustor.

### 3.2.2 Materials

The chemicals used to simulate molten ash were KCl, K<sub>2</sub>SO<sub>4</sub> and the bed material additive used were kaolin (hydrated aluminum silicate) and aluminum sulfate, all purchased from Sigma-Aldrich Co. KCl and K<sub>2</sub>SO<sub>4</sub> were selected on the basis of our previous study and literature work indicating that the most problematic element in biomass combustion is potassium present in the biomass ash [16–19].

In this experiment silica sand (99.88% SiO<sub>2</sub>, melting temperature of 1450°C) with a size range between 200-300µm was used as the bed material for the BFB tests as it is the most common bed material used in fluidized bed boilers. In all the experiments, a fixed amount (approx. 6.2 kg) of the bed material was used, with a static bed height of approx. 50 cm.

### 3.2.3 Procedure

This work aimed to investigate the agglomeration behavior of silica sand particles in a hot BFB with various amounts of KCl, K<sub>2</sub>SO<sub>4</sub> or mixture of KCl-K<sub>2</sub>SO<sub>4</sub> at eutectic composition, and the effects of kaolin or aluminum sulfate additive on the bed material agglomeration.

In the experiments, different amounts of KCl, K<sub>2</sub>SO<sub>4</sub> or eutectic mixture of KCl-K<sub>2</sub>SO<sub>4</sub> (2.85:1 mol/mol) was mixed with silica sand particles (bed material) at various amounts (i.e. 0.0, 0.2, 0.4 and 0.6wt. % with respect to the weight of bed material). To achieve homogenous mixtures of the bed material and the alkali compounds, the compound (s) was first dissolved in a small amount of water, and then mixed with the bed material under agitation, followed by oven drying at 105 °C for at least 24h. The dried bed material sieved to make sure about the homogeneity in size distribution of particles. The BFB column was filled with the prepared homogenous mixture of the bed material-chemical. All experiments were conducted at a superficial air velocity of 3.9 U<sub>mf</sub>. For the tests with KCl, the furnace was ramped up at a rate of 10°C/min to 800°C and controlled at that temperature for about 60-100 min. The furnace was then cooled down to room temperature. The temperature inside the bed and pressure drop across the bed were recorded during the experiment. Finally, the bed material was discharged from the reactor and sieved with sieves of different mesh sizes to determine the agglomerate size distribution. The experiment procedure was similar for the tests with eutectic mixture of KCl-K<sub>2</sub>SO<sub>4</sub> (2.85:1 mol/mol), except that the furnace was controlled at a lower

temperature (700°C), based on its eutectic melting temperature of this eutectic mixture (690°C), soaked for about 60 min followed by cooling.

The effects of additives (kaolin or aluminum sulfate) on the bed material agglomeration was also investigated in the same BFB system with 0.6wt% KCl or 0.6wt% KCl-K<sub>2</sub>SO<sub>4</sub>, respectively.

The collected agglomerates were analyzed by SEM/EDX (LEO (Zeiss) 1540XB FIB/SEM equipped with an Oxford Instruments x-ray system), and XPS (Kratos Axis Ultra spectrometer using a monochromatic Al K(alpha) source) to determine the composition of the agglomerates. ICP (Varian Vista-Pro CCD Simultaneous ICP-OES) analysis was also performed to prove the formation of alkali silicate compounds on the surface of bed materials. 500 g of agglomerates from an experiment containing 0.6wt% KCl were washed with distilled water at 40°C for 20 min under agitating to collect the water-soluble components, then filtered to remove the solid residue. The obtained aqueous solution was characterized by ICP to determine the amount of silica compounds and compared with the solution obtained from washing pure silica sand.

Furthermore, as a side-test to evaluate the evaporation of KCl during the experimental process, 7g of the eutectic mixture of KCl-K<sub>2</sub>SO<sub>4</sub> was placed in a muffle furnace at 800°C for various lengths of time, i.e. 0.5, 1.5 and 3h. The obtained samples were weighed to determine the weight loss of sample before and after experiment. Afterward, the collected samples were washed with distilled water and the washed solutions were analyzed for K and Cl contents using Atomic Absorption Spectroscopy (AAS) (Dionex ICS-2100) and Ion Chromatography (IC) (Perkin Elmer Analyst 100) analysis, respectively.

### **3.3 Results & Discussion**

First of all, our preliminary tests demonstrated that no agglomeration was observed in fluidization of silica sand with addition of various amounts of K<sub>2</sub>SO<sub>4</sub> heated up to 800°C, which could be attributed to the high melting point of K<sub>2</sub>SO<sub>4</sub> (>1024°C). Thus, our tests were focused on the effects of KCl and the eutectic mixture of KCl-K<sub>2</sub>SO<sub>4</sub> on bed material agglomeration, whose results are detailed below.



### 3.3.1 Effects of KCl on formation of agglomerates

Figure 3-2 displays the temperature-differential pressure (T- $\Delta P$ ) curves for BFB of the silica sand particles with various amounts of KCl (0, 0.2, 0.4, and 0.6wt% w.r.t. the weight of sand particles). As shown in the Figure, each test may be generally divided into three zones: heating zone (0-75 min), soaking zone (75-175 min), and cooling zone (>175 min). As given in Figure 3-2 (a), in the blank tests (with pure silica sand), the  $\Delta P$  remained constant in all zones, suggesting smooth fluidization of the bed material. On the other hand, it can be observed from the figure that the values of  $\Delta P$  of the bed material containing KCl in the heating zone are higher than those in the blank tests likely due to an increase in the drag force caused by the friction force between the viscous particle bed and the BFB column wall during the heating period. In the soaking zone, however, a slight decrease in  $\Delta P$  was observed in the presence of a small amount of KCl (0.2wt%), suggesting channeling or slight agglomeration of bed material due to the melting of the KCl at a temperature close to 800°C. Whereas, a large drop in  $\Delta P$  was recorded in the soaking zone of the bed material containing 0.4 and 0.6wt% of KCl, suggesting severe channeling or bed material agglomeration. Compared with other tests, the  $\Delta P$  signals in the test with 0.4wt% KCl exhibited more fluctuation, which might be due to the formation of unstable and weak channels/agglomerates in the bed. With 0.6wt% KCl, the agglomerates formed could be stable and strong, resulting a large decrease in  $\Delta P$  with less fluctuation. These results are in a good agreement with those reported by Montes et al. using KOH as the modeling compound operating at a lower temperature (~ 400°C) [15].

Interestingly, the temperature signals as presented in the Figure 3-2 provide similar information as the  $\Delta P$  signals discussed above. For instance, similar to  $\Delta P$  across the bed, the bed temperature declined sharply with some fluctuation in the tests with a high content of KCl (0.4 or 0.6wt%). This might be caused by the formation of bed material agglomerates with low fluidity which could retard/hinder the heat transfer from the column wall to the bed material, hence sharply reduced the temperature of the bed.

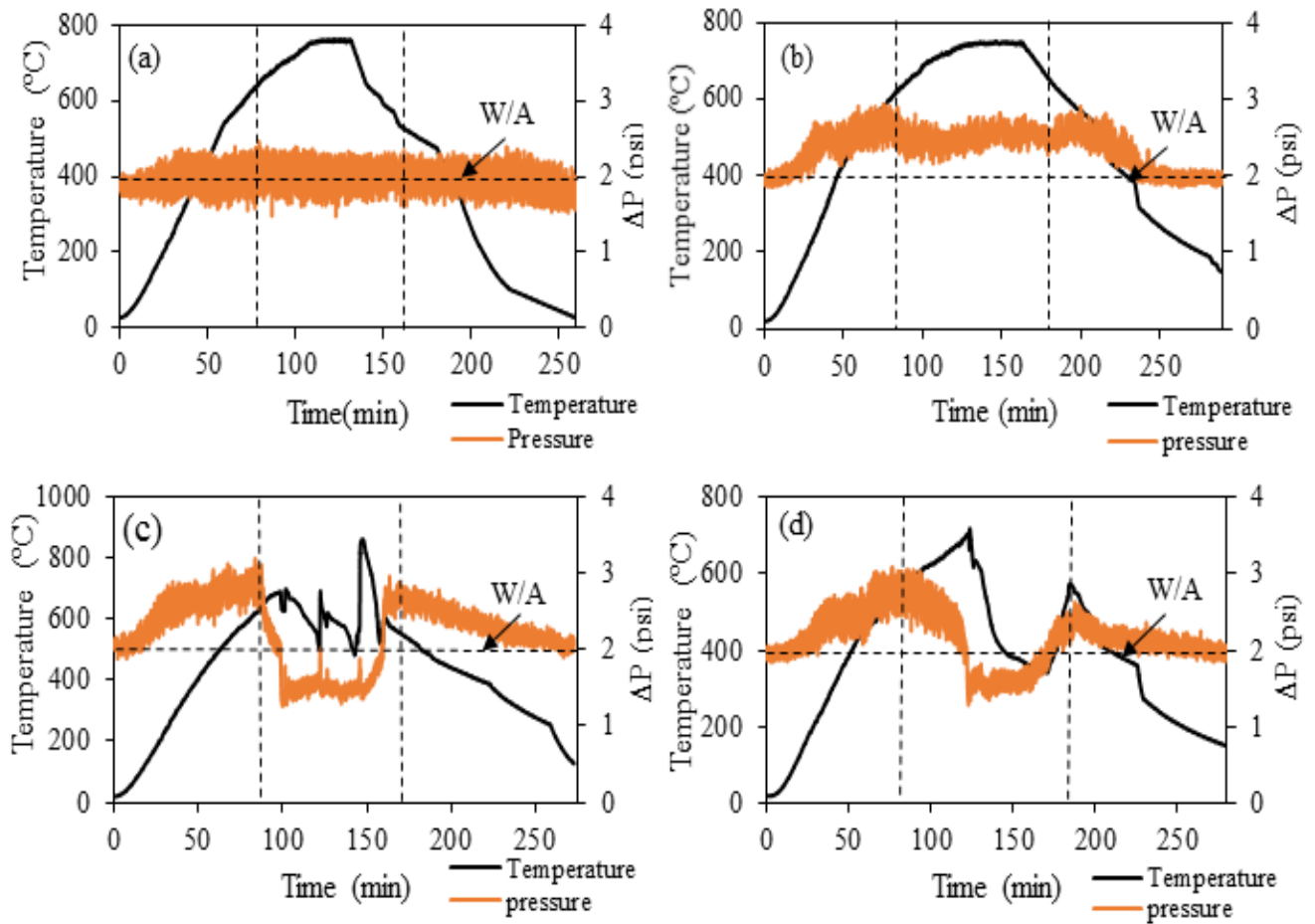


Figure 3-2 Variation of differential pressure ( $\Delta P$ ) and temperature signals with experimental time in BFB of silica sand particles with 0.0wt% KCl (a); 0.2wt% KCl (b); 0.4wt% KCl (c); 0.6wt% KCl (d).

Figure 3-3 displays the agglomerated sand particle and bottom view of the reactor after discharging of the agglomerates. As shown, the formed agglomerates covered the thermocouple and by forming an isolation layer around it, thus hindering the heat transfer.



Figure 3-3 Formed agglomerates and the bottom view of the BFB reactor.

As shown in the Figure 3-2, upon cooling of the BFB, both the pressure and temperature climbed up immediately for a short time period and then decreased as expected during the cooling process. The sharp increase in temperature and pressure could be due to the immediate phase transfer of the molten alkali silicates into a solid phase (resulting in a sudden increase in the bed temperature). Some fragile agglomerates inside the bed bonded with compounds such as alkali silicates could break into fine or smaller agglomerates with improved fluidity upon cooling, accounting for the increased  $\Delta P$  signals.

As mentioned, the formed agglomerates were fragile and easily broken during the discharging process, hence, the agglomerate particle size analysis was extremely challenging, hence the results of particle size distribution are not meaningful. The agglomerates and bed materials collected from the tests were analyzed by SEM-EDX and XPS to investigate the concentration of K and Cl on the surface of bed materials. The SEM-EDX and XPS results are presented in Table 3-1. As well understood, when only KCl was added into the bed, the initial molar ratio of Cl/K of the bed material should be 1 irrespective of the amount of KCl in the bed material. After the tests, interestingly the molar ratio of Cl/K decreased significantly to 0.57 and 0.54 in the agglomerates from the tests with 0.4wt% and 0.6wt% KCl, respectively. The XPS measurement for the agglomerates from the test with 0.6wt% KCl also indicated a marked decrease in molar ratio of Cl/K during the test. This drastic decrease in Cl/K molar ratio suggests that Cl was lost selectively more than K during the experiments via some reactions that convert Cl to gaseous products such as HCl and Cl<sub>2</sub>. Figure 3-4 shows the SEM mapping of elemental distribution for the key elements in the sample with 0.6% KCl. A lighter area in the back-white printed images indicates a higher concentration of the respective element.

Table 3-1 SEM-EDX and XPS analytical results for the agglomerates collected after the tests with various amounts of KCl addition.

Sample	SEM-EDX				XPS		
	K (wt%)	Cl (wt%)	Cl/K molar ratio (-)		K (wt%)	Cl (wt%)	Cl/K (-)
			Before	After			
<b>0.4 wt% KCl</b>	4.05	2.1	1	0.57	-	-	-
<b>0.6 wt% KCl</b>	6.5	3.2	1	0.54	7.3	2.8	0.42

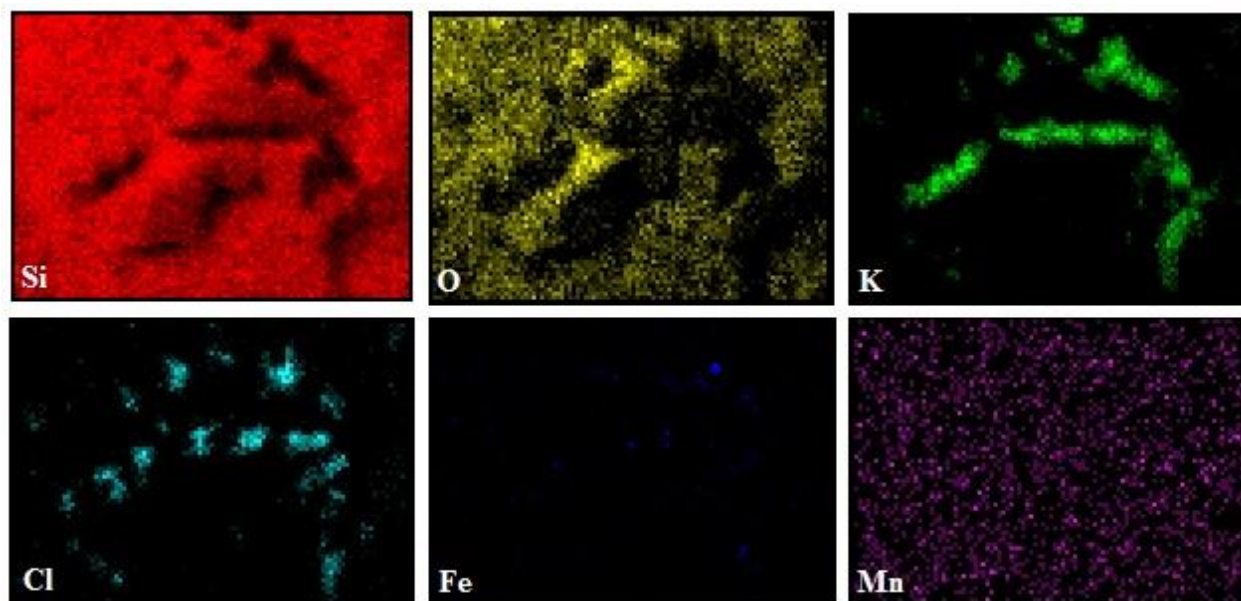


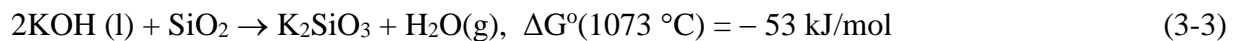
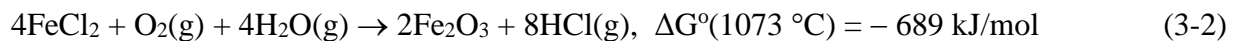
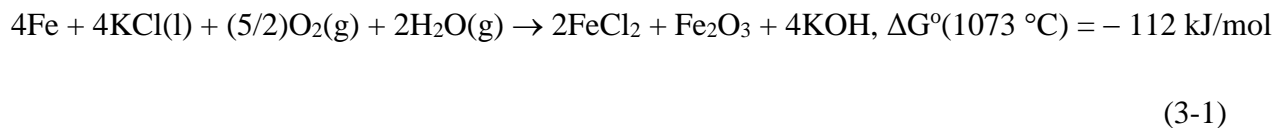
Figure 3-4 SEM mapping images of the agglomerates from the test with 0.6% KCl.

The formed agglomerates were further analyzed to investigate the formation of potassium silicate on the surface of bed materials. Table 3-2 shows the ICP results of aqueous solutions after washing the pure silica sand and the formed agglomerates from the tests with 0.6wt% KCl. As observed, the content of Si was much higher in washing liquid from the agglomerates with 0.6wt% KCl compared to that from the pure silica sand, suggesting the formation of potassium silicates (soluble in water) in the agglomerates. This result may thus evidence that the K could react with silica sand to form the potassium silicates. This formation of potassium silicates that have low melting points would result in formation of sticky layer around the bed material, and hence bed material agglomeration.

Table 3-2 ICP results of washing liquids from pure silica sand and from agglomerates of silica sand with 0.6wt% KCl.

Sample	Ca	K	Mg	Na	S	Si
Washing liquid from pure silica sand	18.8	12.9	6.1	11.9	14.7	3.6
Washing liquid from agglomerates of silica sand with 0.6wt% KCl	18	130	6	12.5	15	11.2

It was proposed by Kiamehr [20] that Fe from the steel-wall of the biomass combustor could react with KCl(s) and H<sub>2</sub>O/O<sub>2</sub> at elevated temperatures (500°C) to produce Fe<sub>2</sub>O<sub>3</sub> (causing corrosion of the reactor wall) and vapor of KOH(g) and HCl(g) [10]. However, considering the KCl and KOH has a melting temperature at 770°C and 406°C and a boiling point of 1420°C and 1327°C, respectively, both KCl and KOH are likely in liquid phase at 700-800°C. Thus, for the 800°C tests the mechanism by Kiamehr [20] may be modified into the following reactions, where KCl (l) reacts with Fe from the reactor wall with H<sub>2</sub>O/O<sub>2</sub> (water was present in un-dried compressed air) at elevated temperatures, forming Fe<sub>2</sub>O<sub>3</sub> and KOH (l) and HCl (g) vapor. The values of ΔG° for these two reactions at 1073K were calculated to be -112 kJ/mol and - 689 kJ/mol, respectively, suggesting that these reactions can spontaneously occur at 800°C. The formed KOH (l) can further react with SiO<sub>2</sub> at elevated temperature to form K<sub>2</sub>SiO<sub>3</sub>. The formed HCl would be entrained by the effluent gas, causing reduced Cl/K ratio as evidenced by the SEM-EDX and XPS analyses (Table 3-1) and the formation of potassium silicates could be evidenced by the ICP results (Table 3-2) However, more analyses are required to validate these hypothetical reactions.



Upon cleaning the reactor after the experiment, we observed an appreciable amount of rust formed on the interior surface of the reactor as illustrated in the photo in Figure 3-5. This may be the evidence for the formation of  $\text{Fe}_2\text{O}_3$  resulted from Reactions (3-1) and (3-2).



Figure 3-5 Photos of the bed material after the experiment with (A) and without (B) 0.6wt% KCl .

### 3.3.2 Effects of eutectic mixture of KCl-K<sub>2</sub>SO<sub>4</sub> on formation of agglomerates

Figure 3-6 shows the T- $\Delta$ P curves from the tests with various amounts of a eutectic mixture of KCl-K<sub>2</sub>SO<sub>4</sub> (0.0, 0.2, 0.4, 0.6wt% w.r.t. the weight of silica sand particles in the BFB column). Similarly, the experiments can be divided into three zones: heating zone, soaking zone and cooling zone, as indicated in the Figure. As expected in the blank tests (with pure silica sand) (Figure 3-6 (a)), the  $\Delta$ P remained stable in all zones. In the experiments with the KCl-K<sub>2</sub>SO<sub>4</sub> mixture (0.2, 0.4, and 0.6wt%), a slight increase in the differential pressure was observed in the heating zone, suggesting adhesion between bed material and the BFB column wall, which was similarly observed in the tests with KCl (Figure 3-2). Similarly as shown previously in Fig. 3-2, in the soaking zone of the experiment however with 0.2 or 0.4wt% KCl-K<sub>2</sub>SO<sub>4</sub>, there was a slight decrease in  $\Delta$ P, which was again likely due to the melting of the alkali compounds causing formation of channels and agglomerates in the bed. The low addition amounts of KCl-K<sub>2</sub>SO<sub>4</sub> (0.2 or 0.4wt%) did not seem to cause severe agglomeration, thus less fluctuation in  $\Delta$ P and temperature was observed. In contrast, a sharp decrease in  $\Delta$ P was observed from the test in the presence of 0.6wt% of KCl-K<sub>2</sub>SO<sub>4</sub> mixture, which might suggest de-fluidization due to severe channeling and agglomeration of the bed materials. Similarly Montes et al. [15] reported that addition of 0.5wt% of KOH resulted in severe agglomeration in BFB at 400°C.

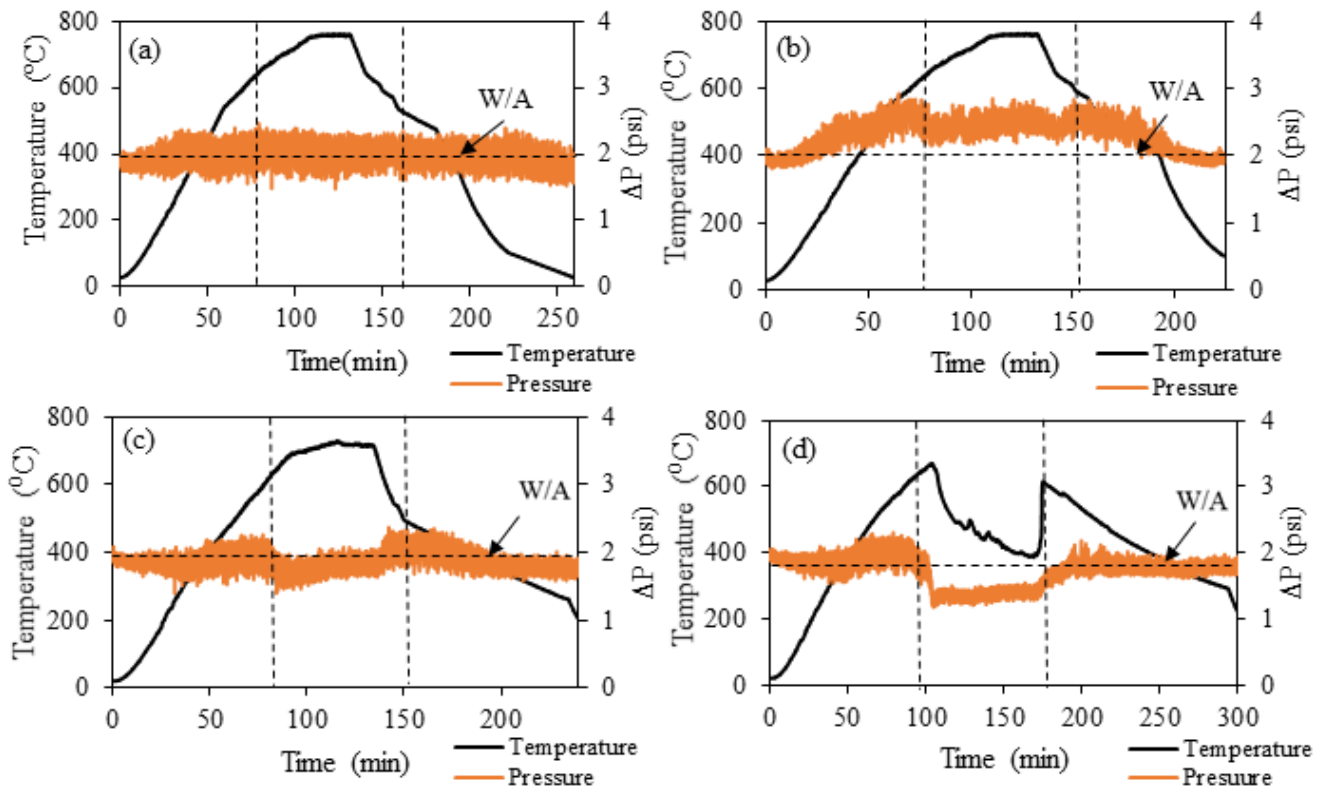


Figure 3-6 Variation of differential pressure ( $\Delta P$ ) and temperature signals with experimental time in BFB of silica sand particles with 0.0wt% KCl-K<sub>2</sub>SO<sub>4</sub> (a); 0.2wt% KCl-K<sub>2</sub>SO<sub>4</sub> (b); 0.4wt% KCl-K<sub>2</sub>SO<sub>4</sub> (c); 0.6wt% KCl-K<sub>2</sub>SO<sub>4</sub> (d).

Figure 3-7 illustrates the SEM-EDX spectra of the agglomerated bed material after the fluidization test with 0.6wt% KCl-K<sub>2</sub>SO<sub>4</sub>. In the Figure, white areas indicate the potassium silicate that formed on the surface of bed material.

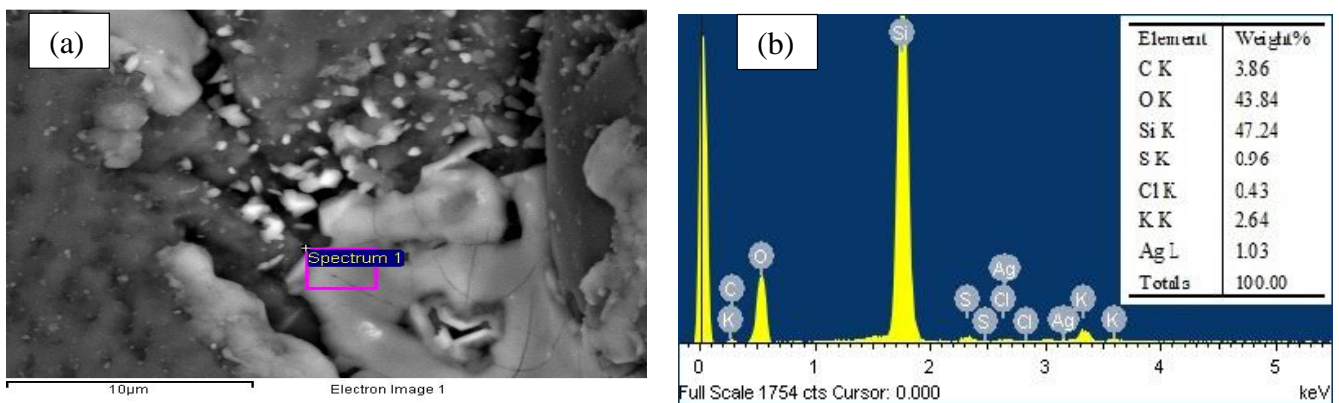


Figure 3-7 SEM image (a) and EDX spectra (b) of the formed agglomerates after the BFB test with 0.6wt% KCl-K<sub>2</sub>SO<sub>4</sub>.



Table 3-3 shows the SEM-EDX and XPS results for the agglomerates collected after the experiments with KCl-K<sub>2</sub>SO<sub>4</sub> addition. As similarly shown and discussed previously in Table 3-1, the results reveal that the molar ratio of Cl/K in the bed material after each experiment dropped from the initial value of 0.59 (irrespective of the addition amount of the KCl-K<sub>2</sub>SO<sub>4</sub> mixture) to 0.12, 0.19, and 0.18 for the test with 0.2, 0.4, and 0.6wt% KCl-K<sub>2</sub>SO<sub>4</sub> respectively. Again, these results suggested more loss of Cl than K in the experiments, likely via the Reactions (3-1) and (3-2) given previously, forming volatile HCl (g).

Table 3-3 SEM-EDX and XPS analysis results for the agglomerates collected after the tests with various amounts of KCl-K<sub>2</sub>SO<sub>4</sub> addition.

Sample	SEM-EDX				XPS		
	K (wt%)	Cl (wt%)	Cl/K molar ratio (-)		K (wt%)	Cl (wt%)	Cl/K (-)
			Before	After			
<b>0.2% KCl-K<sub>2</sub>SO<sub>4</sub></b>	1.1	0.16	0.59	0.12	-	-	-
<b>0.4% KCl-K<sub>2</sub>SO<sub>4</sub></b>	2.4	0.41	0.59	0.19	-	-	-
<b>0.6% KCl-K<sub>2</sub>SO<sub>4</sub></b>	2.64	0.43	0.59	0.18	6.4	1.2	0.21

Figure 3-8 shows the EDX elemental mapping images of bed material agglomerates from the test with 0.6% KCl-K<sub>2</sub>SO<sub>4</sub>. The relative concentrations of selected elements including K, Cl, Si, O, C, Ag, S, and Fe are illustrated with different colors.

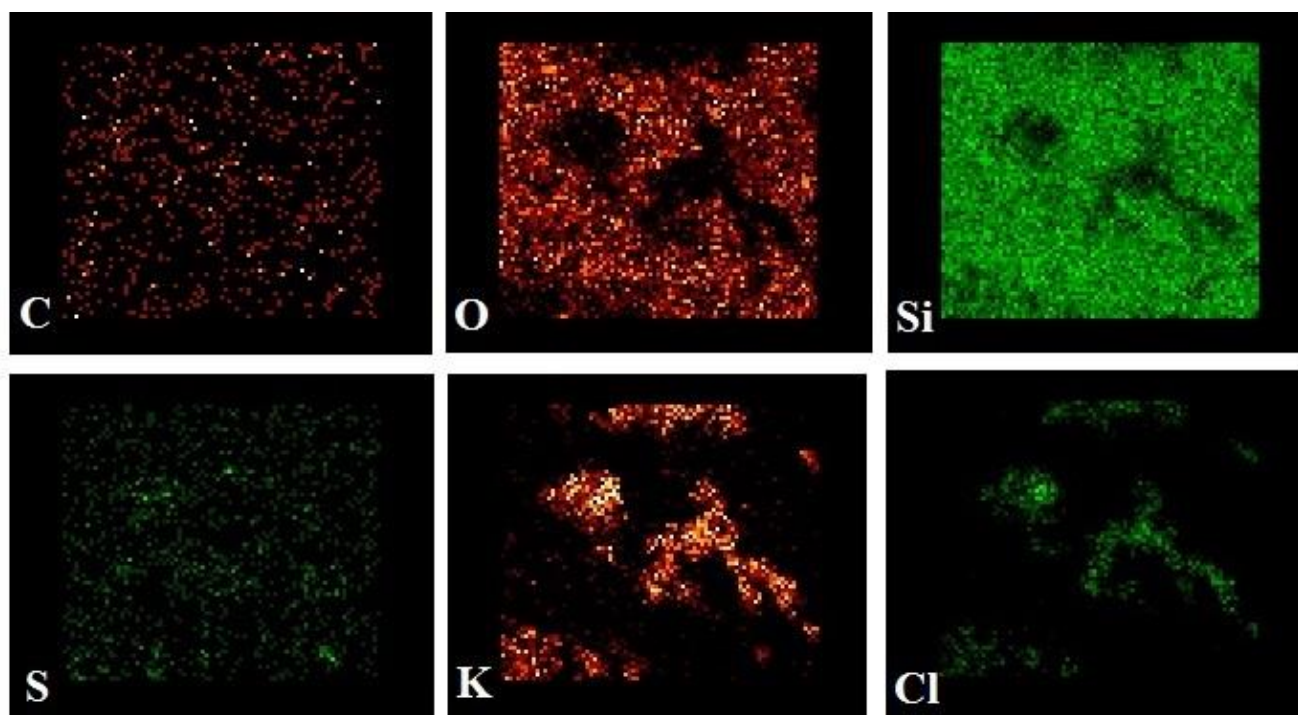


Figure 3-8 SEM mapping images of agglomerates from the test with 0.6% KCl-K<sub>2</sub>SO<sub>4</sub>.



Two possible reasons may be proposed for the reduction of Cl/K molar ratio during the experiment. One mechanism of losing of Cl could be via Reactions (3-1) and (3-2) and the formation of potassium silicate via reaction (3-3), as discussed previously. The other possible cause of decreased Cl/K ration in the experiments might be through evaporation of KCl during the experiment. To investigate the possibility of KCl evaporation, three parallel samples of the eutectic mixture of KCl-K<sub>2</sub>SO<sub>4</sub> (without silica sand) were heated in the muffle furnace at 800°C for 30, 90 and 180 minutes. All samples were weighed before and after the heating to monitor the weight loss. Then, AAS and IC measurements were carried out to determine the amount of K and Cl in the resulted samples after heating, respectively. Table 3-4 shows the AAS and IC results for the samples before and after the heating. As shown in the Table, the molar ratio of Cl/K for all samples before and after the heating remained almost constant (0.54 ~ 0.59), suggesting that KCl evaporation was insignificant at 800°C heating even after 180 mins. Also, the weight loss during the heating was negligible small (0.01 %), another indication of negligible KCl evaporation from the eutectic mixture of KCl-K<sub>2</sub>SO<sub>4</sub> during the heating.

Table 3-4 AAS, IC analysis results of the eutectic mixture of KCl-K<sub>2</sub>SO<sub>4</sub> after heating at 800°C for various lengths of time.

Sample	Time (min)	Temperature (°C)	Weight loss (%)	K (ppm)	Cl (ppm)	Cl/K molar ratio (-)
S1	0	-	-	-	-	0.59
S2	30	800	0.01	682.93	361.60	0.58
S3	90	800	0.01	529.68	251.21	0.54
S4	180	800	0.01	683.64	354.31	0.57

### 3.3.3 Effects of Additives

Figure 3-9 shows the variation of the temperature and  $\Delta P$  signals versus time during the bubbling fluidization of silica sand particles with 0.6wt% KCl or 0.6wt% KCl-K<sub>2</sub>SO<sub>4</sub> in the presence of an additive (Kaolin or Aluminum sulfate) at 0.6wt% w.r.t. the weight of bed material. As can be observed from these figures, the differential pressure remains approximately constant in all three zones of the experiments in the presence of an additive, and the results are comparable with those obtained in the blank test (with silica sand particles only). This is very different from what observed and discussed previously for the tests in the presence of 0.6% KCl or 0.6% of KCl-K<sub>2</sub>SO<sub>4</sub> without an agglomeration additive (Figures 3-2 and 3-6), where the  $\Delta P$  and temperature dropped and fluctuated dramatically in the soaking zone. Thus,

the results demonstrate that the addition of kaolin and aluminum sulfate in such a small amount (0.6wt.%) could effectively prevent the formation of bed material agglomerates in the fluidization of silica sand.

To clarify the possible roles of additives in the experiments, SEM-EDX analysis for the bed materials collected after the experiments was performed. The average contents of Al, K, and Cl in the bed material samples are summarized in Table 3-5. Similarly, as shown previously in Tables 3-1 and 3-3, with the KCl or KCl-K<sub>2</sub>SO<sub>4</sub> addition only without an additive, the molar ratio of Cl/K in the bed material from the tests in co-presence of KCl or KCl-K<sub>2</sub>SO<sub>4</sub> and an agglomeration prevention additive (kaolin or aluminium sulfate) also decreased, suggesting more loss of Cl than K in the experiment, likely due to the forming of volatile HCl (g) via the reactions (3-1) and (3-2), as discussed previously. Therefore, the beneficial effects of these additive might simply be attributed to the formation of higher melting point compounds such as Kalsilite and leucite between the additive and the alkali compounds (KCl, K<sub>2</sub>SO<sub>4</sub> or K<sub>2</sub>SiO<sub>3</sub>) [11]. Presence of Al and K on the surface of silica sands after the experiments could confirm the formation of these two compounds.

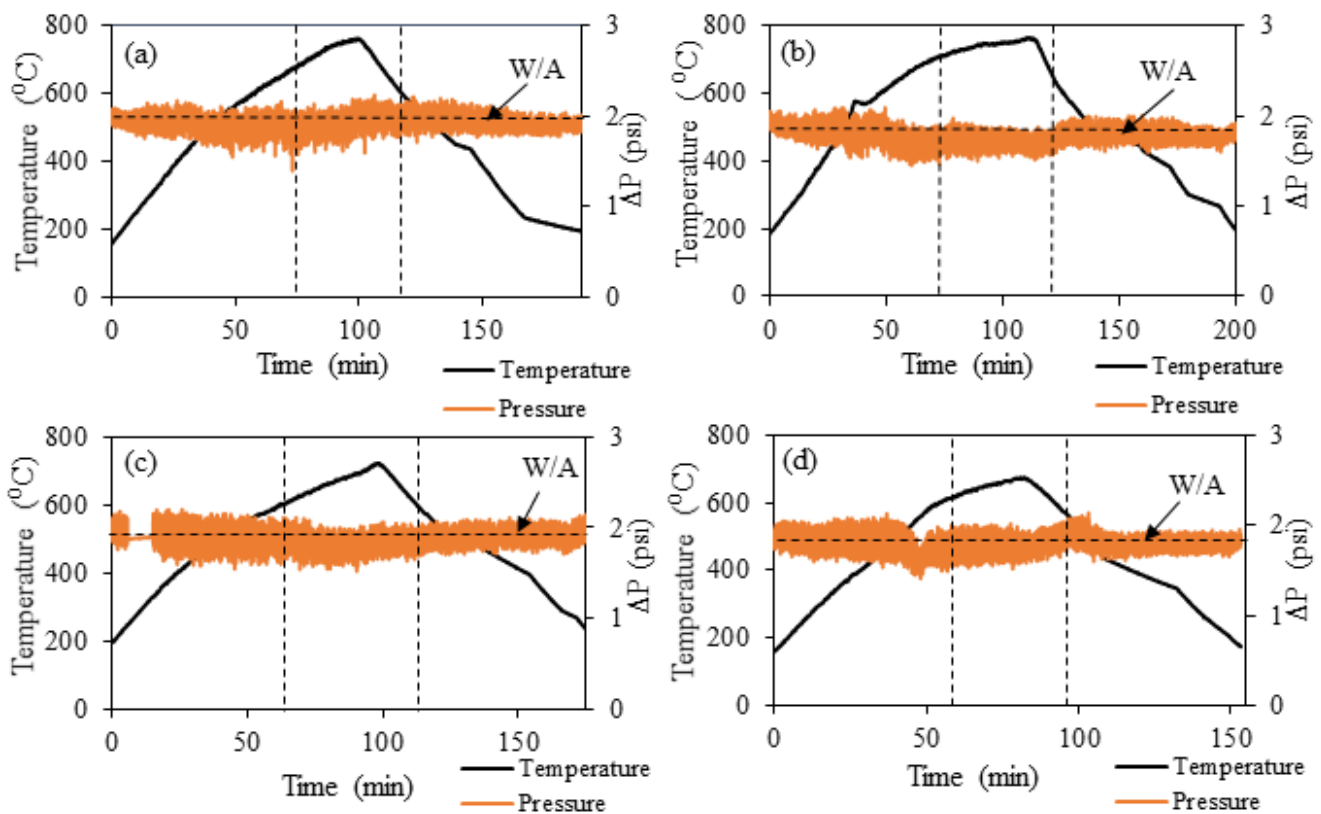


Figure 3-9 Variation of  $\Delta P$  and temperature signals with experimental time in in BFB of silica sand particles with 0.6wt% KCl and 0.6wt% kaolin (a); 0.6wt% KCl and 0.6wt% aluminum sulfate (b); 0.6wt% KCl-K<sub>2</sub>SO<sub>4</sub> and 0.6wt% kaolin(c); 0.6wt% KCl-K<sub>2</sub>SO<sub>4</sub> and 0.6wt% aluminum sulfate (d).

Table 3-5 SEM-EDX analysis results for the bed materials collected after the experiments with co-presence of alkali compounds and an additive (Kaolin or  $\text{Al}_2(\text{SO}_4)_3$ ).

Sample	SEM-EDX				
	Al	K	Cl	Cl/K molar ratio (-)	
	(wt%)	(wt%)	(wt%)	Before	After
0.6 wt% KCl + 0.6 wt% Kaolin <sup>1</sup>	2.01	3.15	1.48	1	0.52
0.6 wt% KCl-K <sub>2</sub> SO <sub>4</sub> + 0.6 wt% Kaolin <sup>1</sup>	2.26	3.19	0.65	0.59	0.22
0.6 wt% KCl + 0.6 wt% $\text{Al}_2(\text{SO}_4)_3$	2.14	3.06	0.88	1	0.32
0.6 wt% KCl-K <sub>2</sub> SO <sub>4</sub> + 0.6 wt% $\text{Al}_2(\text{SO}_4)_3$	2.28	3.11	0.41	0.59	0.14

<sup>1</sup>Kaolin: hydrated aluminum silicate

### 3.4 Conclusions

This research aimed to determine the minimum/critical amount of liquid phase to cause bed material agglomeration in a bubbling fluidized bed of silica sand particles at elevated temperatures up to 700-800°C using KCl, K<sub>2</sub>SO<sub>4</sub> or eutectic mixture of KCl-K<sub>2</sub>SO<sub>4</sub> to simulate the molten ash in biomass combustion. From this study, the following conclusions can be drawn:

- 1) Bubbling fluidization of silica sand particles in the presence of KCl or eutectic mixture of KCl-K<sub>2</sub>SO<sub>4</sub> with an amount of 0.4-0.6wt.% (w.r.t. the weight of bed material) caused severe formation of channeling/agglomeration, leading to de-fluidization. On the contrary, no agglomeration was observed when adding K<sub>2</sub>SO<sub>4</sub> to the bed material heated up to 800°C, which could be attributed to the higher melting point of K<sub>2</sub>SO<sub>4</sub> (>1024°C) than KCl or eutectic mixture of KCl-K<sub>2</sub>SO<sub>4</sub>.
- 2) SEM-EDX and XPS analyses of the agglomerates or bed material samples after the experiments suggested more loss of Cl than K during the experiments, likely via some reactions converting KCl into HCl vapor.
- 3) The proposed reactions are: KCl and Fe from the reactor wall react with H<sub>2</sub>O/O<sub>2</sub> (from the undried compressed air) at elevated temperatures, forming Fe<sub>2</sub>O<sub>3</sub> (causing corrosion of the reactor wall) and KOH (l) and HCl (g) vapor. The reaction between KOH (l) and silica would form potassium silicates, which might contribute to the formation of bed material agglomeration.
- 4) Kaolin and aluminum sulfate can be effective additives used for preventing bed agglomeration in bubbling fluidization of silica sand particles at a high temperature.

### 3.5 References

- [1] Shimizu T, Han J, Choi S, Kim L, Kim H. Fluidized-Bed Combustion Characteristics of Cedar Pellets by Using an Alternative Bed Material. *Energy & Fuels* 2006;20:2737–42. doi:10.1021/ef0601723.
- [2] Bartels M, Lin W, Nijenhuis J, Kapteijn F, van Ommen JR. Agglomeration in fluidized beds at high temperatures: Mechanisms, detection and prevention. *Prog Energy Combust Sci* 2008;34:633–66. doi:10.1016/j.pecs.2008.04.002.
- [3] Ryu C, Yang Y Bin, Khor A, Yates NE, Sharifi VN, Swithenbank J. Effect of fuel properties on biomass combustion: Part I. Experiments—fuel type, equivalence ratio and particle size. *Fuel* 2006;85:1039–46. doi:10.1016/j.fuel.2005.09.019.
- [4] Grimm A, Marcus O, Fredriksson A, Bostro D. Bed Agglomeration Characteristics in Fluidized-Bed Combustion of Biomass Fuels Using Olivine as Bed Material. *Energy & Fuels* 2012;26:4550–9.
- [5] Chirone R, Miccio F, Scala F. Mechanism and prediction of bed agglomeration during fluidized bed combustion of a biomass fuel: Effect of the reactor scale. *Chem Eng J* 2006;123:71–80. doi:10.1016/j.cej.2006.07.004.
- [6] Visser, H., van Lith, S., & Kiel J. Biomass Ash-Bed Material Interactions Leading to Agglomeration in FBC. *J Energy Resour Technol* 2008;130:11801–6.
- [7] Brus E, Marcus O, Nordin A. Mechanisms of Bed Agglomeration during Fluidized-Bed Combustion of Biomass Fuels. *Energy & Fuels* 2005;1:825–32.
- [8] Chaivatamaset P, Sricharoon P, Tia S. Bed agglomeration characteristics of palm shell and corncob combustion in fluidized bed. *Appl Therm Eng* 2011;31:2916–27. doi:10.1016/j.applthermaleng.2011.05.021.
- [9] Öhman M, Nordin A, Skrifvars B-J, Backman R, Hupa M. Bed Agglomeration Characteristics during Fluidized Bed Combustion of Biomass Fuels. *Energy & Fuels* 2000;14:169–78. doi:10.1021/ef990107b.
- [10] Fernández Llorente MJ, Escalada Cuadrado R, Murillo Laplaza JM, Carrasco García JE. Combustion in bubbling fluidised bed with bed material of limestone to reduce the

- biomass ash agglomeration and sintering. *Fuel* 2006;85:2081–92.  
doi:10.1016/j.fuel.2006.03.018.
- [11] Lin W, Dam-Johansen K, Frandsen F. Agglomeration in bio-fuel fired fluidized bed combustors. *Chem Eng J* 2003;96:171–85. doi:10.1016/j.cej.2003.08.008.
- [12] Shiyuan L, Qinggang L, Haipeng T. Agglomeration During Fluidized -Bed Combustion of Biomass. 13th Int. Conf. Fluid. - New Paradig. Fluid. Eng., 2010.
- [13] Yu C, Qin J, Nie H, Fang M, Luo Z. Experimental research on agglomeration in straw-fired fluidized beds. *Appl Energy* 2011;88:4534–43. doi:10.1016/j.apenergy.2011.05.046.
- [14] Montes A, Hamidi M, Briens C, Berruti F, Tran H, Xu C (Charles). Study on the critical amount of liquid for bed material agglomeration in a bubbling fluidized bed. *Powder Technol* 2015;284:437–42. doi:10.1016/j.powtec.2015.07.017.
- [15] Montes A, Ghiasi E, Tran H, Xu C (Charles). Study of bed materials agglomeration in a heated bubbling fluidized bed (BFB) using silica sand as the bed material and KOH to simulate molten ash. *Powder Technol* 2016;291:178–85.  
doi:10.1016/j.powtec.2015.12.030.
- [16] Fryda LE, Panopoulos KD, Kakaras E. Agglomeration in fluidised bed gasification of biomass. *Powder Technol* 2008;181:307–20. doi:10.1016/j.powtec.2007.05.022.
- [17] Arvelakis S, Gehrman H, Beckmann M, Koukios EG. Agglomeration problems during fluidized bed gasification of olive-oil residue: evaluation of fractionation and leaching as pre-treatments. *Fuel* 2003;82:1261–70. doi:10.1016/S0016-2361(03)00013-9.
- [18] Lemoine ML, Civello PM, Martínez GA, Chaves AR. Influence of postharvest UV-C treatment on refrigerated storage of minimally processed broccoli (*Brassica oleracea* var. *Italica*). *J Sci Food Agric* 2007;87:1132–9. doi:10.1002/jsfa.
- [19] Goran O, Ye Z, Bjerle I, Andersson A. Bed Agglomeration Problems in Fluidized-Bed Biomass Combustion. *Ind Eng Chem Res* 2002;41:2888–94.
- [20] Kiamehr S. Material Solutions to Mitigate the Alkali Chloride-Induced High Temperature Corrosion. DTU, 2014.

## **Chapter 4**

### **Behavior and Mechanism of Bed Material Agglomeration in Fluidized-bed Combustion of Corn Stalk Using Silica or Olivine as Bed Material**

## Abstract

In this chapter, the behavior and mechanism of bed material agglomeration for fluidized-bed combustion of corn stalk were studied in a lab scale bubbling fluidized bed (BFB) reactor using olivine or silica sand as bed material at 800°C. The pressure drop across the bed and the temperature in the bed were monitored to evaluate the fluidization behavior, in particular the onset-point of bed material agglomeration or de-fluidization. It was found that the type of bed material could significantly affect the de-fluidization time of the bed, and silica sand bed material had greater tendency of agglomeration compared to the olivine bed material. Interestingly, the composition of the ash-layer on the bed material was strongly dependent on the type of bed material, although the same biomass feed was used in all tests. With the silica bed material, the coated ash-layer, bottom ash or agglomerates were enriched with  $K > Ca \approx Mg$ , whose contents increased with increasing the combustion time, which could eventually lead to bed material agglomeration and de-fluidization. With the olivine bed material, however, the coated ash-layer was enriched with  $Ca > K$ , increasing for a longer combustion time too. It should be also noted that the K content in the coated ash-layer on olivine bed materials is much lower than that on the silica bed materials. This lower deposition tendency of K compounds onto the olivine bed material than that onto the silica sand material might account for the longer de-fluidization time (>12h) for the olivine bed material than that for the silica bed material (8h) during corn stalk combustion. With increasing the superficial gas velocity, the deposited amount of the alkali/alkaline earth elements (K, Ca, Mg) in the bed material (either silica or olivine sand) reduced substantially, which would contribute to reduced tendency of bed agglomeration and de-fluidization.

## 4.1 Introduction

Fluidized bed combustors (FBC) have been widely used for energy conversion from coal or biomass due to high efficiency, low environmental impact and great versatility of fuel resources [1,2]. However, biomass combustion in FBC is still encountering some serious operating problems, of which the major one is associated with bed material agglomeration and sintering, which, in a severe case, may cause complete de-fluidization of the bed material [3,4]. Therefore, preventing of bed material agglomeration is essential to avoid the unwanted plant shutdown for biomass-fired FBC.

The formation of bed agglomeration is mostly associated with the presence of alkali compounds such as sodium and potassium compounds in the ash of biomass. Alkali compounds could form low melting points species which coat the bed materials. After the collision of the coated particles, the liquid bridge force between the particles could lead to formation of larger particles, resulting in bed material agglomeration [5]. Several studies have been conducted to reveal the mechanism of bed material agglomeration. Several mechanisms, such as viscous flow sintering, reactive liquid sintering and chemical reaction sintering, were believed to play a role in the formation of bed material agglomerates in fluidized-bed combustion of biomass [6]. The viscous flow is believed to be the predominant mechanism with a silicate ash. At temperature above the solidus temperature, silicate ash forms a highly viscous layer around the bed materials which may form necks between the particles and cause agglomeration. The second mechanism occurs in the presence of adequate amount of non-viscous liquid phase of molten salts in the fluidized bed. With reducing the operation temperature below solidus temperature, the crystallization and densification of bonding agents control the formation of agglomerates. The last mechanism could be attributed to the chemical reactions to link the bed materials together, which could be the major reason for fuel ashes containing high quantity of calcium compounds such as calcium sulfate and carbonate [5].

Many studies have been also conducted on the effects of operation conditions such as type of bed material, operation temperature, air velocity, and addition of additives on the bed material agglomeration and de-fluidization [7–10]. Shimizu et al. [11] investigated effects of bed materials (silica sand and porous alumina) on de-fluidization during combustion of cedar pellets, where the maximum operating temperature for the system containing silica sand was found to be 800°C as



the system had to be stopped after one hour operation due to severe agglomeration and de-fluidization of bed materials. Whereas, using the porous alumina bed material prevented the de-fluidization and improved the operation up to 950°C without the formation of agglomerates. It was believed that the porous structure of alumina captured the alkali volatile compounds released from the combustion of fuel pellets in the pores, which prevented formation of the coated ash-layer around the bed material. Lin et al. [9] reported that de-fluidization process was very sensitive to temperature and the formation of agglomerates was enhanced when the operation temperature increased as expected. At low temperatures, the sintering of agglomerates happened slowly with a longer de-fluidization time. In contrast, at high temperatures, alkali compounds in the ash of biomass would react with silica sand (bed material) and form low melting point compounds. The low melting point compounds would melt into a viscous liquid phase, which would then coat the bed material's surface and accelerate the de-fluidization.

Effects of gas velocity on de-fluidization time have also been reported. De-fluidization of bed material occurred at a longer time at a higher superficial gas velocity [12]. At a higher gas velocity, both the attrition forces acting on agglomerates and the entrainment of alkali compounds in the flue-gas, increase, which could retard the bed material agglomeration and de-fluidization. Similar results on the effects of gas velocity were reported by other researchers [1,5,13,14].

One of the most practical and effective approaches to mitigate the ash related problems during fluidized-bed combustion of biomass is addition of additives such as kaolin [15,16], zeolite 24A [17], and peat fuels [18]. Additives could retardant the de-fluidization process via four possible mechanisms, (i) increasing the biomass ash melting temperature by increasing the amount of inert in ash residues, (ii) physical adsorption and separating troublesome ash particles from combustion facilities, (iii) capturing problematic ash species via chemical adsorption and reactions, (iv) hindering the biomass ash sintering rate by the diluting effects from the additives [19–22]. The mechanism (iii) was observed to play a dominant role in preventing the bed material agglomeration in BFB of silica particles at 700-800°C in the presence of 0.4-0.6wt% alkali model compounds to simulate molten biomass ash, as discussed previously in Chapter 3.

Interesting research was published recently by our group [23,24], aiming to determine the critical amount of liquid which would cause de-fluidization of bed material. In cold BFB tests using a glycerol-water solution as a model liquid phase, the results showed that the critical liquid amount

resulting in bed agglomeration and de-fluidization was 0.2wt% and 0.7wt%, respectively [23]. In the subsequent warm BFB tests at 400°C using KOH as the model compound, the results revealed that 0.5wt% and 0.8wt% were the critical amount of liquid to cause de-fluidization of the BFB at an superficial gas velocity of  $3.9 U_{mf}$  and  $5.9 U_{mf}$ , respectively. Determination of the critical amount of liquid phase would be extremely important for the operation of biomass fluidized bed boilers as it offers a predictive measure to avoid severe bed material agglomeration and de-fluidization.

As reported in the previous chapter, we had investigated hot BFB fluidization of silica sand particles in the presence of KCl or eutectic mixture of KCl-K<sub>2</sub>SO<sub>4</sub> at 700-800°C, and the critical amount liquid phase was found to be 0.4-0.6wt.% (w.r.t. the weight of bed material) leading to severe agglomeration and de-fluidization. In addition, kaolin and aluminum sulfate demonstrated to be effective additives for preventing bed material agglomeration in bubbling fluidization of silica sand particles at a high temperature. In this chapter, our efforts to investigate the bed material agglomeration continued by conducting real BFB combustion of corn stalk (one of the most difficult biomass feedstock for fluidized bed combustion due to its high alkali ash content). Crop residues have high tendency for the unwanted bed agglomeration problems during fluidized bed combustion due to the presence of high amounts of K, Ca and Mg compounds in the ash.

Therefore, the main objective of this study is to examine the performance of BFB combustion of corn stalk in a lab-scale fluidized bed combustor, and to investigate the effects of bed material types, i.e. olivine and silica sand, and superficial gas velocity on agglomerate formation. The composition of the coated ash-layers on the different bed materials were examined using SEM-EDX and XPS, and the possible agglomeration mechanism for different bed materials are discussed in this chapter.

## **4.2 Experimental**

### **4.2.1 Fluidized Bed Combustor (FBC)**

The combustion experiments were performed in a laboratory scale bubbling fluidized bed reactor, as described in Chapter 3 (Figure 3-1). Briefly, the reactor and freeboard were made of cylindrical stainless steel tube with diameter of 3' and 4", respectively. The total height of the reactor was 2m. Air distributor was located at the bottom of the reactor and pre-heated air was used for the reactor. The reactor was equipped with an electrical furnace for heating of the bed material to desired

operating temperatures for the model compound studies, or for pre-heating the reactor in real biomass combustion tests. The reactor was equipped with a screw feeder coupled with a rotary valve to achieve adjustable feeding rates, assisted with a vibrator in the feeding line along with a compressed air purging system. As the corn stalk is very light and using the vibrator on the feeding line is not enough to feed the feed into the reactor. The compressed air was injected from the top of silo to facilitate the feeding process by pushing the feed through the feeding line into the reactor. Furthermore, the injected air can act as a secondary air and prevent the smoke leakages from rotary valve due to the differential pressure of inside and outside of the reactor. An external cyclone at the exit of the combustor was used to capture the particulate matter entrained by the effluent gas. Two water cooled condensers for tar removal were located after the cyclone. The reactor was also equipped with measuring instrument including pressure transducers (PT), K-type thermocouples (T), flow-meter. A pressure transducer was located at the bottom of the bed just 5 cm above the air distributor and the second one at the top of the reactor to measure the differential pressure across the dense phase of the BFB reactor. Five thermocouples were located on the air line, the bottom of the reactor (T1), the top (T2) and the freeboard (T3) of the reactor and also on the gas outlet line. The signals from the thermocouples and the pressure transducers are collected with an Omega data acquisition system and a personal computer equipped with a custom-designed data logging software.

Pressurized air was used as the primary fluidization gas and secondary air. Silica (98% SiO<sub>2</sub>) and olivine sands were selected as bed materials. They had particle size ranges of 200-300µm and 130-170µm, respectively. The chemical composition of these two bed materials are presented in Table 4-1. For each experiment, 2.5 kg of sand were used corresponding to a static bed height of approx. 20 cm.

Table 4-1 Chemical composition and properties of bed materials.

Component	Olivine sand (wt%)	Silica sand (wt%)
K <sub>2</sub> O	0.041	0.06
Na <sub>2</sub> O	0.052	0.004
CaO	0.32	0.12
MgO	49	0.13
Al <sub>2</sub> O <sub>3</sub>	0.81	0.18
Fe <sub>2</sub> O <sub>3</sub>	8.4	0.12
SiO <sub>2</sub>	41	98.9

In this study, the corn stalk was provided from Ontario Federation of Agriculture (OFA). The ash content and composition of the corn stalk are shown in Table 4-2. The particle size of corn stalk varied in the range of 1- 4 mm. Choosing suitable particle size is critical for this experiment: the very fine particles could start to burn at the feeding line, while big particles could clog the feeding line.

Table 4-2 Mineral composition of corn stalk.

	Al <sup>a</sup>	Fe <sup>a</sup>	Ca <sup>a</sup>	Mg <sup>a</sup>	K <sup>a</sup>	Na <sup>a</sup>	S <sup>a</sup>	Si <sup>a</sup>	Ash <sup>b</sup>
Corn Stalk	1.38	1.05	6.6	2.6	14.8	0.5	1.2	32.3	4.9

<sup>a</sup> wt% of ash, determined by ICP-OES; <sup>b</sup> dry basis wt% determined by ashing in a muffle furnace in air at 575°C for over 8 h.

#### 4.2.2 Fuel Preparation

Feedstock preparation is an important step for obtaining uniform and dried feed particles for combustion process. The corn stalk was firstly crushed by using a rotary mill into small particles, and sieved into 1-4 mm size range. The feed was dried in a pre-heated oven at 105°C for 12 hours before use in the combustion tests.

#### 4.2.3 Methods

The corn stalk combustion was conducted in the lab-scale BFB combustor, as illustrated in the previous Chapter 3 (Figure 3-1), in the presence of two different types of bed material (2.5 kg olivine sand or silica sand) at various superficial air velocities. The agglomerates formed or bed materials after the combustion process were needed to monitor the agglomerate formation process. Limited by the reactor configuration, online sampling was not available during the experiments, thus the combustion tests were carried out for different periods of time, i.e. 2, 4 and 6 hr to investigate the effect of time on the formation of coated ash-layer around the bed materials.

In a typical test, 2.5 kg olivine sand or silica sand was charged into the reactor. The primary air flow was heated up to 550°C by an electrical furnace before injecting to the bed. The superficial air velocity ( $U_g$ ) was set to be 2.5 and 4 times of minimum fluidization velocity ( $U_{mf}$ ) of the bed material.  $U_{mf}$  was calculated for air at 550°C which was the temperature of primary air. As the viscosity and density of air do not change significantly at higher temperature (750°C),  $U_{mf}$  could

be considered unchanged. For silica sand,  $U_g = 0.082$  m/s ( $2.5 U_{mf}$ ) and  $0.132$  m/s ( $4 U_{mf}$ ), and for olivine sand,  $U_g = 0.03$  m/s ( $2.5 U_{mf}$ ) and  $0.048$  m/s ( $4 U_{mf}$ ). The reactor and the bed material was also pre-heated to  $550^\circ\text{C}$  with the main electric furnace, and then the biomass was fed into the reactor at a continuous feeding rate of  $500\text{g/hr}$  for the entire combustion time. The screw feeder was designed for dense feed not light one such as a corn stalk, so it was first calibrated to feed accurate amount of corn stalk to the reactor. Temperature profiles in different locations of the reactor including the bottom of the bed ( $T1$ ), top of the bed ( $T2$ ) and freeboard ( $T3$ ) were recorded during the combustion process.

To determine the de-fluidization time, the corn stalk was fed into the reactor until de-fluidization of the system was detected based on the pressure and temperature signals. In this work, the onset of de-fluidization was characterized by the large decrease in pressure accompanied by a drastic temperature drop during combustion. The total time from the beginning of biomass feeding till the severe formation of agglomerate in the bed was recorded as the de-fluidization time. After detecting the de-fluidization, the fluidization air flow was stopped and the reactor was cooled down to room temperature to collect the formed agglomerates for further analysis. The amount of ash fed to the combustor was calculated using the feeding rate (kg/h), time of de-fluidization (h), and ash content of the biomass feedstock.

After each combustion test, the bed material including the formed agglomerates and the ash remained in the bed (bottom ash) were collected for further analyses by scanning electron microscopy coupled with energy dispersive X-ray (SEM/EDX (LEO (Zeiss) 1540XB FIB/SEM equipped with an Oxford Instruments x-ray system)). Moreover, ash particles collected from the bed (bottom ash) and from cyclone (fly ash) were analyzed by ICP-OES (Varian Vista-Pro CCD Simultaneous ICP-OES).

## **4.3 Results & Discussions**

### **4.3.1 Temperature Profiles**

Generally, biomass combustion is a two-step process [25]: the combustion of volatile matters, followed by the combustion of char which produces ash. Combustion of volatile matters is considered as the main source of heat generation, e.g., the volatile matters in the corn stalk were determining based on ASTM D3172 to be around 76.8%. In a BFB reactor, volatile matters are released when biomass fed into the reactor comes in contact with hot bed materials, and most of

the volatile matters (gas) passes through the bed together with the fluidization gas and burns on the top of the bed. Normally, the char burns mainly in the dense phase of the bed materials. To compare the performance of two different types of bed material (silica sand and olivine sand) in combustion of corn stalk, the temperature profiles along the height of the combustor at  $U_g = 2.5 U_{mf}$  are shown in Figure 4-1. It was found that the type of bed material could affect the temperature profiles along the height of the combustor, but the effects were insignificant considering the fluctuating temperature signals as indicated by the error bars in the Figure. The three temperatures (T1, T2 and T3) are measured by the three thermocouples whose measuring positions are indicated by in the schematic diagram of the BFB reactor as shown previously in Figure 3-1. With either bed material, the average dense phase temperature at the bottom of the bed (T1) was at 797-803°C, the average temperature at the top of the bed (T2) was at 708-771°C, and the average temperature at the freeboard was at 346-379 °C. Although there is not a significant difference between T1 and T2 in particular with the silica sand bed material as most of the volatile matters combust on the top of the bed. While in olivine sand bed material, T2 is lower than T1, suggesting that the a significant of volatile matters can burned in the dense phase of the olivine sand which has rougher surface compare to silica sand. Clearly, due to the heat loss, the introduction of secondary air and the almost complete combustion of volatile matters and char in the dense phase of the bed or at the reactor top, the temperature at the freeboard (T3) is much lower than that T2 and T1.

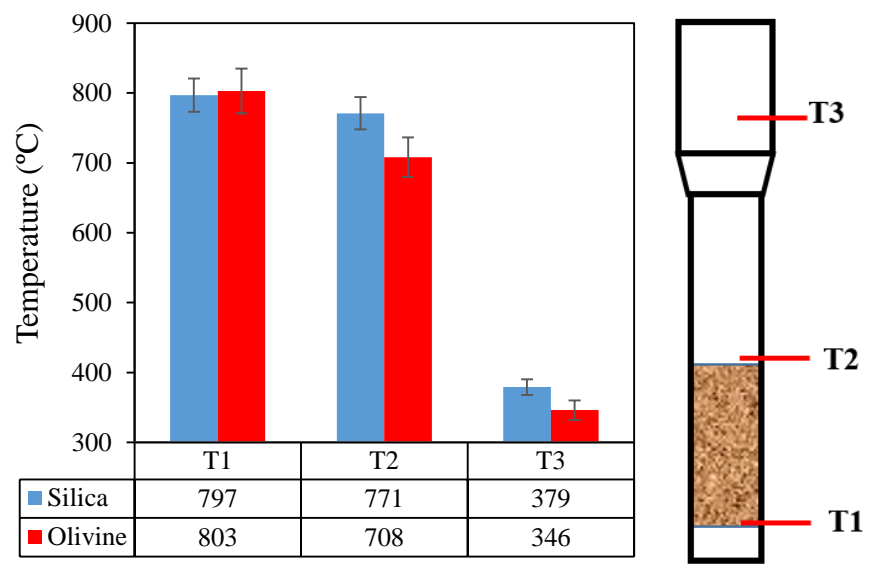


Figure 4-1 Temperature profiles along the height of the reactor in combustion of corn stalk in the presence of silica and olivine sand (at  $U_g = 2.5 U_{mf}$ ).

Effects of superficial air velocity ( $U_g = 2.5 U_{mf}$  or  $4 U_{mf}$ ) on temperature profiles along the reactor height in combustion of corn stalk with different bed materials are shown in Figure 4-2. With increasing  $U_g$  from  $2.5 U_{mf}$  to  $4 U_{mf}$ , T1 declined while both T2 and T3 increased to some extent regardless of the type of bed material. Increasing the air velocity through the bed material reduced the residence time. This result is actually expected, as a higher fluidization gas velocity would transport more ash (char) and volatile matters to the top of the bed and to the freeboard zone. The combustion of the char/volatile matters on the top of the bed would contribute to an increase in T2 and T3.

Bed temperature is one of the most important factors affecting de-fluidization time. A higher temperature can accelerate the formation of agglomerates [14,26,27]. Therefore, keeping the bed temperature at a lower level could prevent or postpone the de-fluidization process in biomass combustion. It was also found that the de-fluidization time occurred at longer time at a higher air velocity compared to a lower air velocity due to better mixing inside the fluidized bed and enhanced attrition acting on agglomerates [14,26]. The other reason why a higher superficial air velocity retards bed de-fluidization could be that a higher air velocity decreases the residence time of volatile matters and char in the dense phase of the bed, leading to a lower temperature dense phase of the bed and hence reduced bed agglomeration. This is evidenced from Figure 4-2, clearly showing that that increasing  $U_g$  from  $2.5 U_{mf}$  to  $4 U_{mf}$ , T1 (the dense-phase temperature) declines regardless of the type of bed material. As a result, the tendency of bed material agglomeration in biomass combustion should reduce at a higher superficial air velocity, which will be discussed in the subsequent sections of this chapter.

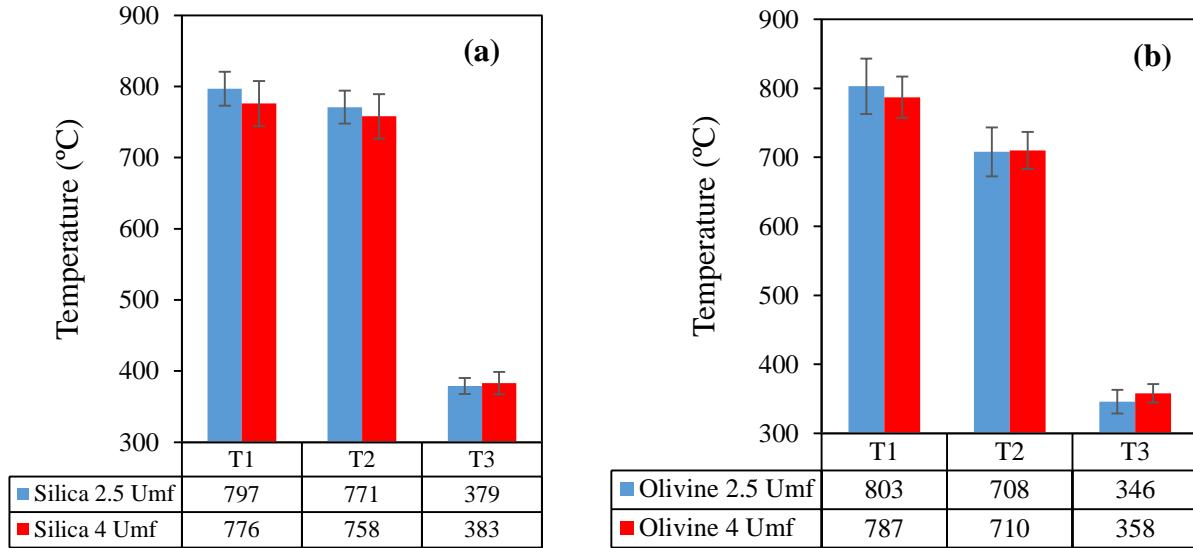


Figure 4-2 Effects of superficial air velocity on the temperature profiles along the reactor height in combustion of corn stalk with silica sand (a) or olivine sand (b) bed material.

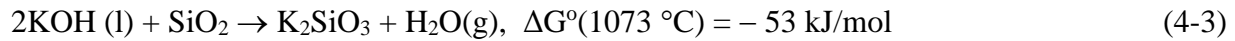
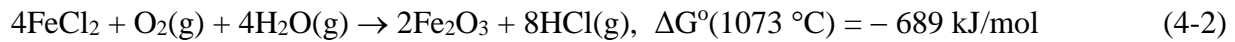
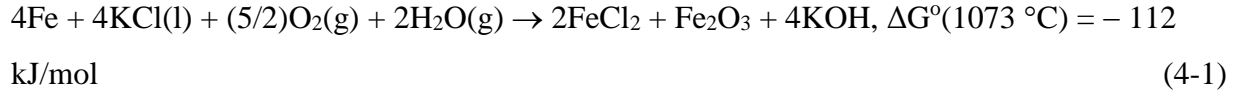
### 4.3.2 Composition of Coated Ash-layer on Bed Material

Combustion of corn stalk in silica or olivine sand led to formation of ash-layer coated around the bed material. The chemical composition of the surface of the bed materials was characterized by SEM-EDX elemental analysis before and after the combustion test. Figure 4-3 shows the EDX results of the surface composition of bed material (silica or olivine sand) after 2, 4, and 6h combustion of corn stalk at two air velocities  $U_g = 2.5U_{mf}$  (a) and  $4U_{mf}$  (b). As shown in the Figure, silica sand particles before and after corn stalk combustion contain similar content of Si on the surface which is apparently originated from the silica sand. However, compared with the virgin bed material before corn stalk combustion, the silica particles after the corn stalk combustion test are enriched with  $K > Ca \approx Mg$ , whose contents increase with increasing the combustion time, suggesting deposition of these elements from the biomass ash onto the bed material surface, which could eventually lead to bed material agglomeration and de-fluidization. Similarly, as shown in this Figure, surface of olivine sand particles before and after corn stalk combustion is composed of mainly Mg and Si, originated from the olivine sand (Table 4-1). When compared with the virgin bed material before corn stalk combustion, however, the coated ash-layer was enriched with  $Ca > K$ , increasing for a longer combustion time too. It should also be noted that the K content in the coated ash-layer on olivine bed materials is much lower than that on the silica bed materials. This much less deposition amount of alkali K compounds onto the olivine bed material than that onto



the silica sand material might contribute to the longer de-fluidization time (>12h) for the olivine bed material than that for the silica bed material (8h) during corn stalk combustion.

A possible reason for the much less deposition tendency of alkali K compounds onto the olivine bed material than that onto the silica sand material might be related to the following reactions (as discussed previously in Chapter 3):



From the above reactions, reaction (4-3) will play a significant role in capturing more K in the coated ash-layer around the silica bed material, compared with that with the olivine bed material which contains less SiO<sub>2</sub>,

As shown in Table 4-2, K (14.8wt%), Ca (6.6wt%) are Mg (2.6wt%) are three major alkali/alkaline earth elements in corn stalk ash. These elements may form low-boiling point compounds, hence have high tendency for the formation of molten ash-layer on the bed material, which would lead to the bed material agglomeration and de-fluidization eventually.

Comparing the results presented in Figures 4-3a and 4-3b, with increasing the superficial gas velocity  $U_g$  from  $2.5U_{mf}$  to  $4U_{mf}$ , the deposited amount of the alkali/alkaline earth elements (K, Ca, Mg) in the bed material (either silica or olivine sand) reduced substantially, which could be explained by the fact that at higher air velocity the residence time of volatile matters and char shortens in the dense phase of the bed materials and hence the deposition of the alkali/alkaline earth elements (K, Ca, Mg) from the biomass ash on the surface of bed materials reduces. This again would contribute to reduced tendency of bed agglomeration and de-fluidization.

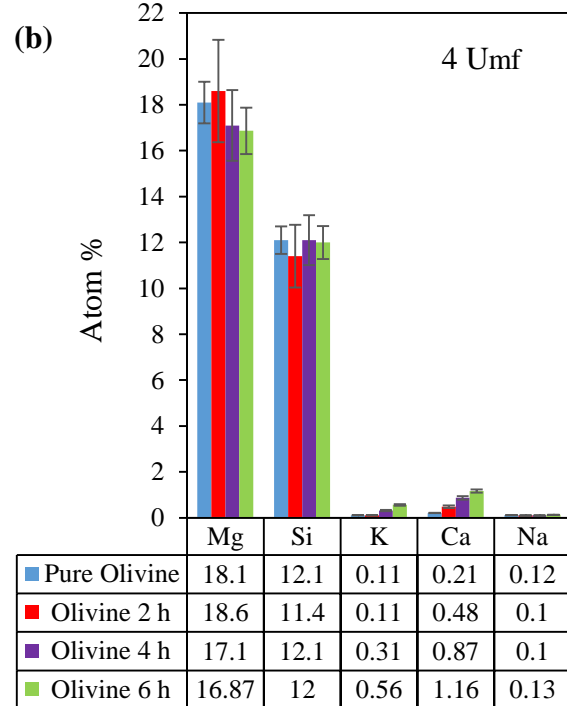
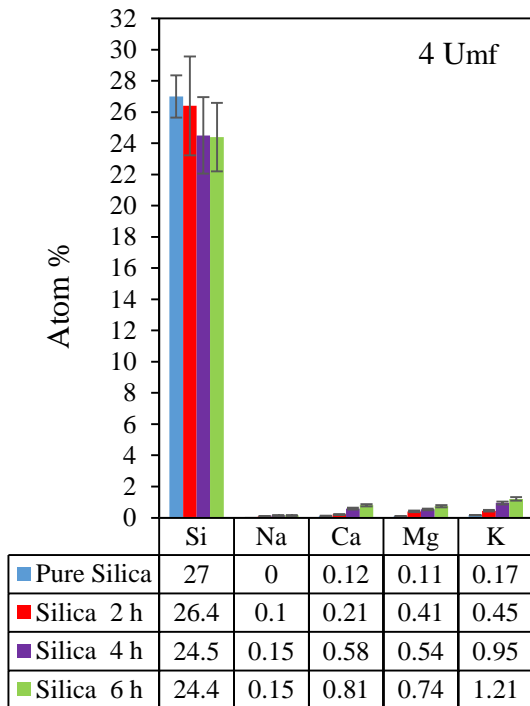
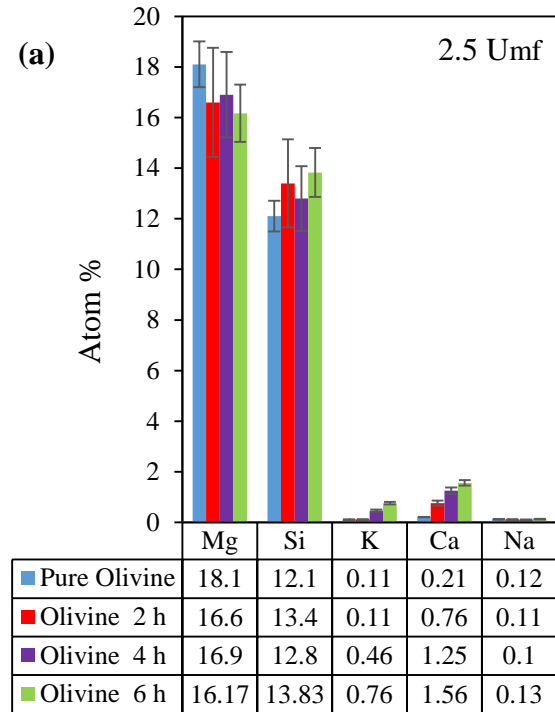
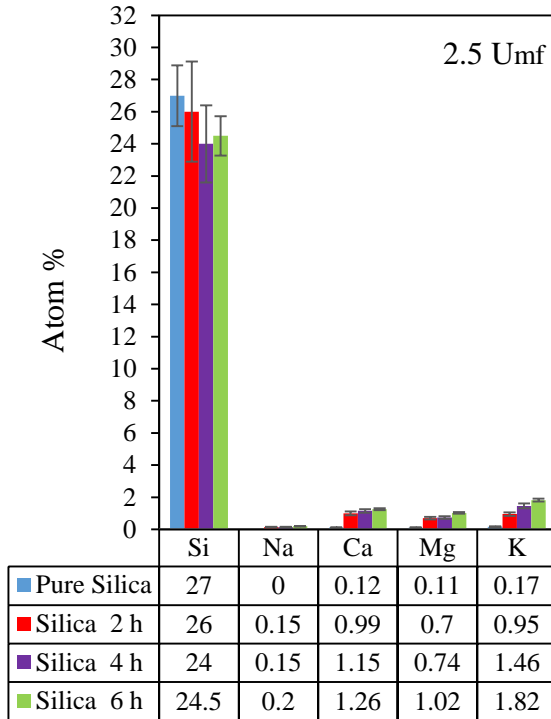


Figure 4-3 EDX results of the surface composition of bed material (silica or olivine sand) after 2, 4, and 6 hours combustion of corn stalk at two air velocities  $U_g = 2.5U_{mf}$  (a) and  $4U_{mf}$  (b).

### 4.3.3 De-Fluidization Time and Surface Composition of Agglomerates

De-fluidization time was determined by operating the corn stalk combustion at  $U_g = 2.5U_{mf}$  with two different bed materials for a long time until the onset of de-fluidization characterized by the rapid increases in pressure accompanied by a drastic temperature drops during the combustion. Determining the de-fluidization time was actually a long process > 8-12h by combustion of corn stalk in BFB of silica or olivine sand at  $U_g = 2.5U_{mf}$ , when the T- $\Delta P$  signals at the dense phase bed are monitored, as displayed in Figures 4-4a and 4-4b. Same as the procedure as described in the experimental section, biomass feeding was started when the bed temperature reached 550°C. As clearly illustrated in this figure, the de-fluidization appeared to occur after 8h combustion test. However, both the pressure drop and the dense-phase temperature signals are rather stable with the olivine sand even after 12h operation with de-fluidization.

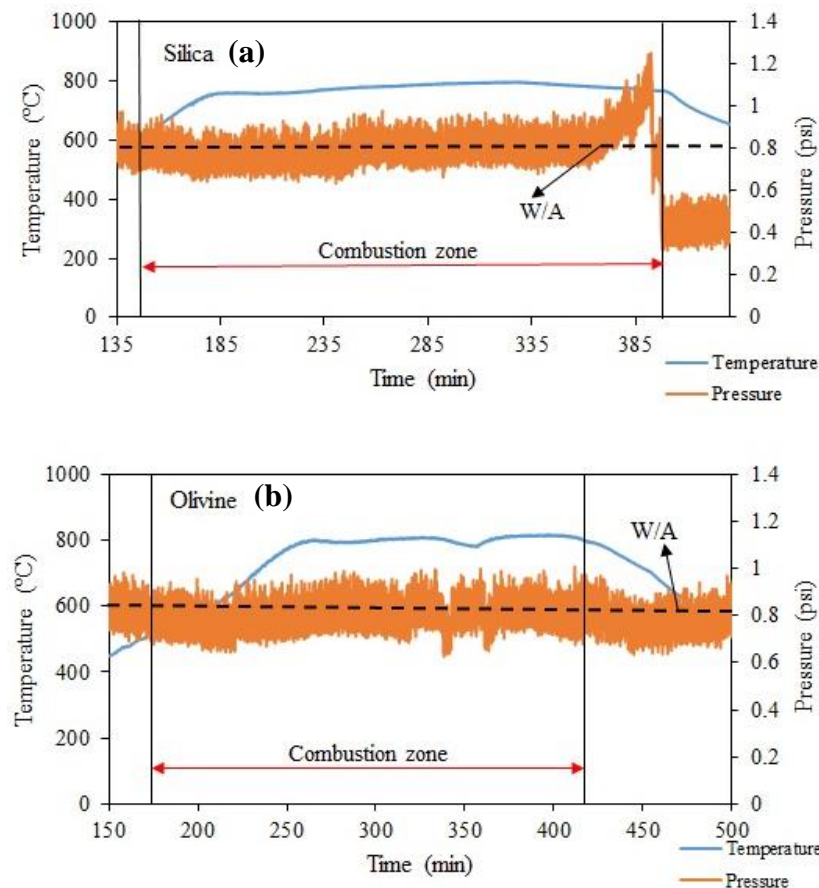


Figure 4-4 T- $\Delta P$  signals at the dense phase bed during combustion of corn stalk in BFB of silica (2<sup>nd</sup> day) (a) and olivine sand (3<sup>rd</sup> day) (b) at  $U_g = 2.5U_{mf}$ .

Table 4-3 presents the operation conditions and de-fluidization time for the combustion of corn stalk in a BFB combustor using silica sand and olivine sand as bed material at  $2.5U_{mf}$ . De-fluidization time defines as a specific time from the feeding the biomass into the reactor until the onset of the severe bed material agglomeration or de-fluidization, determined based on the T- $\Delta$ P signals as discussed previously. The results indicate that the de-fluidization time for the silica sand system was 8 hours, whereas no de-fluidization was detected for the olivine sand system even after 12h operation.

Table 4-3 Operation conditions and de-fluidization time for the combustion of corn stalk in a BFB combustor using silica sand and olivine sand as bed material at  $2.5U_{mf}$ .

Bed material	Air rate (m/s)	Feed rate (g/h)	Bed temperature	Ash* /Bed	$d_p(\mu\text{m})$	De-fluidization time (h)
Silica Sand	0.082	500	~797	0.078	200-250	8
Olivine Sand	0.03	500	~803	0.117	130-170	>12

\*Total amount of ash which was calculated based on feeding rate and the operating time.

After the de-fluidization, the air flow was shut down and the reactor was cooled down to the room temperature. Afterward, the bed material was discharged and sieved very gently to collect the agglomerated particles. As the formed agglomerates were quite fragile, the size distribution of particles was not determined. The collected agglomerates from silica bed (after 8h combustion) and olivine (after 12h combustion) were analysed by SEM-EDX. Figure 4-5 displays the EDX elemental analysis of the agglomerated silica in two points (A and B as shown in Figure 4-7 (I)) and non-agglomerated olivine particles after the combustion tests. Both point (A) and (B) are enriched in  $K > Ca \approx Mg$  although with a large difference in K content in these two points (suggesting non-uniform deposition of K on the silica particles). Whereas, the SEM-EDX analysis of olivine particles from the 12h combustion test revealed the presence of  $Ca > K$  originated from the biomass ash. The much less deposition amount of alkali K onto the olivine bed material than that onto the silica sand material might partially account for the longer de-fluidization time (>12h) for the olivine bed material than that for the silica bed material (8h).

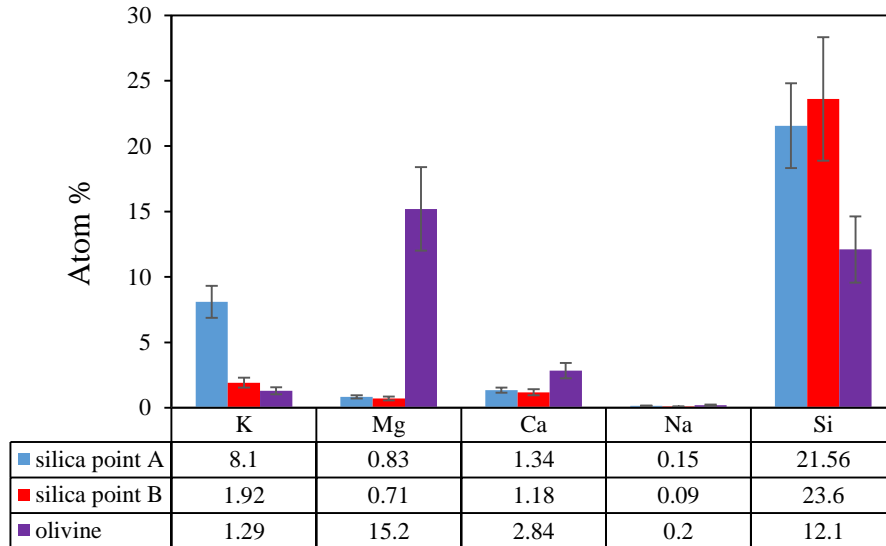


Figure 4-5 EDX elemental analysis of the agglomerated silica in two points (A and B as shown in Figure 4-7 (I)) and non-agglomerated olivine particles after 12h combustion tests.

It is worth to mention that the complex alkali compounds have different melting temperatures depending on their compositions. For instance, mixture of CaO-MgO-SiO<sub>2</sub> has the lowest melting point at around 1300°C [10,28]. On the other hand, for a complex system containing K<sub>2</sub>O-CaO-SiO<sub>2</sub>, the ratio of Ca/K plays an important role in determining the melting point. With increasing Ca/K ratio, the melting point of the system will increase, whereas the melting point of the system will decrease at a lower Ca/K ratio.

In case of olivine, based on the EDX elemental analysis (Figure 4-5) of the bed materials after 12h combustion test, the ternary phase diagram of K<sub>2</sub>O-CaO-SiO<sub>2</sub> is presented in Figure 4-6. The diagram reveals that the coated ash-layer around olivine with a high ratio of Ca/K around 2.84/1.29 had a higher melting temperature compared to silica agglomerates with low content of Ca/K ratio (Ca/K ratio is 1.34/8.1 for spot A and 1.18/1.92 for spot B (Figure 4-7), respectively). This could be another reason explaining that no severe agglomerate or de-fluidization was observed even after 12h operation of the olivine system at ~850°C. The operating temperature (~850°C) is much lower than the melting temperatures of the complex K<sub>2</sub>O-CaO-SiO<sub>2</sub> alkali compounds.

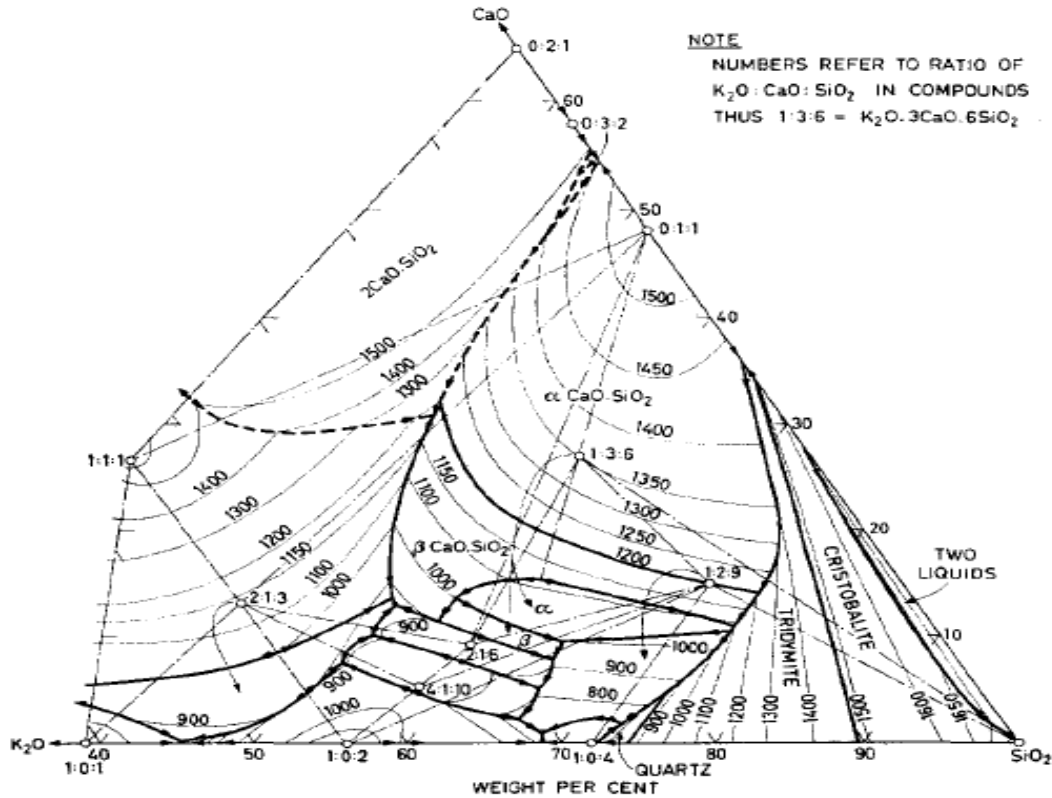


Figure 4-6 Ternary phase diagram of CaO-K<sub>2</sub>O-SiO<sub>2</sub> [5].

Figure 4-7 shows the SEM and optical microscopy images of the obtained agglomerates from the silica system. It was found that the formed agglomerates have the hollow structure. Formation of hollow structure could be explained by initiation of agglomeration through the accumulation of bed particles around the burning fuel particles. Based on Figure 4-7(I), two possible mechanisms could be proposed for the formation of agglomerates. Firstly, as a result of the burning of char particles, the temperature of ash is higher than the operation temperature, which forms molten ash media to glue the silica particles. Secondly, some alkali compounds such as K and Ca could react with silica sand and form low melting alkali silicates which could cover the silica particles to form a coated ash-layer and the coated particles might contact each other and form a bridge connection between the particles, forming agglomerates.

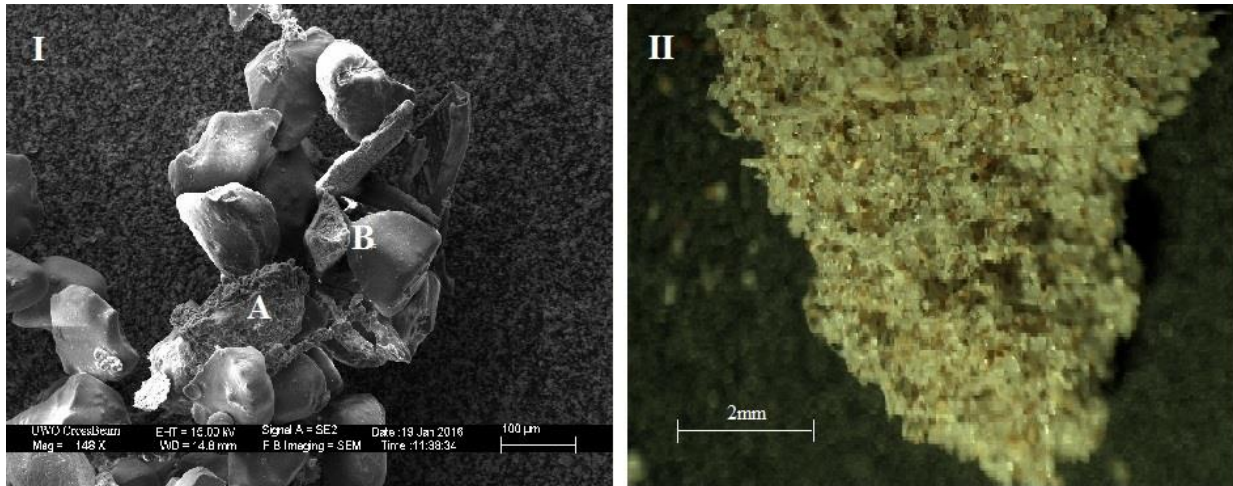


Figure 4-7 SEM micrograph of typical silica agglomerates (I), optical photograph of a small silica sand agglomerate (II).

#### 4.3.4 Composition of Bottom and Fly Ash

After 8 hours of combustion of cornstalk, the bed materials were discharged to collect the agglomerates. Along with the agglomerates, bottom ash particles were also collected in both silica and olivine systems. Meanwhile fly ash samples were also collected from the cyclone. Figures 4-8a and 4-8b show the bottom ash particles collected from both silica and olivine beds after 8h combustion of corn stalk. As observed, the colors of the collected samples are much different, depending on the type of the bed material used in the combustion tests.

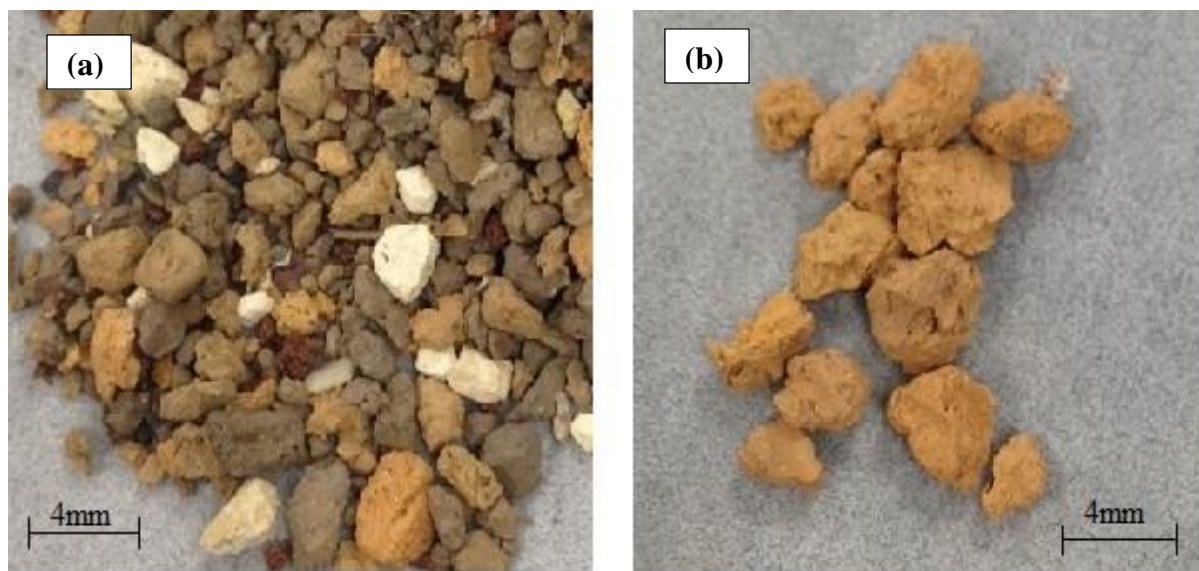


Figure 4-8 Bottom ash particles collected from the olivine bed (a) and silica bed (b) after 8h BFB combustion of corn stalk.

The collected bottom ash particles were analyzed by ICP to determine the elemental composition, and the results are presented in Figure 4-9. The bottom ash particles collected from the olivine bed are rich in  $\text{Ca} > \text{Mg} > \text{K} > \text{Na}$ , in a good agreement with the composition of the coated ash-layer on the bed material (Figures 4-3 and 4-5), where the  $\text{Ca/K/Na}$  species are originated from the biomass feedstock (Table 4-2) and the  $\text{Mg}$  is mainly from olivine bed material (Table 4-1). In contrast, the most significant element in the bottom ash particles from the silica bed is  $\text{K} > \text{Ca} > \text{Mg} > \text{Na}$ , all are likely originated from the biomass feedstock (Table 4-2). The high  $\text{K}$  content in the bottom ash from the silica bed is in a good agreement with that of the coated ash-layer on the bed material or agglomerates of silica bed material (Figures 4-3 and 4-5). As previously discussed, the high content of  $\text{K}$  species in the bottom ash and their possible reactions with silica material in the silica bed would form low-melting point compounds during the biomass combustion, eventually leading to severe agglomeration and de-fluidization.



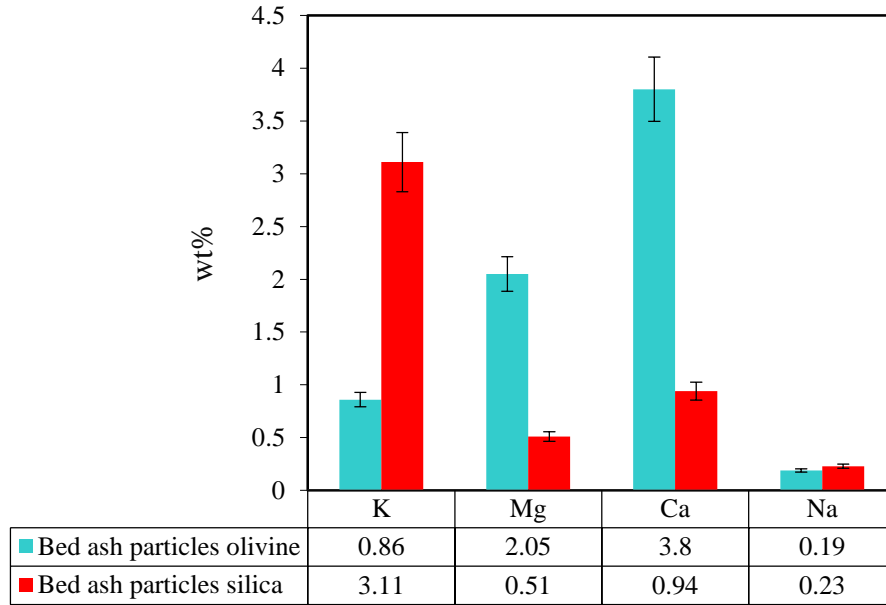


Figure 4-9 Results of ICP analysis of bottom ash particles collected from the silica or olivine bed after 8h BFB combustion of corn stalk.

Figure 4-10 presents results of ICP analysis of fly ashes collected after 8h BFB combustion of corn stalk in silica sand or olivine sand in comparison with composition of the original corn stalk ash. Generally, the relative compositions of both fly ash samples are similar to that of the original ash of the feedstock, containing mainly K, Ca, Mg and Na. However, the elemental composition of the fly ash samples shows a reduction in the composition of all these elements. For instance, the content of K in the fly ash is 2.7~2.9wt%, compared with 14.8% in the original ash of corn stalk. Such reduction of K, Ca, Mg and Na contents in the fly ash is actually expected due to accumulation of these alkali/alkaline earth compounds in the bed by forming coated ash-layers or agglomerates) or bottom ash during the combustion.

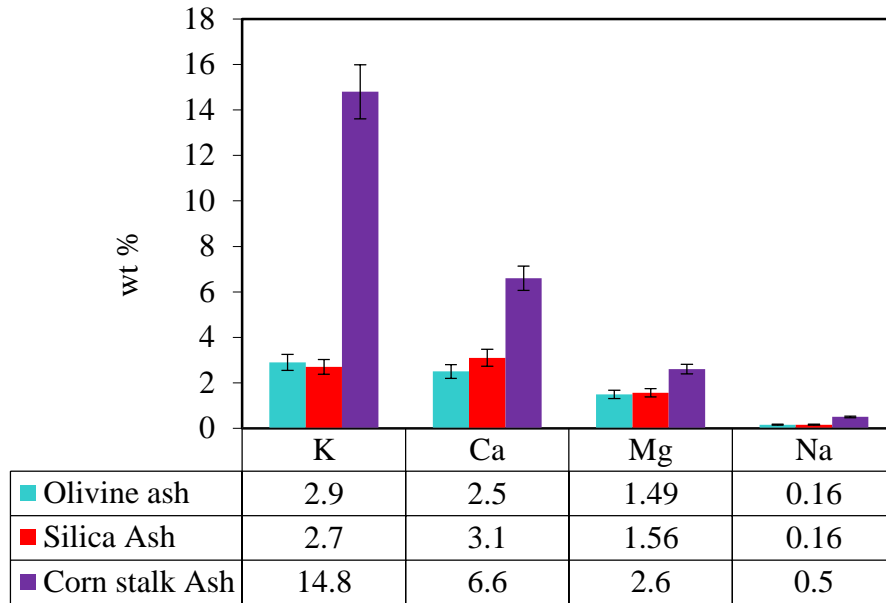


Figure 4-10 Results of ICP analysis of fly ashes collected after 8h BFB combustion of corn stalk in silica sand or olivine sand in comparison with composition of the original corn stalk ash.

#### 4.4 Conclusions

Bed material agglomeration behaviours during the combustion of corn stalk were studied in a BFB reactor using different bed materials (silica and olivine sand) at two different superficial air velocities ( $U_g = 2.5U_{mf}$  and  $4U_{mf}$ ). During the combustion tests, T- $\Delta$ P signals were monitored to determine the de-fluidization time. In addition, the composition of the ash-lay coated around the bed material, the agglomerates formed as well as the bottom/fly ash particles collected in the combustion tests were analyzed by SEM-EDX and ICP. Some major conclusions can be drawn from this study, as summarized as follows:

- 1) Different bed materials exhibited different agglomeration tendencies during BFB combustion of corn stalk. Silica sand system showed a shorter de-fluidization time, approximately 8h after combustion of cornstalk, whereas no de-fluidization was observed in the olivine system even after 12h combustion,
- 2) Compared with the virgin bed material before corn stalk combustion, the silica particles or agglomerates after the corn stalk combustion tests are enrich with  $K > Ca \approx Mg$ , whose contents increase with increasing the combustion time, suggesting deposition of these elements from the biomass ash onto the bed material surface, which could eventually lead

to bed material agglomeration and de-fluidization. With olivine sand bed material, however, the coated ash-layer was enriched with  $Ca > K$ , increasing for a longer combustion time too.

- 3) The K content in the coated ash-layer on olivine bed materials and in the bottom ash from the olivine bed system is much lower than that with the silica bed material, suggesting much less deposition tendency of K compounds on the olivine bed material than that on the silica sand material. This might contribute to the longer de-fluidization time (>12h) for the olivine bed material than that for the silica bed material (8h) during corn stalk combustion.
- 4) With increasing the superficial gas velocity, the deposited amount of the alkali/alkaline earth elements (K, Ca, Mg) in the bed material (either silica or olivine sand) reduced substantially, which would contribute to reduced tendency of bed agglomeration and de-fluidization.

#### 4.5 References

- [1] Yu C, Qin J, Nie H, Fang M, Luo Z. Experimental research on agglomeration in straw-fired fluidized beds. *Appl Energy* 2011;88:4534–43. doi:10.1016/j.apenergy.2011.05.046.
- [2] Ninduangdee P, Kuprianov VI. Study on burning oil palm kernel shell in a conical fluidized-bed combustor using alumina as the bed material. *J Taiwan Inst Chem Eng* 2013;44:1045–53. doi:10.1016/j.jtice.2013.06.011.
- [3] Brus E, Marcus O, Nordin A. Mechanisms of Bed Agglomeration during Fluidized-Bed Combustion of Biomass Fuels. *Energy & Fuels* 2005;1:825–32.
- [4] Chirone R, Miccio F, Scala F. Mechanism and prediction of bed agglomeration during fluidized bed combustion of a biomass fuel: Effect of the reactor scale. *Chem Eng J* 2006;123:71–80. doi:10.1016/j.cej.2006.07.004.
- [5] Chaivatamaset P, Sricharoon P, Tia S, Bilitewski B. The characteristics of bed agglomeration/defluidization in fluidized bed firing palm fruit bunch and rice straw. *Appl Therm Eng* 2014;70:737–47. doi:10.1016/j.applthermaleng.2014.05.061.
- [6] Öhman M, Nordin A, Skrifvars B-J, Backman R, Hupa M. Bed Agglomeration Characteristics during Fluidized Bed Combustion of Biomass Fuels. *Energy & Fuels* 2000;14:169–78. doi:10.1021/ef990107b.
- [7] Gatternig B, Karl J. The influence of particle size, fluidization velocity and fuel type on ash-induced agglomeration in biomass combustion. *Front Energy Res* 2014;2:1–12. doi:10.3389/fenrg.2014.00051.
- [8] Rozainee M, Ngo SP, Salema a. a., Tan KG, Ariffin M, Zainura ZN. Effect of fluidising velocity on the combustion of rice husk in a bench-scale fluidised bed combustor for the production of amorphous rice husk ash. *Bioresour Technol* 2008;99:703–13. doi:10.1016/j.biortech.2007.01.049.
- [9] Lin C-L, Peng T-H, Wang W-J. Effect of particle size distribution on agglomeration/defluidization during fluidized bed combustion. *Powder Technol* 2011;207:290–5. doi:10.1016/j.powtec.2010.11.010.
- [10] Grimm A, Marcus O, Fredriksson A, Bostro D. Bed Agglomeration Characteristics in

- Fluidized-Bed Combustion of Biomass Fuels Using Olivine as Bed Material. *Energy & Fuels* 2012;26:4550–9.
- [11] Shimizu T, Han J, Choi S, Kim L, Kim H. Fluidized-Bed Combustion Characteristics of Cedar Pellets by Using an Alternative Bed Material. *Energy & Fuels* 2006;20:2737–42. doi:10.1021/ef0601723.
- [12] Shiyuan L, Qinggang L, Haipeng T. Agglomeration During Fluidized -Bed Combustion of Biomass. 13th Int. Conf. Fluid. - New Paradig. Fluid. Eng., 2010.
- [13] Liu H, Feng Y, Wu S, Liu D. The role of ash particles in the bed agglomeration during the fluidized bed combustion of rice straw. *Bioresour Technol* 2009;100:6505–13. doi:10.1016/j.biortech.2009.06.098.
- [14] Chaivatamaset P, Sricharoon P, Tia S. Bed agglomeration characteristics of palm shell and corncob combustion in fluidized bed. *Appl Therm Eng* 2011;31:2916–27. doi:10.1016/j.applthermaleng.2011.05.021.
- [15] Öhman M, Nordin A. The Role of Kaolin in Prevention of Bed Agglomeration during Fluidized Bed Combustion of Biomass Fuels 2000, Volume 14. *Energy & Fuels* 2000;14:737–737. doi:10.1021/ef000065n.
- [16] Öhman M, Boström D, Nordin A, Hedman H. Effect of kaolin and limestone addition on slag formation during combustion of wood fuels. *Energy and Fuels* 2004;18:1370–6. doi:10.1021/ef040025+.
- [17] Wang L, Becidan M, Skreiberg Ø. Testing of Zeolite and Kaolin for Preventing Ash Sintering and Fouling during Biomass Combustion. *Chem Eng Trans* 2013;35:1159–64. doi:10.3303/CET1335193.
- [18] Lundholm K, Nordin A, Marcus O, Bostro D. Reduced Bed Agglomeration by Co-combustion Biomass with Peat Fuels in a Fluidized Bed. *Energy & Fuels* 2005;19:2273–8.
- [19] Wang L, Hustad JE, Skreiberg Ø, Skjevraak G, Grønli M. A critical review on additives to reduce ash related operation problems in biomass combustion applications. *Energy Procedia* 2012;20:20–9. doi:10.1016/j.egypro.2012.03.004.

- [20] Steenari BM, Lundberg A, Pettersson H, Wilewska-Bien M, Andersson D. Investigation of ash sintering during combustion of agricultural residues and the effect of additives. *Energy and Fuels* 2009;23:5655–62. doi:10.1021/ef900471u.
- [21] Steenari BM, Lindqvist O. High-temperature reactions of straw ash and the anti-sintering additives kaolin and dolomite. *Biomass and Bioenergy* 1998;14:67–76. doi:10.1016/S0961-9534(97)00035-4.
- [22] Boström D, Grimm A, Boman C, Björnbom E, Öhman M. Influence of kaolin and calcite additives on ash transformations in small-scale combustion of oat. *Energy and Fuels* 2009;23:5184–90. doi:10.1021/ef900429f.
- [23] Montes A, Hamidi M, Briens C, Berruti F, Tran H, Xu C (Charles). Study on the critical amount of liquid for bed material agglomeration in a bubbling fluidized bed. *Powder Technol* 2015;284:437–42. doi:10.1016/j.powtec.2015.07.017.
- [24] Montes A, Ghiasi E, Tran H, Xu C (Charles). Study of bed materials agglomeration in a heated bubbling fluidized bed (BFB) using silica sand as the bed material and KOH to simulate molten ash. *Powder Technol* 2016;291:178–85. doi:10.1016/j.powtec.2015.12.030.
- [25] Overend RP. Direct Combustion of Biomass. *Renew. Energy Sources Charg. with Energy from Sun Orig. from Earth– Moon Interaction*, vol. I, 2012.
- [26] Lin W, Dam-Johansen K, Frandsen F. Agglomeration in bio-fuel fired fluidized bed combustors. *Chem Eng J* 2003;96:171–85. doi:10.1016/j.cej.2003.08.008.
- [27] Goran O, Ye Z, Bjerle I, Andersson A. Bed Agglomeration Problems in Fluidized-Bed Biomass Combustion. *Ind Eng Chem Res* 2002;41:2888–94.
- [28] Osborn, E F. The Compound Merwinite ( $3\text{CaO}\cdot\text{MgO}\cdot 2\text{SiO}_2$ ) and its Stability Relations within the System  $\text{CaO}\text{-MgO}\text{-SiO}_2$ . *Am Ceram Soc* 1943;26:321–32.
- [1] Yu C, Qin J, Nie H, Fang M, Luo Z. Experimental research on agglomeration in straw-fired fluidized beds. *Appl Energy* 2011;88:4534–43. doi:10.1016/j.apenergy.2011.05.046.

- [2] Ninduangdee P, Kuprianov VI. Study on burning oil palm kernel shell in a conical fluidized-bed combustor using alumina as the bed material. *J Taiwan Inst Chem Eng* 2013;44:1045–53. doi:10.1016/j.jtice.2013.06.011.
- [3] Brus E, Marcus O, Nordin A. Mechanisms of Bed Agglomeration during Fluidized-Bed Combustion of Biomass Fuels. *Energy & Fuels* 2005;1:825–32.
- [4] Chirone R, Miccio F, Scala F. Mechanism and prediction of bed agglomeration during fluidized bed combustion of a biomass fuel: Effect of the reactor scale. *Chem Eng J* 2006;123:71–80. doi:10.1016/j.cej.2006.07.004.
- [5] Chaivatamaset P, Sricharoon P, Tia S, Bilitewski B. The characteristics of bed agglomeration/defluidization in fluidized bed firing palm fruit bunch and rice straw. *Appl Therm Eng* 2014;70:737–47. doi:10.1016/j.applthermaleng.2014.05.061.
- [6] Öhman M, Nordin A, Skrifvars B-J, Backman R, Hupa M. Bed Agglomeration Characteristics during Fluidized Bed Combustion of Biomass Fuels. *Energy & Fuels* 2000;14:169–78. doi:10.1021/ef990107b.
- [7] Gatternig B, Karl J. The influence of particle size, fluidization velocity and fuel type on ash-induced agglomeration in biomass combustion. *Front Energy Res* 2014;2:1–12. doi:10.3389/fenrg.2014.00051.
- [8] Rozainee M, Ngo SP, Salema a. a., Tan KG, Ariffin M, Zainura ZN. Effect of fluidising velocity on the combustion of rice husk in a bench-scale fluidised bed combustor for the production of amorphous rice husk ash. *Bioresour Technol* 2008;99:703–13. doi:10.1016/j.biortech.2007.01.049.
- [9] Lin C-L, Peng T-H, Wang W-J. Effect of particle size distribution on agglomeration/defluidization during fluidized bed combustion. *Powder Technol* 2011;207:290–5. doi:10.1016/j.powtec.2010.11.010.
- [10] Grimm A, Marcus O, Fredriksson A, Bostro D. Bed Agglomeration Characteristics in Fluidized-Bed Combustion of Biomass Fuels Using Olivine as Bed Material. *Energy & Fuels* 2012;26:4550–9.
- [11] Shimizu T, Han J, Choi S, Kim L, Kim H. Fluidized-Bed Combustion Characteristics of

- Cedar Pellets by Using an Alternative Bed Material. *Energy & Fuels* 2006;20:2737–42. doi:10.1021/ef0601723.
- [12] Shiyuan L, Qinggang L, Haipeng T. Agglomeration During Fluidized -Bed Combustion of Biomass. 13th Int. Conf. Fluid. - New Paradig. Fluid. Eng., 2010.
- [13] Liu H, Feng Y, Wu S, Liu D. The role of ash particles in the bed agglomeration during the fluidized bed combustion of rice straw. *Bioresour Technol* 2009;100:6505–13. doi:10.1016/j.biortech.2009.06.098.
- [14] Chaivatamaset P, Sricharoon P, Tia S. Bed agglomeration characteristics of palm shell and corncob combustion in fluidized bed. *Appl Therm Eng* 2011;31:2916–27. doi:10.1016/j.applthermaleng.2011.05.021.
- [15] Öhman M, Nordin A. The Role of Kaolin in Prevention of Bed Agglomeration during Fluidized Bed Combustion of Biomass Fuels 2000, Volume 14. *Energy & Fuels* 2000;14:737–737. doi:10.1021/ef000065n.
- [16] Öhman M, Boström D, Nordin A, Hedman H. Effect of kaolin and limestone addition on slag formation during combustion of wood fuels. *Energy and Fuels* 2004;18:1370–6. doi:10.1021/ef040025+.
- [17] Wang L, Becidan M, Skreiberg Ø. Testing of Zeolite and Kaolin for Preventing Ash Sintering and Fouling during Biomass Combustion. *Chem Eng Trans* 2013;35:1159–64. doi:10.3303/CET1335193.
- [18] Lundholm K, Nordin A, Marcus O, Bostro D. Reduced Bed Agglomeration by Co-combustion Biomass with Peat Fuels in a Fluidized Bed. *Energy & Fuels* 2005;19:2273–8.
- [19] Wang L, Hustad JE, Skreiberg Ø, Skjevraak G, Grønli M. A critical review on additives to reduce ash related operation problems in biomass combustion applications. *Energy Procedia* 2012;20:20–9. doi:10.1016/j.egypro.2012.03.004.
- [20] Steenari BM, Lundberg A, Pettersson H, Wilewska-Bien M, Andersson D. Investigation of ash sintering during combustion of agricultural residues and the effect of additives. *Energy and Fuels* 2009;23:5655–62. doi:10.1021/ef900471u.



- [21] Steenari BM, Lindqvist O. High-temperature reactions of straw ash and the anti-sintering additives kaolin and dolomite. *Biomass and Bioenergy* 1998;14:67–76. doi:10.1016/S0961-9534(97)00035-4.
- [22] Boström D, Grimm A, Boman C, Björnbom E, Öhman M. Influence of kaolin and calcite additives on ash transformations in small-scale combustion of oat. *Energy and Fuels* 2009;23:5184–90. doi:10.1021/ef900429f.
- [23] Montes A, Hamidi M, Briens C, Berruti F, Tran H, Xu C (Charles). Study on the critical amount of liquid for bed material agglomeration in a bubbling fluidized bed. *Powder Technol* 2015;284:437–42. doi:10.1016/j.powtec.2015.07.017.
- [24] Montes A, Ghiasi E, Tran H, Xu C (Charles). Study of bed materials agglomeration in a heated bubbling fluidized bed (BFB) using silica sand as the bed material and KOH to simulate molten ash. *Powder Technol* 2016;291:178–85. doi:10.1016/j.powtec.2015.12.030.
- [25] Overend RP. Direct Combustion of Biomass. *Renew. Energy Sources Charg. with Energy from Sun Orig. from Earth– Moon Interation*, vol. I, 2012.
- [26] Lin W, Dam-Johansen K, Frandsen F. Agglomeration in bio-fuel fired fluidized bed combustors. *Chem Eng J* 2003;96:171–85. doi:10.1016/j.cej.2003.08.008.
- [27] Goran O, Ye Z, Bjerle I, Andersson A. Bed Agglomeration Problems in Fluidized-Bed Biomass Combustion. *Ind Eng Chem Res* 2002;41:2888–94.
- [28] Osborn, E F. The Compound Merwinite ( $3\text{CaO}\cdot\text{MgO}\cdot 2\text{SiO}_2$ ) and its Stability Relations within the System CaO-MgO-SiO<sub>2</sub>. *Am Ceram Soc* 1943;26:321–32.

## **Chapter 5**

### **Conclusions and Recommendations**

## 5.1 Conclusions

To the best of our knowledge there is no answer yet to what is the minimum or critical amount of liquid (molten alkali compounds) required to agglomerate the bed material and cause de-fluidization of the bed, except for some research results obtained by our group based on cold/mild-temperature tests using model compounds. Therefore, the main objective of the present thesis work is to determine experimentally the critical amount of liquid required to agglomerate silica sand particles in a bubbling fluidized bed (BFB) leading to de-fluidization at higher temperatures, and to examine effects of kaolin or aluminum sulfate additive. To simulate the real biomass combustion in BFB, various model systems have been employed, including hot BFB with KCl, and KCl-K<sub>2</sub>SO<sub>4</sub> eutectic compounds to simulate molten biomass ash in real biomass combustion. The main conclusions drawn from this part of research are summarized as follows:

- 1) Bubbling fluidization of silica sand particles in the presence of KCl or eutectic mixture of KCl-K<sub>2</sub>SO<sub>4</sub> with an amount of 0.4-0.6 wt.% (w.r.t. the weight of bed material) caused severe formation of channeling/agglomeration, leading to de-fluidization. On the contrary, no agglomeration was observed when adding K<sub>2</sub>SO<sub>4</sub> to the bed material heated up to 800 °C, which could be attributed to the higher melting point of K<sub>2</sub>SO<sub>4</sub> (>1024 °C) than KCl or eutectic mixture of KCl-K<sub>2</sub>SO<sub>4</sub>.
- 2) SEM-EDX and XPS analyses of the agglomerates or bed material samples after the experiments suggested more loss of Cl than K during the experiments, likely via some reactions converting KCl into HCl vapor.
- 3) The proposed reactions are: KCl and Fe from the reactor wall react with H<sub>2</sub>O/O<sub>2</sub> (from the undried compressed air) at elevated temperatures, forming Fe<sub>2</sub>O<sub>3</sub> (causing corrosion of the reactor wall) and KOH (l) and HCl (g) vapor. The reaction between KOH (l) and silica would form potassium silicates, which might contribute to the formation of bed material agglomeration.
- 4) Kaolin and aluminum sulfate demonstrated to be effective additives for preventing bed material agglomeration in bubbling fluidization of silica sand particles at a high temperature.

The second part of the thesis work aimed to examine the de-fluidization time for BFB combustion of corn stalk (with a high K, Mg, Ca-containing ash) with different bed materials operating at different superficial air velocities. Some major conclusions are summarized as follows

- 5) Different bed materials exhibited different agglomeration tendencies during BFB combustion of corn stalk. Silica sand system showed a shorter de-fluidization time, approximately 8h after combustion of cornstalk, whereas no de-fluidization was observed in the olivine system even after 12h combustion,
- 6) Compared with the virgin bed material before corn stalk combustion, the silica particles or agglomerates after the corn stalk combustion tests are enriched with  $K > Ca \approx Mg$ , whose contents increase with increasing the combustion time, suggesting deposition of these elements from the biomass ash onto the bed material surface, which could eventually lead to bed material agglomeration and de-fluidization. With olivine sand bed material, however, the coated ash-layer was enriched with  $Ca > K$ , increasing for a longer combustion time too.
- 7) The K content in the coated ash-layer on olivine bed materials and in the bottom ash from the olivine bed system is much lower than that with the silica bed material, suggesting much less deposition tendency of K compounds on the olivine bed material than that on the silica sand material. This might contribute to the longer de-fluidization time (>12h) for the olivine bed material than that for the silica bed material (8h) during corn stalk combustion.
- 8) With increasing the superficial gas velocity, the deposited amount of the alkali/alkaline earth elements (K, Ca, Mg) in the bed material (either silica or olivine sand) reduced substantially, which would contribute to reduced tendency of bed agglomeration and de-fluidization.

## 5.2 Recommendations

- I suggest to install a separate probe for pressure transducers using snubber connection. With the current configuration, a shared probe was used for pressure transducer and thermocouples which leading to clogging during the experiment and cleaning after several experiments.
- If possible, the feeding line may better be replaced with a straight line instead of the elbow joint to prevent the clogging during biomass feeding for the combustion tests.

- It would be of interest to test the de-fluidization behavior for olivine sand system at a higher operation temperature, e.g.,  $> 900^{\circ}\text{C}$ .

## **Appendix**

## Appendix 1: Permission to Reuse Copyrighted Materials

Permission of Figure 2-2

### SPRINGER LICENSE TERMS AND CONDITIONS

Mar 01, 2016

---

This is a License Agreement between Ehsan Ghiasi ("You") and Springer ("Springer") provided by Copyright Clearance Center ("CCC"). The license consists of your order details, the terms and conditions provided by Springer, and the payment terms and conditions.

**All payments must be made in full to CCC. For payment instructions, please see information listed at the bottom of this form.**

License Number	3820300986517
License date	Mar 01, 2016
Licensed content publisher	Springer
Licensed content publication	Mitigation & Adaptation Strategies for Global Change
Licensed content title	Modern Biomass Conversion Technologies
Licensed content author	Andre Faaij
Licensed content date	Jan 1, 2006
Volume number	11
Issue number	2
Type of Use	Thesis/Dissertation
Portion	Figures/tables/illustrations
Number of figures/tables/illustrations	1
Author of this Springer article	No
Order reference number	None
Original figure numbers	Figure 1
Title of your thesis / dissertation	Bed Agglomeration Behavior in Bubbling Fluidized-Bed Combustor
Expected completion date	May 2016
Estimated size(pages)	100
Total	0.00 CAD
Terms and Conditions	

**ELSEVIER LICENSE  
TERMS AND CONDITIONS**

Mar 01, 2016

This is a License Agreement between Ehsan Ghiasi ("You") and Elsevier ("Elsevier") provided by Copyright Clearance Center ("CCC"). The license consists of your order details, the terms and conditions provided by Elsevier, and the payment terms and conditions.

**All payments must be made in full to CCC. For payment instructions, please see information listed at the bottom of this form.**

Supplier	Elsevier Limited The Boulevard, Langford Lane Kidlington, Oxford, OX5 1GB, UK
Registered Company Number	1982084
Customer name	Ehsan Ghiasi
Customer address	
License number	3820331392991
License date	Mar 01, 2016
Licensed content publisher	Elsevier
Licensed content publication	Biomass and Bioenergy
Licensed content title	An SEM/EDX study of bed agglomerates formed during fluidized bed combustion of three biomass fuels
Licensed content author	Fabrizio Scala, Riccardo Chirone
Licensed content date	March 2008
Licensed content volume number	32
Licensed content issue number	3
Number of pages	15
Start Page	252
End Page	266
Type of Use	reuse in a thesis/dissertation
Intended publisher of new work	other
Portion	figures/tables/illustrations
Number of figures/tables/illustrations	1
Format	electronic
Are you the author of this Elsevier article?	No
Will you be translating?	No

<https://www.copyright.com/DispatchServlet>



Original figure numbers	Figure 8
Title of your thesis/dissertation	Bed Agglomeration Behavior in Bubbling Fluidized-Bed Combustor
Expected completion date	May 2016
Estimated size (number of pages)	100
Elsevier VAT number	GB 494 6272 12
Permissions price	0.00 CAD
VAT/Local Sales Tax	0.00 CAD / 0.00 GBP
Total	0.00 CAD
Terms and Conditions	

### INTRODUCTION

1. The publisher for this copyrighted material is Elsevier. By clicking "accept" in connection with completing this licensing transaction, you agree that the following terms and conditions apply to this transaction (along with the Billing and Payment terms and conditions established by Copyright Clearance Center, Inc. ("CCC"), at the time that you opened your Rightslink account and that are available at any time at <http://myaccount.copyright.com>).

### GENERAL TERMS

2. Elsevier hereby grants you permission to reproduce the aforementioned material subject to the terms and conditions indicated.
3. Acknowledgement: If any part of the material to be used (for example, figures) has appeared in our publication with credit or acknowledgement to another source, permission must also be sought from that source. If such permission is not obtained then that material may not be included in your publication/copies. Suitable acknowledgement to the source must be made, either as a footnote or in a reference list at the end of your publication, as follows:  
"Reprinted from Publication title, Vol /edition number, Author(s), Title of article / title of chapter, Pages No., Copyright (Year), with permission from Elsevier [OR APPLICABLE SOCIETY COPYRIGHT OWNER]." Also Lancet special credit - "Reprinted from The Lancet, Vol. number, Author(s), Title of article, Pages No., Copyright (Year), with permission from Elsevier."
4. Reproduction of this material is confined to the purpose and/or media for which permission is hereby given.
5. Altering/Modifying Material: Not Permitted. However figures and illustrations may be altered/adapted minimally to serve your work. Any other abbreviations, additions, deletions and/or any other alterations shall be made only with prior written authorization of Elsevier Ltd. (Please contact Elsevier at [permissions@elsevier.com](mailto:permissions@elsevier.com))
6. If the permission fee for the requested use of our material is waived in this instance, please be advised that your future requests for Elsevier materials may attract a fee.
7. Reservation of Rights: Publisher reserves all rights not specifically granted in the combination of (i) the license details provided by you and accepted in the course of this licensing transaction, (ii) these terms and conditions and (iii) CCC's Billing and Payment terms and conditions.
8. License Contingent Upon Payment: While you may exercise the rights licensed immediately upon issuance of the license at the end of the licensing process for the transaction, provided that you have disclosed complete and accurate details of your proposed

**ELSEVIER LICENSE  
TERMS AND CONDITIONS**

Mar 01, 2016

This is a License Agreement between Ehsan Ghiasi ("You") and Elsevier ("Elsevier") provided by Copyright Clearance Center ("CCC"). The license consists of your order details, the terms and conditions provided by Elsevier, and the payment terms and conditions.

**All payments must be made in full to CCC. For payment instructions, please see information listed at the bottom of this form.**

Supplier	Elsevier Limited The Boulevard, Langford Lane Kidlington, Oxford, OX5 1GB, UK
Registered Company Number	1982084
Customer name	Ehsan Ghiasi
Customer address	
License number	3820320484694
License date	Mar 01, 2016
Licensed content publisher	Elsevier
Licensed content publication	Chemical Engineering Journal
Licensed content title	Agglomeration in bio-fuel fired fluidized bed combustors
Licensed content author	Weigang Lin, Kim Dam-Johansen, Flemming Frandsen
Licensed content date	15 December 2003
Licensed content volume number	96
Licensed content issue number	1-3
Number of pages	15
Start Page	171
End Page	185
Type of Use	reuse in a thesis/dissertation
Portion	figures/tables/illustrations
Number of figures/tables/illustrations	1
Format	electronic
Are you the author of this Elsevier article?	No
Will you be translating?	No
Original figure numbers	Figre 4
Title of your	Bed Agglomeration Behavior in Bubbling Fluidized-Bed Combustor



---

thesis/dissertation

Expected completion date	May 2016
Estimated size (number of pages)	100
Elsevier VAT number	GB 494 6272 12
Permissions price	0.00 CAD
VAT/Local Sales Tax	0.00 CAD / 0.00 GBP
Total	0.00 CAD

Terms and Conditions

### INTRODUCTION

1. The publisher for this copyrighted material is Elsevier. By clicking "accept" in connection with completing this licensing transaction, you agree that the following terms and conditions apply to this transaction (along with the Billing and Payment terms and conditions established by Copyright Clearance Center, Inc. ("CCC"), at the time that you opened your Rightslink account and that are available at any time at <http://myaccount.copyright.com>).

### GENERAL TERMS

2. Elsevier hereby grants you permission to reproduce the aforementioned material subject to the terms and conditions indicated.

3. Acknowledgement: If any part of the material to be used (for example, figures) has appeared in our publication with credit or acknowledgement to another source, permission must also be sought from that source. If such permission is not obtained then that material may not be included in your publication/copies. Suitable acknowledgement to the source must be made, either as a footnote or in a reference list at the end of your publication, as follows:

"Reprinted from Publication title, Vol /edition number, Author(s), Title of article / title of chapter, Pages No., Copyright (Year), with permission from Elsevier [OR APPLICABLE SOCIETY COPYRIGHT OWNER]." Also Lancet special credit - "Reprinted from The Lancet, Vol. number, Author(s), Title of article, Pages No., Copyright (Year), with permission from Elsevier."

4. Reproduction of this material is confined to the purpose and/or media for which permission is hereby given.

5. Altering/Modifying Material: Not Permitted. However figures and illustrations may be altered/adapted minimally to serve your work. Any other abbreviations, additions, deletions and/or any other alterations shall be made only with prior written authorization of Elsevier Ltd. (Please contact Elsevier at [permissions@elsevier.com](mailto:permissions@elsevier.com))

6. If the permission fee for the requested use of our material is waived in this instance, please be advised that your future requests for Elsevier materials may attract a fee.

7. Reservation of Rights: Publisher reserves all rights not specifically granted in the combination of (i) the license details provided by you and accepted in the course of this licensing transaction, (ii) these terms and conditions and (iii) CCC's Billing and Payment terms and conditions.

8. License Contingent Upon Payment: While you may exercise the rights licensed immediately upon issuance of the license at the end of the licensing process for the transaction, provided that you have disclosed complete and accurate details of your proposed use, no license is finally effective unless and until full payment is received from you (either by publisher or by CCC) as provided in CCC's Billing and Payment terms and conditions. If full payment is not received on a timely basis, then any license preliminarily granted shall be

**ELSEVIER LICENSE  
TERMS AND CONDITIONS**

Mar 01, 2016

This is a License Agreement between Ehsan Ghiasi ("You") and Elsevier ("Elsevier") provided by Copyright Clearance Center ("CCC"). The license consists of your order details, the terms and conditions provided by Elsevier, and the payment terms and conditions.

**All payments must be made in full to CCC. For payment instructions, please see information listed at the bottom of this form.**

Supplier	Elsevier Limited The Boulevard, Langford Lane Kidlington, Oxford, OX5 1GB, UK
Registered Company Number	1982084
Customer name	Ehsan Ghiasi
Customer address	
License number	3820320892598
License date	Mar 01, 2016
Licensed content publisher	Elsevier
Licensed content publication	Applied Energy
Licensed content title	Experimental research on agglomeration in straw-fired fluidized beds
Licensed content author	Chunjiang Yu, Jianshuang Qin, Hu Nie, Mengxiang Fang, Zhongyang Luo
Licensed content date	December 2011
Licensed content volume number	88
Licensed content issue number	12
Number of pages	10
Start Page	4534
End Page	4543
Type of Use	reuse in a thesis/dissertation
Intended publisher of new work	other
Portion	figures/tables/illustrations
Number of figures/tables/illustrations	2
Format	electronic
Are you the author of this Elsevier article?	No
Will you be translating?	No



Original figure numbers	Figure 5, figure 10
Title of your thesis/dissertation	Bed Agglomeration Behavior in Bubbling Fluidized-Bed Combustor
Expected completion date	May 2016
Estimated size (number of pages)	100
Elsevier VAT number	GB 494 6272 12
Permissions price	0.00 CAD
VAT/Local Sales Tax	0.00 CAD / 0.00 GBP
Total	0.00 CAD
Terms and Conditions	

### INTRODUCTION

1. The publisher for this copyrighted material is Elsevier. By clicking "accept" in connection with completing this licensing transaction, you agree that the following terms and conditions apply to this transaction (along with the Billing and Payment terms and conditions established by Copyright Clearance Center, Inc. ("CCC"), at the time that you opened your Rightslink account and that are available at any time at <http://myaccount.copyright.com>).

### GENERAL TERMS

2. Elsevier hereby grants you permission to reproduce the aforementioned material subject to the terms and conditions indicated.

3. Acknowledgement: If any part of the material to be used (for example, figures) has appeared in our publication with credit or acknowledgement to another source, permission must also be sought from that source. If such permission is not obtained then that material may not be included in your publication/copies. Suitable acknowledgement to the source must be made, either as a footnote or in a reference list at the end of your publication, as follows:

"Reprinted from Publication title, Vol /edition number, Author(s), Title of article / title of chapter, Pages No., Copyright (Year), with permission from Elsevier [OR APPLICABLE SOCIETY COPYRIGHT OWNER]." Also Lancet special credit - "Reprinted from The Lancet, Vol. number, Author(s), Title of article, Pages No., Copyright (Year), with permission from Elsevier."

4. Reproduction of this material is confined to the purpose and/or media for which permission is hereby given.

5. Altering/Modifying Material: Not Permitted. However figures and illustrations may be altered/adapted minimally to serve your work. Any other abbreviations, additions, deletions and/or any other alterations shall be made only with prior written authorization of Elsevier Ltd. (Please contact Elsevier at [permissions@elsevier.com](mailto:permissions@elsevier.com))

6. If the permission fee for the requested use of our material is waived in this instance, please be advised that your future requests for Elsevier materials may attract a fee.

7. Reservation of Rights: Publisher reserves all rights not specifically granted in the combination of (i) the license details provided by you and accepted in the course of this licensing transaction, (ii) these terms and conditions and (iii) CCC's Billing and Payment terms and conditions.

8. License Contingent Upon Payment: While you may exercise the rights licensed immediately upon issuance of the license at the end of the licensing process for the transaction, provided that you have disclosed complete and accurate details of your proposed use, no license is finally effective unless and until full payment is received from you (either

## Curriculum Vitae

**Name:** Ehsan Ghiasi

**Post-secondary Education and Degrees:** Amirkabir University of Technology  
Tehran, Iran  
2000-2004, B.Sc.

The University of Western Ontario  
London, Ontario, Canada  
2014-2016, M.Sc.

**Honours and Awards:** Western Graduate Research Scholarship  
Faculty of Engineering, Western University  
2014-2016

**Related Work Experience**

Graduate Research Assistant  
University of Western Ontario  
2014-2016

Graduate Teaching Assistant  
University of Western Ontario  
2014-2015

### Publications

- **Journal Publications**

1. Montes, A., Ghiasi, E., Tran, H., Xu, C. "Study of bed materials agglomeration in a heated bubbling fluidized bed (BFB) using silica sand as the bed material and KOH to simulate molten ash", *Powder Technology* 291, 2016, Pages **178-185**.

- **Manuscript to be submitted**

1. **Ghiasi, E.**, Montes, A., Nanda, M., Honghi, T and Xu, C. "Study of Bed Materials Agglomeration in a Bubbling Fluidized Bed (BFB) Using Silica Sand as the Bed Material and KCl and K<sub>2</sub>SO<sub>4</sub> at high temperature to simulate molten ash". *In preparation*.

2. Ghiasi, E., Tran, H. and Xu, C. “Bed Agglomeration Characteristics in Fluidized-bed Combustion of Corn Stalk Using Silica and Olivine as Bed Materials”. *In preparation*.

**Conference Presentations:**

1. 65<sup>th</sup> Canadian Chemical Engineering Conference, 4-7 Oct. 2015 Calgary, AB
2. Annual Research Review Meeting on Effective Energy and Chemical Recovery in Pulp and Paper Mills. University of Toronto 10-12 Nov. 2015
3. Annual Research Review Meeting on Effective Energy and Chemical Recovery Efficiency in the Kraft Process III. University of Toronto, 11-13 Nov. 2014